

Summer 8-19-2016

# Sediment Accumulations Patterns in the Damariscotta River Estuary

Emily A. Chandler

*University of Maine*, [emily.a.chandler@maine.edu](mailto:emily.a.chandler@maine.edu)

Follow this and additional works at: <http://digitalcommons.library.umaine.edu/etd>



Part of the [Geomorphology Commons](#), [Oceanography Commons](#), and the [Sedimentology Commons](#)

---

## Recommended Citation

Chandler, Emily A., "Sediment Accumulations Patterns in the Damariscotta River Estuary" (2016). *Electronic Theses and Dissertations*. 2470.

<http://digitalcommons.library.umaine.edu/etd/2470>

This Open-Access Thesis is brought to you for free and open access by DigitalCommons@UMaine. It has been accepted for inclusion in Electronic Theses and Dissertations by an authorized administrator of DigitalCommons@UMaine.

**SEDIMENT ACCUMULATION PATTERNS IN THE  
DAMARISCOTTA RIVER ESTUARY**

By

Emily A. Chandler

B.A. Bates College, 2009

A THESIS

Submitted in Partial Fulfillment of the

Requirements for the Degree of

Master of Science

(in Earth and Climate Sciences)

The Graduate School

The University of Maine

August 2016

Advisory Committee:

Joseph T. Kelley, Professor of Earth and Climate Sciences, Advisor

Daniel F. Belknap, Professor of Earth and Climate Sciences

Lawrence M. Mayer, Professor of Oceanography



## **THESIS ACCEPTANCE STATEMENT**

On behalf of the Graduate Committee for Emily A. Chandler, I affirm that this manuscript is the final and accepted thesis. Signatures of all committee members are on file with the Graduate School at the University of Maine, 42 Stodder Hall, Orono, Maine.

---

Joseph T. Kelley, Professor of Earth and Climate Sciences

Date

Copyright 2016 Emily Archer Chandler

All Rights Reserved

## **LIBRARY RIGHTS STATEMENT**

In presenting this thesis in partial fulfillment of the requirements for an advanced degree at The University of Maine, I agree that the Library shall make it freely available for inspection. I further agree that permission for "fair use" copying of this thesis for scholarly purposes may be granted by the Librarian. It is understood that any copying or publication of this thesis for financial gain shall not be allowed without my written permission.

Signature:

Date:

# **SEDIMENT ACCUMULATION PATTERNS IN THE DAMARISCOTTA RIVER ESTUARY**

By Emily A. Chandler

Thesis Advisor: Dr. Joseph T. Kelley

An Abstract of the Thesis Presented  
in Partial Fulfillment of the Requirements for the  
Degree of Master of Science  
(in Earth and Climate Sciences)  
August 2016

The tidally dominated Damariscotta River estuary is located on the south-central Maine coast. The elongate, north-south orientation of the estuary is characteristic of the indented shoreline in this region and a consequence of the bedrock structural framework, comprised of Paleozoic high-grade metasedimentary rocks. Pegmatite sills form bedrock constriction points that divide the estuary into seven distinct basins. The narrow, bending geometry and sill and basin morphology impact the distribution of sediment within the estuary and the hydrodynamics of the system. This study employs multibeam bathymetry surveys, sediment grab samples and radionuclide analysis ( $^{210}\text{Pb}$  and  $^{137}\text{Cs}$ ) of sediment cores to evaluate the impact of the bedrock framework on sediment accumulation patterns in the estuary. Sedimentation rates in the estuary are lower than those of other estuaries in the region, indicative of a sediment-starved system. As a result of extensive reworking of sediment within the estuary, the inner estuary is sediment choked and the volume and distribution of sediment control the hydrodynamics in this region. Current lineations mark a transition from the inner to middle and outer estuary, where the volume of

sediment is reduced and constriction points formed by bedrock sills dominate the morphology of the system.

The role of the bedrock framework in the morphology of the system is not unique to the Damariscotta River but also applies to other estuaries in the region. Despite its absence from many published conceptual models, bedrock framework is critical to development of estuaries in rocky, formerly glaciated regions. Furthermore its role in the distribution of sediment, as well as pollutants and contaminants, is significant in the context of global climate change, continued shoreline development in the region and expansion of Maine's aquaculture industry.

## **ACKNOWLEDGEMENTS**

I would like to acknowledge the University of Maine's Sustainable Ecological Aquaculture Network (SEANET) project, the Experimental Program to Stimulate Competitive Research (EPSCoR) and National Science Foundation (NSF) for supporting this research (grant award number IIA-1355457). The Graduate Student Government and Geological Society of America provided funds to support the presentation of this work at regional and national conferences. I thank Professor C. Thomas Hess of the University of Maine Physics Department and his student, John Cummings, for analysis of radionuclides in sediment core samples.

I offer my heartfelt thanks to Professor Joe Kelley, my advisor, for his patience, guidance and sense of humor throughout this project. I thank Professor Dan Belknap for his thorough approach and willingness to help in the field, lab and writing process. Thank you to Professor Larry Mayer for his enthusiasm for and interest in this project, as well as insights into lead-210 and cesium-137 activity in the marine environment. I am also indebted to Professor Steve Norton for his help and patience deciphering radionuclide analysis results, and his willingness to share his expert knowledge of the subject with me. I want to thank the faculty, staff and graduate students of the School and Earth & Climate Sciences, the Darling Marine Center and SEANET for their support and assistance throughout my graduate career. In particular, I thank Dianne Perro for patiently answering all of my persistent questions.

Finally, I am grateful for the professors, students, family and friends who assisted me in the field, namely Dr. Joe Kelley, Dr. Dan Belknap, Dr. Larry Mayer, Carl Wilson, Robbie Downs, Eliza Kane, Ellen Park, Robin Arnold, Katie Coupland, Sam Hodge,

Catie Mitchell, Peter Chandler, Elsa Chandler, and Margo, Ross and Jackson Wade. This work would not have been possible without your help.

## TABLE OF CONTENTS

|  |    |
|--|----|
| ACKNOWLEDGEMENTS .....                       | iv |
| LIST OF TABLES .....                         | ix |
| LIST OF FIGURES .....                        | x  |
| CHAPTER 1: INTRODUCTION .....                | 1  |
| 1.1 Damariscotta River .....                 | 2  |
| 1.2 Estuaries .....                          | 3  |
| 1.3 Present Study .....                      | 6  |
| CHAPTER 2: BACKGROUND .....                  | 8  |
| 2.1 Geologic Settling .....                  | 8  |
| 2.2 Deglaciation and Sea Level History ..... | 9  |
| 2.3 Estuarine Stratigraphy .....             | 12 |
| 2.4 An Estuarine Model .....                 | 15 |
| 2.5 Sediment Distribution .....              | 17 |
| 2.6 Significance of Oysters .....            | 17 |
| 2.7 Previous Work .....                      | 18 |
| 2.7.1 Damariscotta River .....               | 18 |
| 2.7.2 Sedimentation Rates .....              | 21 |



|   |        |
|---|--------|
| CHAPTER 3: METHODS.....                     | 23     |
| 3.1 Approach.....                           | 23     |
| 3.2 Sediment Characterization.....          | 23     |
| 3.2.1 Geophysical Survey .....              | 23     |
| 3.2.2 Sediment Characterization Survey..... | 28     |
| 3.3 Sediment Accumulation Patterns.....     | 30     |
| 3.4 Sediment Thickness .....                | 31     |
| <br>CHAPTER 4: RESULTS.....                 | <br>33 |
| 4.1 Geophysical Survey .....                | 33     |
| 4.1.1 Bathymetry.....                       | 33     |
| 4.1.2 Estuarine Volume.....                 | 37     |
| 4.2 Sediment Characterization.....          | 38     |
| 4.2.1. Grab Sample Analysis.....            | 38     |
| 4.2.2. Backscatter Intensity.....           | 39     |
| 4.3 Submerged Landforms.....                | 39     |
| 4.3.1 River Thalweg.....                    | 39     |
| 4.3.2 Subtidal Drainage Networks .....      | 41     |
| 4.3.3 Current Lineations .....              | 41     |
| 4.3.4 Relict and Modern Oyster Beds.....    | 43     |
| 4.3.5 Recessional Moraines .....            | 45     |
| 4.4 Sediment Accumulation Patterns.....     | 46     |
| 4.4.1 Sediment Cores .....                  | 46     |

|  |    |
|--|----|
| 4.4.2 Radionuclide Analysis .....                              | 51 |
| CHAPTER 5: DISCUSSION.....                                     | 54 |
| 5.1 Sediment Accumulation Patterns.....                        | 54 |
| 5.1.1 Age Models and Sediment Accumulation Rates .....         | 56 |
| 5.1.2 Sediment Mixing and Maximum Sedimentation Estimates..... | 61 |
| 5.2 Estuarine Framework .....                                  | 63 |
| 5.3 Estuarine models.....                                      | 70 |
| CHAPTER 6: CONCLUSION .....                                    | 77 |
| REFERENCES CITED.....  | 78 |
| APPENDIX A: SECONDARY ANALYSIS OF CORE DR-PC-15-07 .....       | 85 |
| APPENDIX B: SEDIMENT CORE PHOTOS AND LOGS .....                | 86 |
| APPENDIX C: SEDIMENT GRAB SAMPLE SITES AND ANALYSIS.....       | 88 |
| APPENDIX D: SEDIMENT CORE ANALYSIS .....                       | 90 |
| BIOGRAPHY OF AUTHOR .....                                      | 93 |

## LIST OF TABLES

|   |    |
|---|----|
| Table 4.1: Piston core sites, locations and core lengths.....                   | 47 |
| Table 4.2: Piston core sediment samples utilized in radionuclide analysis. .... | 47 |
| Table 5.1: Sedimentation rates and ages determined from CRS model. ....         | 57 |
| Table 5.2: Estimated sediment accumulation rates.....                           | 62 |
| Table 5.3: Regional comparison of sediment accumulation rates. ....             | 63 |
| Table C.1: Sediment grab sample sites.....                                      | 88 |
| Table C.2: Grain Size Analysis Results.....                                     | 89 |
| Table D.1: Summary of sediment core analysis. ....                              | 90 |

## LIST OF FIGURES

|   |    |
|---|----|
| Figure 1.1: Compartmentalization of the Maine coast.....  | 3  |
| Figure 1.2: The relative energy distribution in an idealized estuary.....   | 4  |
| Figure 2.1: Maine's inner marine limit.....   | 10 |
| Figure 2.2: Maine's local relative sea-level curve.....   | 11 |
| Figure 2.3: Schematic cross-section of the Damariscotta River .....   | 12 |
| Figure 2.4: Cross sections of the Damariscotta River.....   | 14 |
| Figure 2.5: Schematic of idealized Indented Shoreline estuary.....  | 16 |
| Figure 2.6: Map of bottom sediments in the middle and lower estuarine zones of the<br>Damariscotta River estuary..... | 19 |
| Figure 3.1: Extent of MBES coverage in the Damariscotta River Estuary .....   | 25 |
| Figure 3.2: Research vessel R/V Mud Queen and equipment .....   | 27 |
| Figure 3.3: Sediment grab sample sites in the estuary.....  | 29 |
| Figure 3.4: Piston Corer used to collect cores .....  | 31 |
| Figure 3.5: Sites at which piston cores were collected in the Damariscotta River .....                                | 32 |
| Figure 4.1: Maps generated with MBES.....   | 34 |
| Figure 4.2: Location map indicating places referenced in text.....  | 35 |
| Figure 4.3: Location map indicating the location of figures included in this text .....                               | 36 |
| Figure 4.4: Hypsometry of the Damariscotta River estuary .....  | 37 |
| Figure 4.5: Backscatter intensity vs. sand and gravel content .....   | 38 |
| Figure 4.6: MBES data in Days Basin.....  | 40 |
| Figure 4.7. Current-oriented striations present on the seafloor .....   | 42 |
| Figure 4.8: Vertical relief and backscatter intensity of current lineations. ....                                     | 42 |

|  |    |
|--|----|
| Figure 4.9: Dodge Cove relict and Hog Island modern oyster beds .....                                      | 44 |
| Figure 4.10: Recessional moraines in the Damariscotta River estuary .....                                  | 46 |
| Figure 4.11: DR-PC-15-04 sediment core log from Lowe's Cove. ....  | 48 |
| Figure 4.12: DR-PC-15-08 sediment core log from the shoal south of Hog Island. ....                        | 50 |
| Figure 4.13: Specific activity of $^{210}\text{Pb}$ in sediment cores from the southern estuary .....      | 52 |
| Figure 4.14: Specific activity of $^{210}\text{Pb}$ in sediment cores from the northern estuary.....       | 52 |
| Figure 4.15: Specific activity of $^{137}\text{Cs}$ in sediment cores from the southern estuary .....      | 53 |
| Figure 4.16: Specific activity of $^{137}\text{Cs}$ in sediment cores from the northern estuary.....       | 53 |
| Figure 5.1: Sedimentation rates determined from CRS age-depth model .....                                  | 58 |
| Figure 5.2: Core locations in the context of MBES data .....   | 60 |
| Figure 5.3: Excess $^{210}\text{Pb}$ activities vs. core depth.....  | 61 |
| Figure 5.4: Selected seismic reflection profile cross-sections in the southern<br>Damariscotta River ..... | 65 |
| Figure 5.5: Selected seismic reflection profile cross-sections in the northern<br>Damariscotta River. .... | 65 |
| Figure 5.6: Total sediment thickness in the Damariscotta River estuary. ....                               | 66 |
| Figure 5.7: A schematic rendering of the Damariscotta River estuary.....                                   | 74 |
| Figure A.1. Secondary analysis of DR-PC-15-07.....   | 85 |
| Figure B.1. DR-PC-15-02 sediment core log from Long Cove.....  | 86 |
| Figure B.2: DR-PC-15-07 sediment core log from Upper Dodge Cove.....                                       | 87 |

# **CHAPTER 1**

## **INTRODUCTION**

Estuaries are ubiquitous coastal environments that link fresh and marine water systems. Recognized as effective sediment traps (Dalrymple et al., 1992), estuaries also are biologically productive coastal regions (Roman et al., 2000) that can be ideal environments for aquaculture industries. Many economically important ports and cities are located in and around estuaries. With climate change and associated sea-level rise, as well as increasing human population and coastal development (Roman et al., 2000), estuaries face increasing pressure from multiple sources. Increasing coastal populations contribute to shoreline development and nutrient loading associated with wastewater, fertilizers and runoff. These affect the stability and water quality of estuarine systems, and the effects of climate change compound the impact of coastal development. Rising sea level and increased storm events pose greater threats to the population in areas that are densely populated and of economic importance.

The rockbound coast of Maine is home to a number of estuaries that vary greatly in terms of development. This study is focused on the Damariscotta River estuary (Figure 1.1), which supports a year-round local population and a tourism industry in the summer months, as well as 70% the state's oyster aquaculture industry. It is an elongate, bending estuary with multiple bedrock sills that divide the embayment into several discrete basins. The Damariscotta River estuary provides an excellent opportunity to study Maine estuaries in the context of the Holocene sea-level transgression and modern sea-level rise, as well as the chance to consider geomorphology and substrates as constraints on the modern shellfish aquaculture industry in Maine.

## 1.1 Damariscotta River

The Damariscotta River is a tidally dominated estuary on the coast of Maine. With minimal freshwater input from upstream Damariscotta Lake, the system is a river only by name and more properly termed an estuary. The north-south orientation of the estuary is characteristic of the indented shoreline in this region of the coast and is a consequence of the bedrock structural framework that comprises high-grade metasedimentary rocks of Paleozoic ages (Figure 1.1, Kelley, 1987; Belknap et al., 1987). The Damariscotta River presents an opportunity to study the evolution of estuarine systems in this region in the context of late Quaternary and Holocene sea-level changes. Located between the inland marine limit, associated with high-stand sea level and the retreat of the Laurentide ice sheet, and the low-stand sea level, associated with isostatic rebound of the continental crust, this system was extensively reworked in subaerial and subaqueous environments associated with sea-level fluctuations in the late Pleistocene and Holocene (Belknap et al., 1987, 1994; Shipp, 1989).

With little freshwater input ( $1-3 \text{ m}^3/\text{s}$ ) into the estuarine system (McAlice, 1974), the Damariscotta River receives little new sediment from upstream sources; thus modern sedimentation relies on the reworking of material within the system or perhaps the import of new material from offshore sources. The tidal range of the system is 3.1 m in the outer river and 3.3 m in the upper river (McAlice, 1977). The magnitude of the tidal prism,  $5.6 \times 10^6 \text{ m}^3$  (McAlice, 1977), relative to the comparatively low freshwater input indicates the role of tidal processes in the reworking of sediment within the system. Tidal reworking, particularly evident in modern ravinement unconformities (Belknap et al., 1994), continues to erode sediment from the thalweg of the estuary, but where that

sediment is re-deposited is not known. It may be exported from the estuarine system by tidal currents and deposited offshore or transported farther upstream and deposited on tidal flats and salt marshes (Belknap et al., 1986).

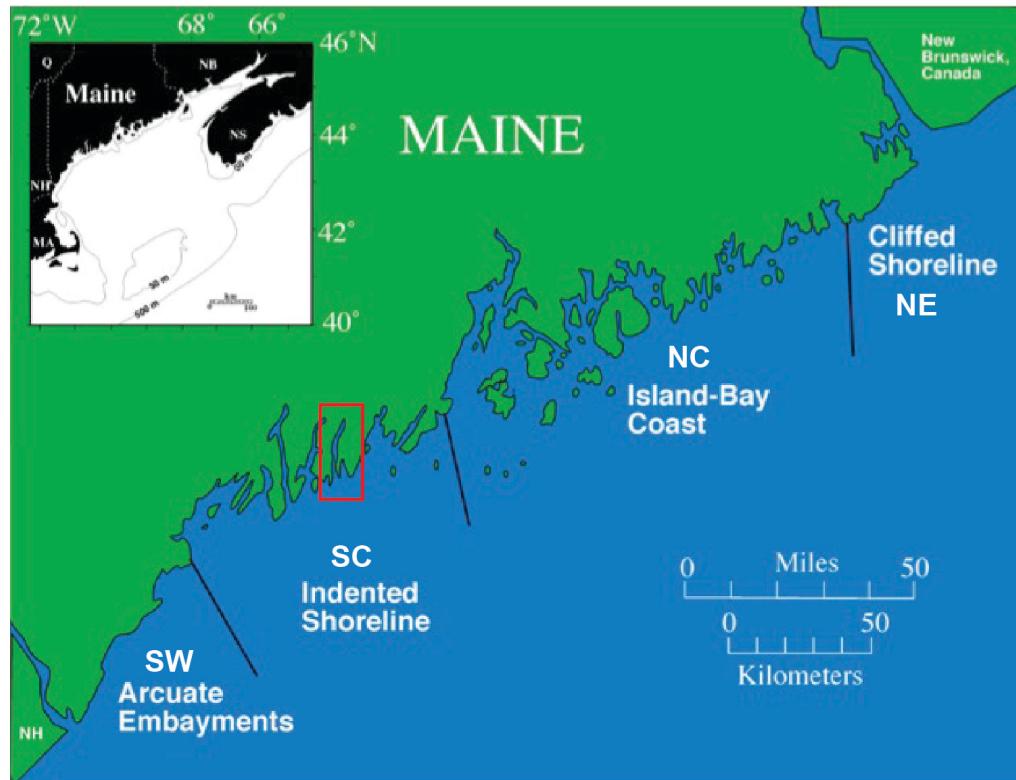


Figure 1.1: Compartmentalization of the Maine coast. The Damariscotta River is located in the south central (SC) compartment and delineated by a red rectangle (after Kelley, 1987).

## 1.2 Estuaries

Estuaries are areas of transition; from fresh to ocean water composition, from fluvial to marine processes, from terrestrial and freshwater to marine biota. The range of transitions found within these environments is broad and can be examined from biological, chemical, physical and geological perspectives. Regarded as transgressive valleys that have been flooded by the ocean, most estuaries exist in river mouths that are low in sediment and therefore without active deltas (Dalrymple et al., 1992, Belknap et



al., 1986, 1994). Pritchard (1967), however, defined estuaries based only on salinity, as the region in which the salinity of the water is greater than 0‰ and less than 30-35‰. Such a definition, based purely on salinity, is broad in scope and encompasses environments such as lagoons and delta distributaries, which are considered by some to be distinct from estuaries (Dalrymple et al., 1992). In an effort to limit the scope of estuarine definitions, Dalrymple et al. (1992) incorporated geologic setting and hydrodynamic processes into a new definition. Farther from the mouth of an estuary, the effect of marine processes (e.g. tides and waves) is reduced whereas the effect of fluvial processes increases (Figure 1.2). This depiction illustrates relative energetics within an estuary and must be scaled appropriately to relate to individual systems.

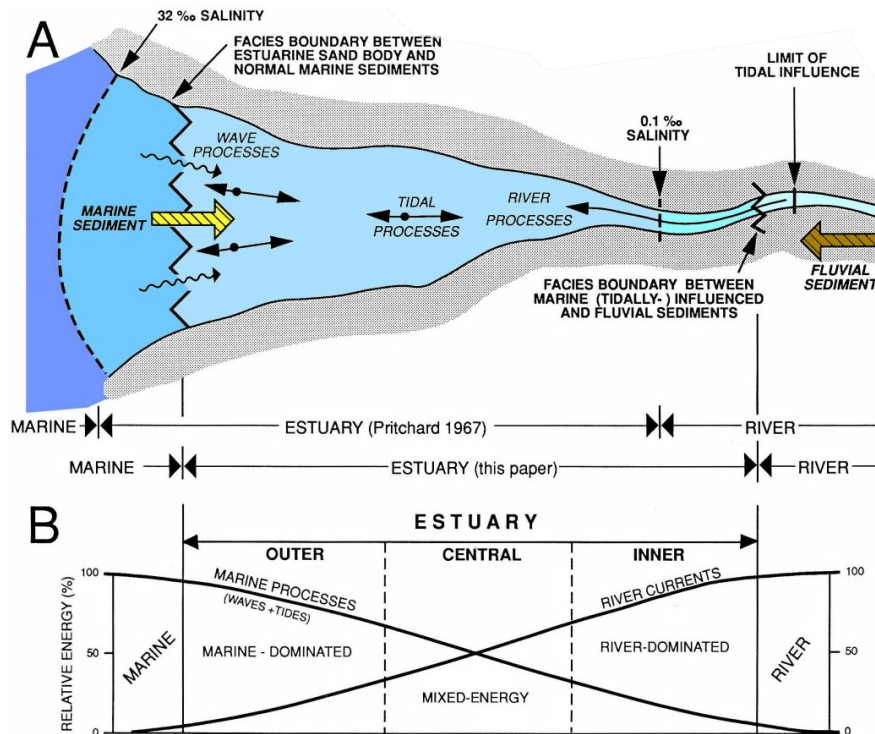


Figure 1.2: The relative energy distribution in an idealized estuary. A) Estuary schematic and B) relative energy levels of energy in the estuary. The estuary gradually transitions from a marine-dominated to fluvial-dominated environment from Dalrymple et al. (1992).

Estuaries are regarded as sediment sinks because of their balanced fluvial and marine processes. Rivers with stronger fluvial velocities and higher sediment loads can overwhelm marine processes and construct a delta (e.g., the Mississippi River). On the other hand, those with insufficient fluvial discharge and sediment loads and/or relatively large embayments with great accommodation space, terminate in estuaries. The physical marine processes affecting estuaries are waves and tides, and these forces play a critical role in the geomorphologic development of estuaries (Dalrymple et al., 1992). Dalrymple et al. (1992) consider wave-dominated and tide-dominated estuaries idealized end-members, while virtually all estuarine systems experience a degree of both. The role of the antecedent bedrock topography and framework is not considered in their discussion. Other factors influencing estuaries, including evaporation versus precipitation and runoff, wind, and biological and ecological systems that relate to latitude and other climatic variables, are not considered here.

Roman et al. (2000) specifically describe different habitats found in estuaries in the northeastern United States, distinguishing them from habitats in the Coastal Plain and identifying the bedrock framework as the primary “signature” (control) of northeastern estuarine shoreline configuration and therefore estuarine geometry. Roman et al. (2000) consider estuaries from a much more biological perspective than Dalrymple et al. (1992); however, beyond acknowledging the overarching control of bedrock geometry, they do not expand on the role of bedrock in estuarine development or energetics. Habitats identified in northeastern estuaries include tidal marshes, seagrass beds, intertidal mudflats and rocky shorelines (Roman et al., 2000). These habitats are critical to different organisms and ecosystems found within this region and have changed in recent history in

association with land-use changes and the anthropogenic nutrient contributions (Roman et al., 2000). Modern estuaries continue to change with local, regional and global anthropogenic influences, from increased residential development and population growth as well as changing climate (Roman et al., 2000).

### 1.3 Present Study

This study utilizes multi-beam echosounder (MBES) bathymetry to generate high-resolution bathymetric and bottom backscatter intensity maps of the estuary, from near the head of the estuary (the Newcastle-Damariscotta Bridge) to navigation aid buoy “10” at the Fort Island Narrows. The Fort Island Narrows mark the outer extent of estuarine salinities (McAlicie, 1977). Building on the well-understood stratigraphy and evolution of the estuarine system, I assess spatial and temporal patterns in sediment accumulation and distribution within the estuary, using sediment cores in conjunction with multi-beam bathymetry data and bottom grab samples. Of particular interest are sediment accumulation rates in the upper and middle estuary, as variations in such rates may relate to anthropogenic and other disturbances to the estuarine system. Such disturbances may include land-use changes associated with colonization, economic development and environmental alteration (Brush et al., 1982; Cooper and Brush, 1991; Cronon, 1983; Köster et al., 1997; Lu and Matsumoto, 2005; Meade, 1982; Wolman, 1967). It is also possible that the recent introduction of aquaculture into the estuary, particularly of bottom-seeded growing techniques, which utilize trawling to harvest oysters, may have some effect on sedimentation in the estuary.

As a tidally dominated estuary, it is not known whether the Damariscotta estuary primarily reworks material from the outer and middle zones of the estuary to be deposited in the upper zone or if sediment is gradually stripped from the system and exported offshore at the mouth of the estuary. In addition to considering sediment accumulation rates in the context of disturbances to the estuarine system, the present study seeks to identify whether the system is a net source or sink of sediment in the south-central region of the Maine coast. The extent of upstream reworking of sediment is controlled by accommodation space in shallow waters. The lack of sediment in the outer estuary (Shipp, 1989; Belknap et al., 1994) suggests that sediment may be simultaneously reworked upstream and exported from the outer and middle zones of the estuary, and reducing the volume of sediment in the middle zone of the estuary (Figure 2.5).

## **CHAPTER 2**

### **BACKGROUND**

#### **2.1 Geologic Settling**

Although popularly considered a “rockbound coast”, only 20% of more than 1,200 km of nearby Casco Bay shoreline were mapped as exposed bedrock on the shoreline. Still, bedrock remains the skeleton of the coast. The shoreline of Maine is classified into four distinct compartments based on the antecedent bedrock geology (Kelley, 1987), with the Damariscotta River located in the south-central compartment. The rockbound coast is comprised of metamorphosed and deformed Paleozoic sedimentary and volcanic rock (Osberg et al., 1985). The south-central compartment of the coast is composed of high-grade amphibolite metasedimentary rocks of Cambrian to Ordovician age (Osberg et al., 1985). The northeasterly strike creates the elongate, north/northeast-south/southwest oriented peninsulas and estuaries that characterize this compartment (Kelley, 1987). Bedrock constrictions throughout the river valleys serve as ledges or sills that punctuate estuaries into distinct basins (Shipp, 1989). Bedrock-controlled waterfalls separate the freshwater from the estuarine systems of some Maine estuaries (e.g., Saco River, Damariscotta River, Machias River), and reversing falls or rapids commonly occur at other rock sills (e.g., Sheepscot River). The narrow geometry of the Damariscotta Estuary restricts wave energy to the mouth of the estuary and results in well-protected, tidally dominated system, characterized by tidal flats and, to a much lesser degree, salt marshes (Kelley, 1987).

Estuarine sediments in this coastal compartment are generally underlain by the glaciomarine Presumpscot Formation and comprised of muddy tidal flats with fringing

salt marshes in the inner estuary (Kelley, 1987). The outer estuary is typically sediment-depleted as a result of tidal ravinement and some reworking by waves (Dalrymple et al., 1992; Belknap et al., 1994).

## **2.2 Deglaciation and Sea Level History**

At the last glacial maximum, the late-Pleistocene Laurentide ice sheet overrode New England, the Canadian Maritime provinces and extended seaward across the Gulf of Maine to George's and Brown's Banks (Schnitker et al., 2001). Ice retreated in contact with the ocean in the Gulf of Maine and in a sequential progression across a series of basins and troughs in the Gulf of Maine (Schnitker et al., 2001). Retreat continued inland and Gulf waters inundated the isostatically depressed mainland, reaching an inner marine limit of ~70-129 m above present sea level (Dorion et al., 2001; Borns et al., 2004) approximately 16 ka (Figure 2.1; Belknap et al., 1987; Barnhardt et al., 1997; Kelley et al., 2010, 2013). Submergence of the coastal zone coincided with the deposition of the glaciomarine Presumpscot Fm. over large parts of the coastal zone (Bloom, 1963; Stuiver and Borns, 1975; Thompson and Borns, 1985; Belknap et al., 1987; Barnhardt et al., 1997). Subsequent isostatic rebound resulted in rapid sea-level fall to a low stand of ~60 m below present by 12.5 ka in southwestern Maine (Kelley et al., 2013) during which period the Presumpscot Fm. was subaerially exposed and eroded (Bloom, 1963; Stuiver and Borns, 1975; Belknap et al., 1987; Barnhardt et al., 1997). A second, initially rapid transgression followed, as sea level rose to 25 m below present at 11.5 ka, at which point the rate of sea-level rise slowed to less than 5 m from 11.5-7.5 ka (Kelley et al., 2010, 2013). This period was characterized by the reworking of coastal and littoral sediments

(Thompson et al., 2011) and is marked in the stratigraphic record as a basal unconformity (Belknap and Shipp, 1991; Barnhardt et al., 1997, Belknap et al., 1994).

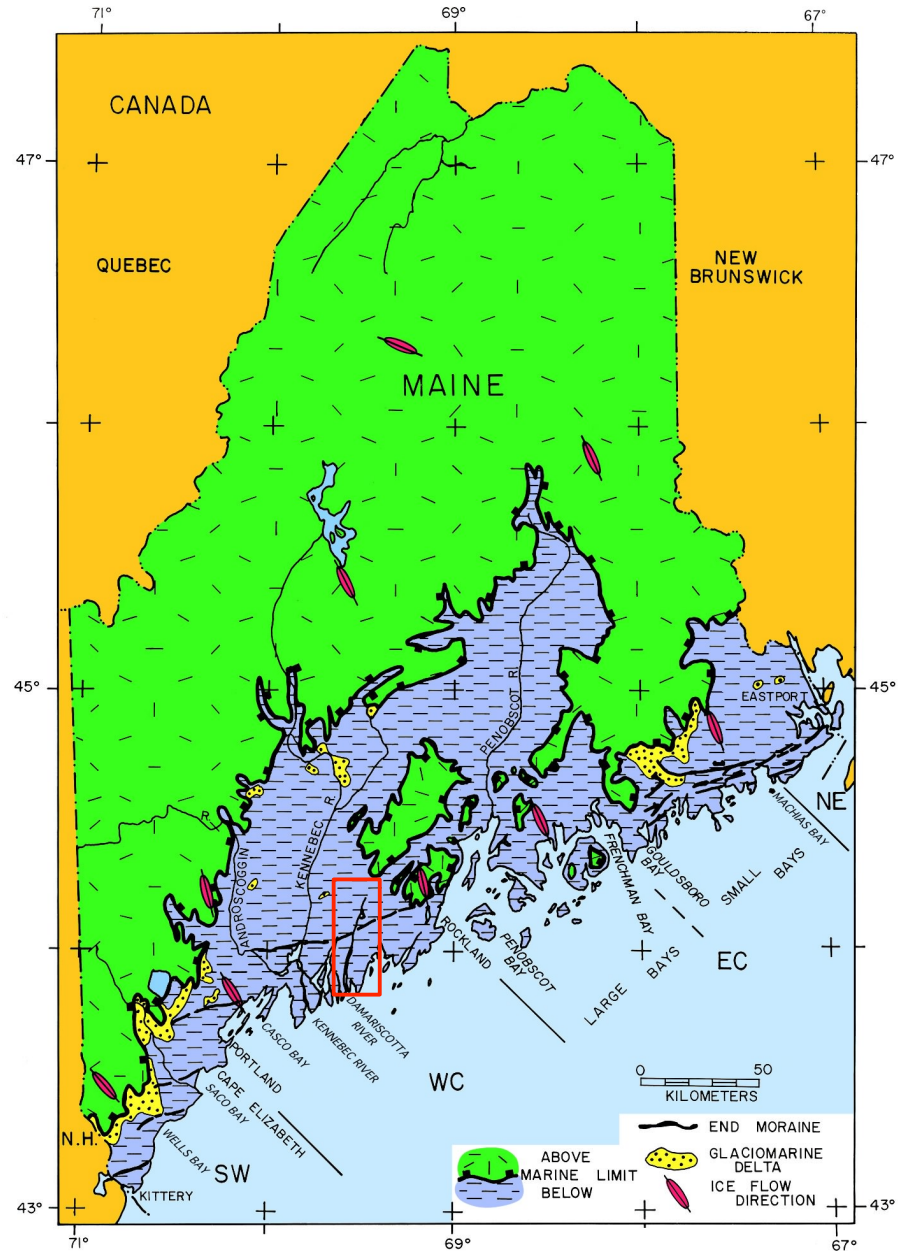


Figure 2.1: Maine's inner marine limit. The inland marine limit is delineated by thick black line with the location of Damariscotta River in red rectangle (after Belknap et al., 1987 and Thompson and Borns, 1985).

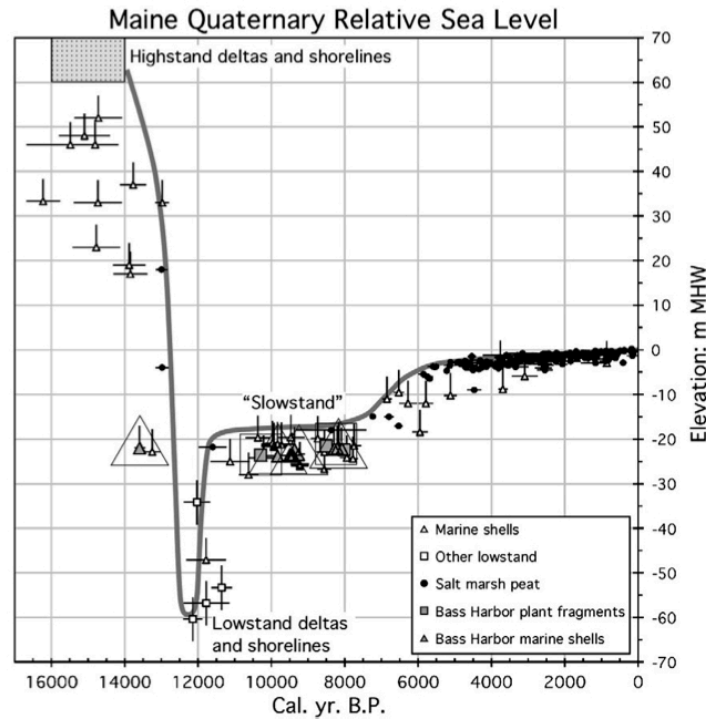


Figure 2.2: Maine's local relative sea-level curve. The solid line represents mean high water (from Kelley et al., 2010).

Located between the inner marine limit and the low-stand shoreline (Figure 2.1), the bedrock in the Damariscotta River valley was blanketed by the Presumpscot Fm. during glacial retreat (Shipp, 1989; Belknap et al., 1994). Till and washboard moraine deposits are extensive in the vicinity of the river and comprise bluffs along the modern shoreline (Thompson and Borns, 1985; Shipp, 1989). The ice sheet margin retreated to the Damariscotta River by 12.5 ka (Belknap and Shipp, 1986). As sea level fell from the high to low-stand limit, bedrock sills within the Damariscotta River valley sequentially isolated basins from the marine environment, creating lacustrine environments (Belknap and Shipp, 1986). Following the low-stand at 12.5 ka, rising sea level gradually overtopped the sills and the basins were reincorporated into the estuarine system (Figure 2.3; Shipp 1989; Belknap et al., 1994).



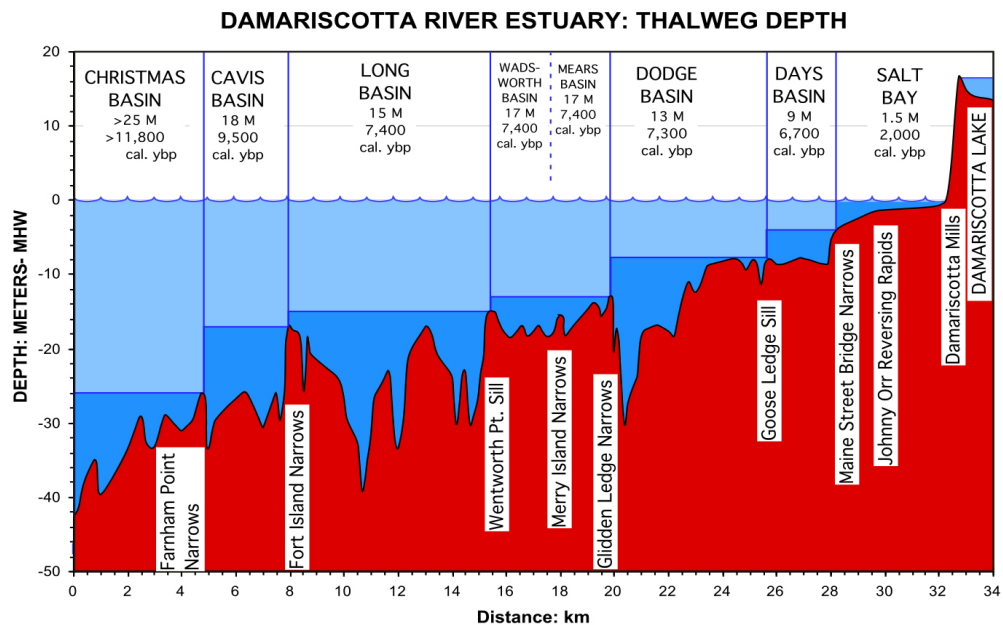


Figure 2.3: Schematic cross-section of the Damariscotta River. The cross-section illustrates discrete basins and dates correspond to approximately when bedrock sills were overtopped by rising sea level (after Shipp, 1989 and Belknap et al., 1994).

### 2.3 Estuarine Stratigraphy

Extensive seismic reflection profiles and many sediment vibracores have revealed the distinct estuarine zones and reconstruct sediment accumulation and transport trends within in the estuary (Figure 2.4; Shipp, 1989; Belknap et al., 1994). The innermost zone is dominated by the draped Presumpscot Fm., overlain by a basal unconformity associated with subaerial and littoral erosion at low-stand sea level that created a depression in the glaciomarine facies directly above the bedrock valley (Belknap et al., 1994). The inner estuary was isolated from the marine environment for the greatest period of time between the sea-level fall and second transgression; thus the formation of lakes in the innermost basins is likely (Belknap and Shipp, 1986). Damariscotta Lake, located just upstream from Great Salt Bay in the valley, remains isolated today at ~15 m

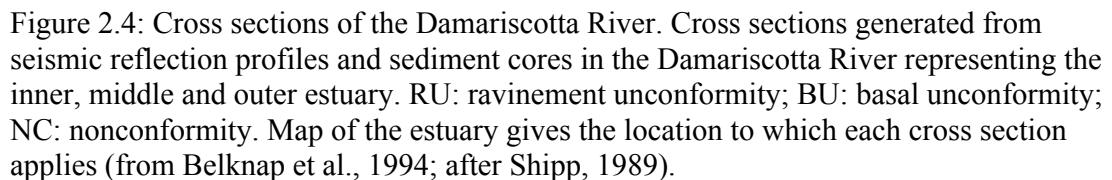
above present sea level and separated from the estuary by a waterfall. A washed-out seismic reflection signal in the upper estuary is interpreted as natural gas and, in the inner estuary, may result from the decay of organic material in estuarine sediments, or possibly transgressed lacustrine environments (Shipp, 1989; Hannum, 1997)). Glaciomarine facies are unconformably overlain by Holocene estuarine sediments, which contain extensive *Mya arenaria* and *Crassostrea virginica* shells (Belknap et al., 1994).

The middle estuary profile, associated with the more eroded estuarine zone, exhibits the same sequence found in the inner estuary, albeit further eroded (Figure 2.4). The glaciomarine facies are thinner, as is expected due to the longer time of reworking of sediments during the second sea-level transgression. Estuarine mud overlies the glaciomarine facies, with both *Mya arenaria* and *Crassostrea virginica* recovered in Holocene units of sediment cores (Belknap et al., 1994). Further erosion of the estuarine sediment is apparent particularly by a depression in middle of the cross section (Figure 2.4, middle cross section). This represents a ravinement unconformity, created by modern tidal processes and erosion.

Finally, the outermost zone of the estuary, known only through seismic profiles, is nearly stripped of sediments, with discrete packets of glaciomarine and estuarine sediments preserved only in isolated bedrock depressions (Belknap et al. 1994). Erosion associated with both the basal low-stand and modern ravinement unconformities is responsible for the lack of sediment in this zone, as sediment is either exported from estuarine system or recycled northward through the system.

While the stratigraphy throughout the estuarine system is similar, the degree of preservation is directly related to distribution of energy within the estuary through space

DAMARISCOTTA RIVER ESTUARY



## **2.4 An Estuarine Model**

An idealized estuarine model presented by Belknap et al., (1986) and Kelley (1987) is representative of the Damariscotta River (Figure 2.5). The estuary can be considered in three, generalized but distinct zones with varying energies and sedimentation trends. The innermost zone is stable and characterized by tidal flats, marshes and relatively rapid accumulation of sediment. Sediment sources consist primarily of reworked Holocene and Pleistocene deposits from within the estuary as well as erosion of bluffs that border middle zone (Belknap et al., 1986). With fewer marshes and more tidal and subtidal flats than the inner estuary, sediment accumulation in the middle zone is more episodic (Belknap et al., 1986; Kelley, 1987). This zone is generally more eroded than the inner zone as a result of sediment recycling in the transgressive environment (Belknap et al., 1986; Kelley, 1987). The outer zone is most exposed to the Gulf of Maine and as such, experiences the greatest wave influence. Wave and tidal energy, associated with the modern ravinement unconformity, has largely stripped the outer zone of sediment, and Pleistocene and Holocene sediments are only preserved below wave base (Belknap et al., 1986; 1994).

While this model applies in a longitudinal sense to the estuarine system, it also applies to the many coves and protected areas along the Damariscotta River. As the head of the estuary is a well-protected, low-energy zone of sediment accumulation, so too are innermost points in smaller protected coves in the middle and outer estuary, such as Lowes and Pleasant Coves (Shipp, 1989).

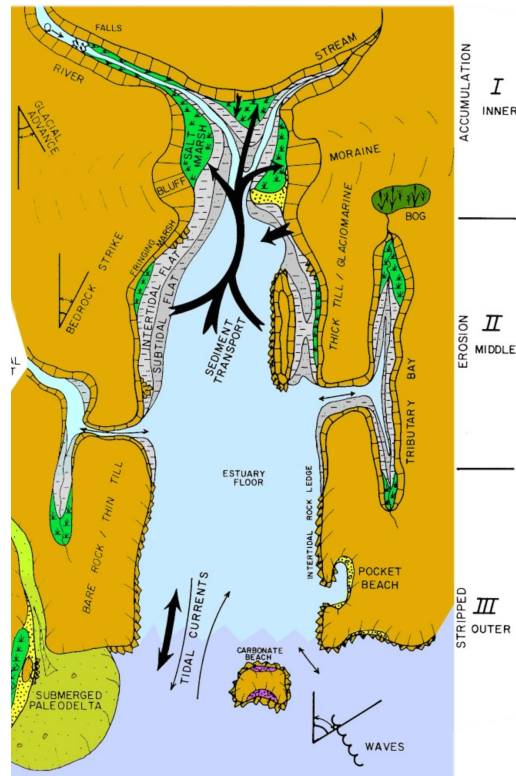


Figure 2.5: Schematic of idealized Indented Shoreline estuary. Schematic depicts the landward zone of sediment accumulation, the middle erosive zone and the seaward zone stripped of sedimentary material (from Belknap et al., 1986).

McAlicie (1977) established the baseline hydrographic conditions for the Damariscotta River system to serve as a reference point for future studies. The river, 29 km in length, has limited freshwater input from Damariscotta Lake at the head of the estuary (spring maximum of  $2.83 \text{ m}^3/\text{s}$ , McAlicie, 1977). The narrow geometry of the system restricts the influence of waves, resulting in a tidally dominated estuary. The elongate nature of the estuary also creates a tidal lag at the head of the estuary of  $\sim 20$  minutes behind East Boothbay at the mouth and results in sequential filling and draining of basins with each tidal cycle (McAlicie, 1977). The estuarine system is ebb-dominated and the tidal prism for the area north of Fort Island is approximately  $5.6 \times 10^6 \text{ m}^3$ . McAlicie (1977) approximated the summer flushing time of four to five weeks from

morphometric and tidal-range data. The southern extent of the estuarine environment is Fort Island, where salinity transitions to those that are representative of the open Gulf of Maine (McAlice, 1977).

## **2.5 Sediment Distribution**

In addition to compiling preliminary oceanographic data for the Damariscotta River system, McAlice (1977) conducted an early survey of bottom sediments using 50 grab samples, concluding that areas that are not comprised of bedrock consist of poorly to extremely poorly sorted clayey to sandy silts. Rocky lag deposits characterize the constrictions of bedrock sills that isolate individual basins, where tidal currents are sufficiently strong to remove finer sediments (McAlice, 1977). Using seismic reflection profiles, side-scan sonar lines, sediment cores as well as sediment grab sample data, Hannum (1997) built on the work of McAlice (1977) and Shipp (1989) and created a surficial sediment map based on side-scan sonar for the estuary from Perkins Point to Fort Island (Figure 1.7). Much of this middle to outer section of the estuary is characterized by mud, sand with mud, and generally lined by rock with gravel along the shorelines and at constriction points.

## **2.6 Significance of Oysters**

Although their recent reintroduction into the estuary is a result of aquaculture, oysters, *Crassostrea virginica*, are historically and ecologically significant in the history and evolution of the estuarine system. The presence of shell middens in several locations along the river provide minimum age constraints on rising sea level and suggest when

basins were overstepped (Sanger and Belknap, 1987). As oysters require a minimum salinity of 6 ppt, the appearance of middens in basins along the river and an oyster bioherm in Dodge Basin correspond with the reincorporation of isolated basins into the estuarine system (Leach, 2007; Leach and Belknap, 2007). The expansive Whaleback and Glidden Middens are indicative of the vast quantity of oysters that once inhabited the Damariscotta River and the significance of this species to the local indigenous population. Furthermore, the local extirpation of the oyster population may correspond to exploitation by local indigenous populations and/or increasing salinity within the estuarine system that enabled the inland migration of the oyster drill, a key oyster predator requiring salinities greater than 20 ppt (Sanger and Belknap, 1987).

## **2.7 Previous Work**

### **2.7.1 Damariscotta River**

Previous studies in the Damariscotta River have reconstructed the evolution of the estuarine system in the context of Holocene sea-level fluctuations. Extensive seismic reflection profiles and sediment cores form the basis for understanding the evolution of the estuarine system in the context of late Quaternary and Holocene sea-level changes (Shipp, 1989; Belknap et al., 1994). With sediment cores in the middle to upper estuary, the evolutionary model for the estuary is correlated with sea-level changes for the Maine coast region (Shipp, 1989; Belknap et al., 1994).

Side-scan sonar surveys in the middle estuary revealed that the dominant sediment types are silt and mud, with mud blanketing coves, inlets as well as many of the deep basins (Figure 2.6, Hannum, 1997). Deposits of muddy sand, and smaller deposits

of sandy gravel, are often found associated with bedrock outcrops and narrow constrictions within the river (Hannum, 1997). Gross sedimentation rates for the middle estuary, as measured by sediment traps, are roughly  $4 \text{ g/cm}^2\text{yr}^{-1}$  (Hannum, 1997).

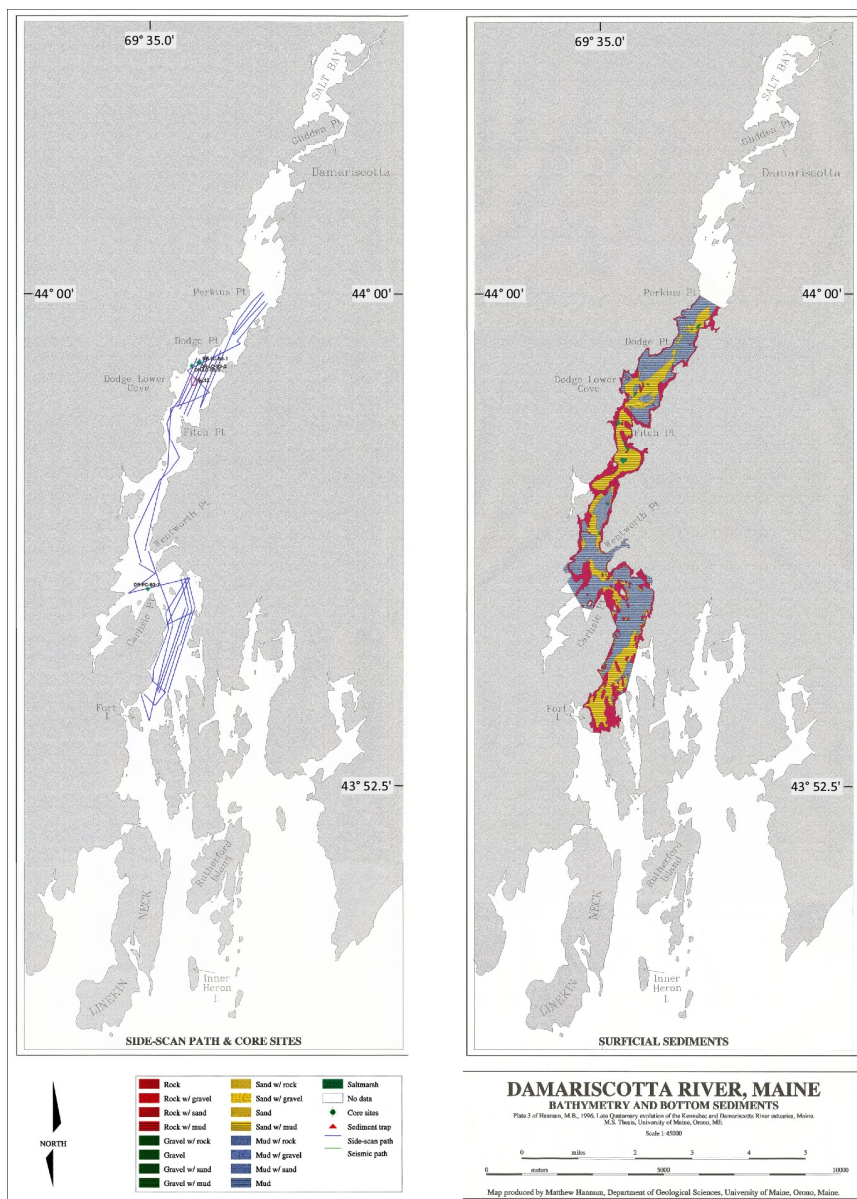


Figure 2.6: Map of bottom sediments in the middle and lower estuarine zones of the Damariscotta River estuary (from Hannum, 1997).



Tidal mudflats, abundant in the upper estuary and all adjacent coves, are generally considered depositional environments (Anderson et al., 1981). Precise leveling surveys utilized in Lowe's Cove, in upper Long Basin, measure both spatial and temporal changes in sediment to reveal that mudflats experience both erosion and deposition, at times simultaneously on different parts of the flat (Anderson et al., 1981).

Several archeological studies have focused extensively in Dodge Basin, looking for shell middens comprised of *Crassostrea virginica* (Davies, 1992; Leach, 2007). Utilizing seismic reflection profiles and sediment cores, Davies (1992) built on the work of Shipp (1989) in this region to identify natural oyster biomes preserved in Dodge Cove, though not shell middens. With detailed seismic reflection profiles, side-scan sonar and sediment cores, Leach (2007) confirmed the presence of natural oyster bioherms and developed a predictive model for identifying submerged shell middens.

Oyster bioherms are found in other large rivers in the Northeast, such as the Hudson River, where oysters flourished during the Holocene and were extirpated by cooler seawater temperatures around 4,000-5,000 years ago (Carbotte et al., 2014). Oysters later returned to the Hudson River valley but the population again disappeared with the onset of the Little Ice Age (Carbotte, et al., 2014). Relict oyster beds, that resist wave erosion, remain in the Hudson River today (Carbotte et al., 2014). Oyster bioherms are also present in many estuaries and bays along the mid- and southeastern United States, including the Piscataqua River (Grizzle et al., 2008), Chesapeake Bay (Bratton et al., 2002) and Mobile Bay (Ryan and Goodell, 1972).

### 2.7.2 Sedimentation Rates

Lead-210 is a naturally occurring isotope in the uranium-238 decay series. It is removed from the atmosphere by precipitation and dry fallout and is then scavenged by sediments and organic material in lakes and the marine environments (Appleby and Oldfield, 1983; Nittrouer et al., 1984).  $^{210}\text{Pb}$  geochronologies were effectively used to constrain sedimentation rates in lakes (Appleby and Oldfield, 1983) and estuarine environments, such as the Chesapeake Bay (Brush, et al., 1982, 1989; Colman and Bratton, 2003; Cronin et al., 2000), Narragansett Bay (Goldberg et al., 1977), San Francisco Bay (Nichols et al., 1986) and Merymeeting Bay (Köster et al., 2007). These studies have focused particularly in instances related to anthropogenic disturbance to and pollution of estuarine environments. This technique is most effective when combined with other proxies, such as pollen (Brush et al., 1982) and Cesium-137 (Köster et al., 2007; Lu and Matsumoto, 2005; Sugai et al., 1994). Nittrouer et al. (1979) also used lead-210 geochronology to successfully constrain sediment accumulation patterns on the Washington continental shelf.

While Lead-210 geochronology is a proven and effective tool for constraining sediment accumulation rates, it has limitations. It is ideal for areas with steady accumulation ( $>1$  mm/yr) of modern sediments that are not extensively mixed by physical or biological processes (Nittrouer, et al., 1979). Alternatively this tool is difficult or impossible to use in sediment cores with low accumulation rates ( $<1$  mm/yr), complex stratigraphies (such as grain-size fluctuations or interbedding or sand and mud), low initial activities or thick surface mixed layers (Nittrouer, 1979). In environments such as salt marshes, Cesium-137 can lend credibility to geochronologies derived from Lead-

$^{210}\text{Po}$  activities (Wilson et al., 2010). However, environments low in clay content, such as regions in nearby Merrymeeting Bay,  $^{137}\text{Cs}$  can diffuse upward and downward throughout sediments, which can limit its use when paired with  $^{210}\text{Pb}$  age models (Köster, et al., 2007; Anderson et al., 1987).

## **CHAPTER 3**

### **METHODS**

#### **3.1 Approach**

This thesis is part of an EPSCoR-funded project to understand the social ecological systems framework and environmental effects of aquaculture in Maine through the establishment of a sustainable ecological aquaculture network (SEANET). As such, this study provides detailed bathymetry and backscatter intensity data for the creation of coupled hydrodynamic and biogeochemical models (Coupland, 2016) and further SEANET applications. It also provides an opportunity to characterize the distribution of sediment and quantify spatial and temporal trends in sediment accumulation throughout the Damariscotta River estuary.

#### **3.2 Sediment Characterization**

##### **3.2.1 Geophysical Survey**

To understand the distribution of sediment as well as sedimentary composition found within the Damariscotta River estuary, the University of Maine Marine Geology research team conducted a detailed multibeam bathymetry and backscatter intensity survey in the summer of 2015. The survey area extends from the US Route 1 bridge in Damariscotta, the inner extent of navigable waters, to immediately south of Fort Island (Figure 3.1), where the river transitions from estuarine to fully marine conditions (McAlice, 1977). The total area surveyed is 13.7 km<sup>2</sup>.

Basins were generally surveyed discretely, with the outer, deeper basins surveyed before the inner, shallower basins. Coves and sub-intertidal transition mudflats were surveyed to the maximum extent possible. Limitations on the survey extent included tidal stage and near-shore navigation hazards. Whenever possible, near-shore areas were surveyed at high tide to maximize survey coverage.

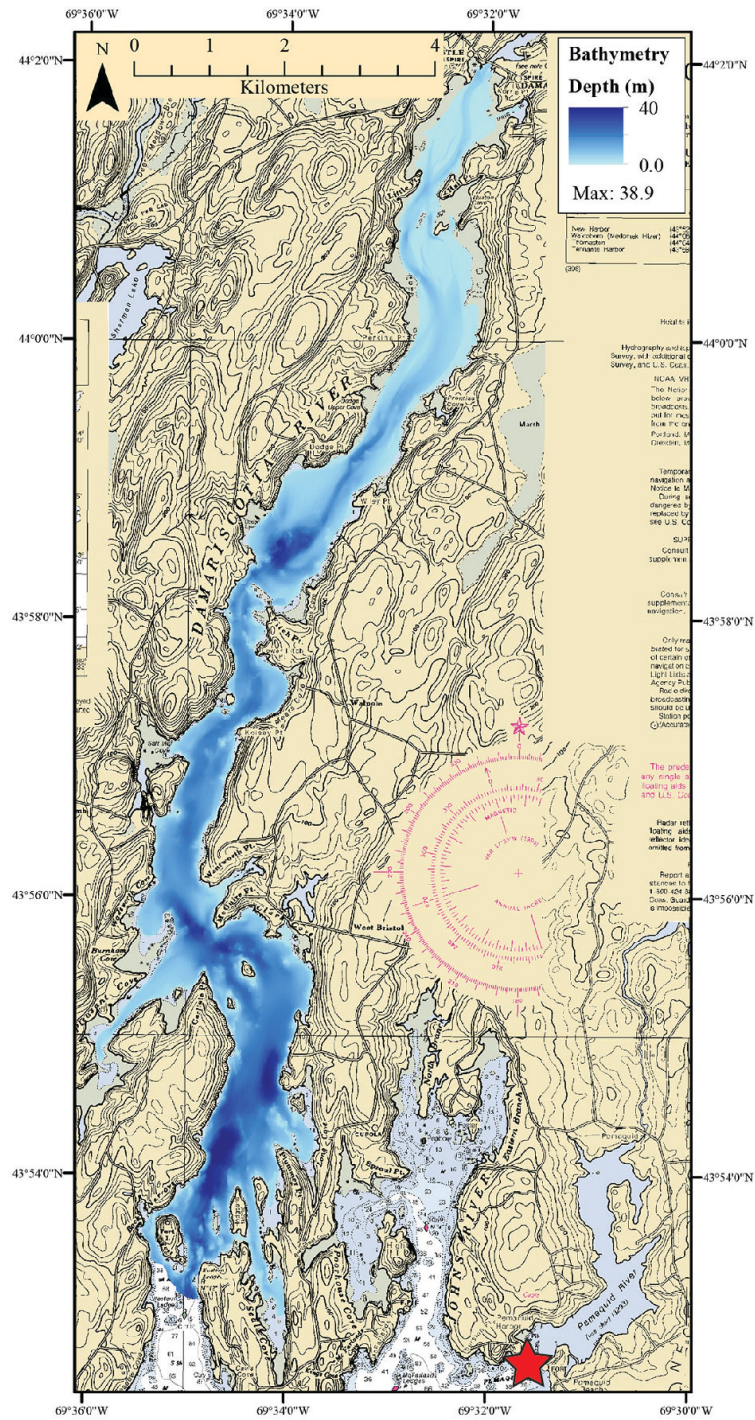


Figure 3.1: Extent of MBES coverage in the Damariscotta River Estuary. The red star indicates location of Pemaquid Harbor, the tide station from which bathymetry data is corrected for tide state.

Multibeam bathymetry and backscatter intensity data were collected using a coupled Olex/WASSP system mounted on an 18-foot Sweetwater Challenger pontoon boat (Figure 3.2). Additional technology included a Furuno GPS and Maretron digital compass. The survey was conducted over 27 days at a 0.23 m resolution and 9.3 m radius. Data were corrected for tidal state in real time using tide tables for Pemaquid Harbor and are referenced to mean low low-water (MLLW) and World Geodetic System (WGS) 1984. While the MBES system was corrected for the pitch and roll of the vessel, some artifacts remain present in the MBES datasets due to the effect of environmental conditions (i.e. wind and currents) on the research vessel. Bathymetry artifacts appear as vertical steps at the outer extent of the MBES swath. Occasional backscatter intensity artifacts appear as anomalously hard or soft returns in a swath relative to the surrounding data.

In processing the resolution was coarsened to 1.9 m to reduce file size. Data were then processed using multiple geographic information system (GIS) platforms (QGIS, Global Mapper and ArcGIS), with support from the University of Maine Advanced Computing Group and their high-performance visualization machines. Once inserted into a GIS, it is possible to examine bathymetry and backscatter intensity data in the context of previous geophysical studies, utilizing seismic reflection observations and side-scan sonar surveys (Shipp, 1989; Hannum, 1997; Davies, 1992; Leach, 2007).





Figure 3.2: Research vessel *R/V Mud Queen* and equipment. A) *R/V Mud Queen*, with WASSP transducer and Furuno GPS mast mounted forward of the steering console, B) Equipment locker with Olex/WASSP computer displays, power supplies and power inverters.



### 3.2.2 Sediment Characterization Survey

To better understand and ground truth the backscatter intensity data in terms of sediment composition, 22 grab samples were collected with a Ponar-style grab sampler throughout the estuary on August 27, 2015 (Figure 3.3) with the Maine Coastal Program's Maine Coast Mapping Initiative team aboard the *R/V Amy Gale*. The samples were analyzed for bulk gravel, sand, silt and clay content using procedures described by Folk (1980) as well as water content (90 °C for at least four hours) and mass lost on ignition (LOI). LOI samples were heated to 550° C for not less than three hours and allowed to cool in a desiccating jar. Grab sample composition was then compared against backscatter intensity data for the same sites.

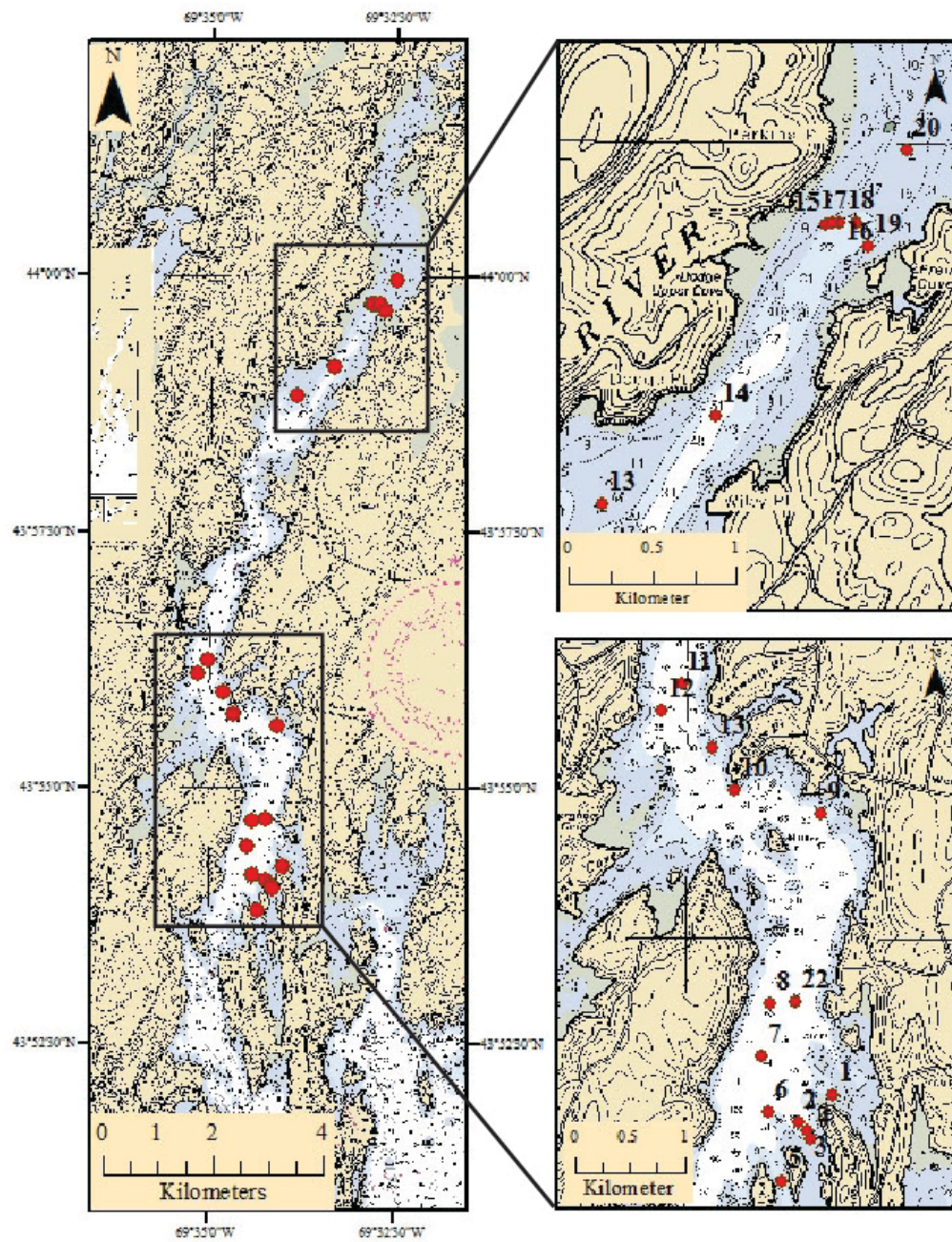


Figure 3.3: Sediment grab sample sites in the estuary. A) locations throughout the estuary, B) northern sample sites between Dodge Cove and Perkins Point and C) southern sample sites between Seal Cove and Salt Marsh Cove.

### 3.3 Sediment Accumulation Patterns

A series of eight short piston cores (7.62 cm diameter aluminum core barrels, ranging in length from 0.83 m to 1.73 m) were collected on August 17, 2015 (Figure 2.4). Core sites were selected using backscatter intensity data to identify areas where values were lowest, indicating softer, muddier substrate (Figure 2.5). Four cores, selected for wide spatial distribution and overall core length, were used to determine sediment accumulation rates throughout the estuary (Figure 2.5). Each of these cores was opened, photographed and logged. The top ~16-30 cm of each core was sub-sampled at 1 cm intervals for gamma-spectroscopy analysis in horizontal, high-purity germanium, well detectors (HPGe) capable of directly measuring trace concentrations of Lead-210 and Cesium-137. The germanium detector uses a low noise lead shield that allows for the accurate retrieval of the relatively low energy gamma ray that  $^{210}\text{Pb}$  emits (46.5 keV) and the comparatively higher energy gamma ray that  $^{137}\text{Cs}$  emits (661.5 keV) (Cahl, 2012). For each sample, after HPGe analysis, organic content was determined using LOI (samples were heated to 550° C for not less than three hours and allowed to cool in a desiccating jar). Carbonate content was determined for core DR-PC-15-02 (because of shelly layers present, Figure B.1) by measuring weight loss after rinsing each sample with hydrochloric acid to dissolve carbonate materials (Molnia, 1974). Using  $^{210}\text{Pb}$  and  $^{137}\text{Cs}$  activity profiles, as well as organic and carbonate content for each sub-sample, age-depth models were developed for each core. Age models were then used to determine sediment accumulation rates in the surface sediments at core sites.

### 3.4 Sediment Thickness

Extensive seismic reflection profiles and sediment cores collected by Shipp (1989) resulted in an isopach map of the estuary. Using ArcGIS, the map was geo-referenced to satellite imagery (Maine GIS, 2009) and digitized. Once digital, the area was calculated and volume estimated for each isobath.



Figure 3.4: Piston Corer used to collect cores. Cores were collected aboard aboard the *R/V Ira C* (photo: Belknap, D.F. 2015).



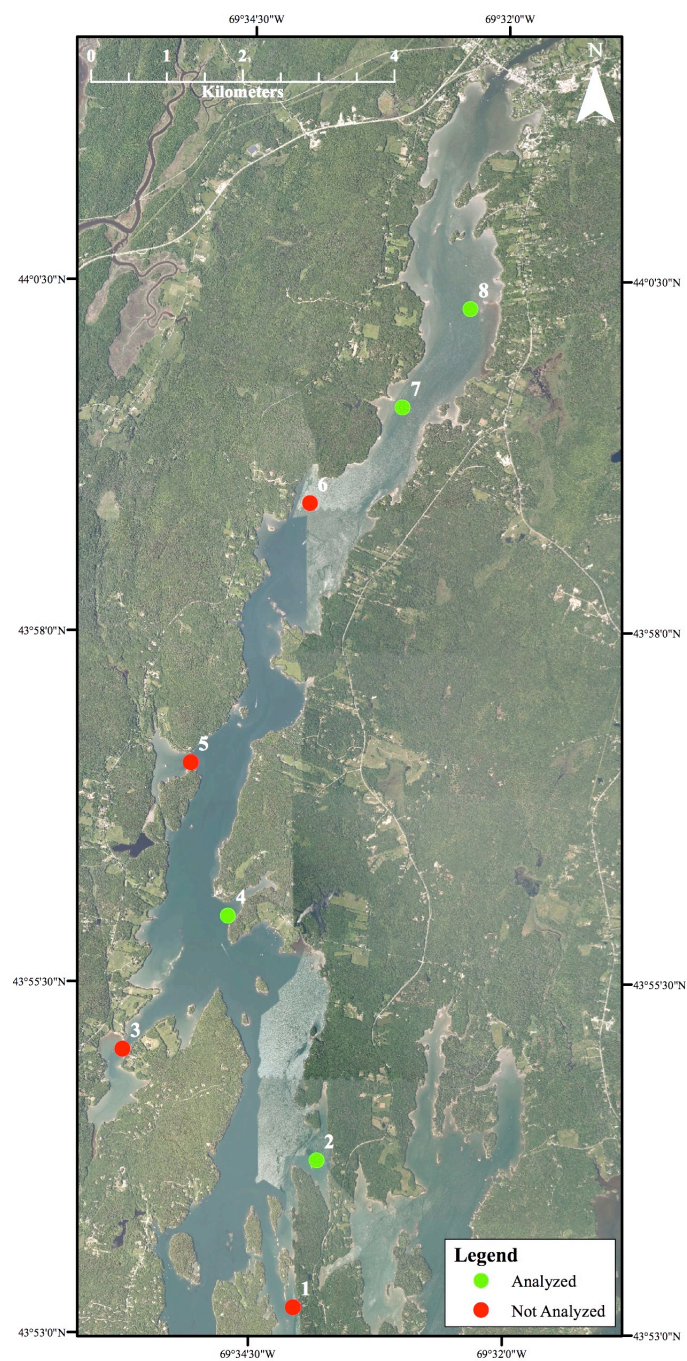


Figure 3.5: Sites at which piston cores were collected in the Damariscotta River. Green circles indicate cores that were analyzed for  $^{210}\text{Pb}$  and  $^{137}\text{Cs}$ , whereas red circles represent those that were not.

## CHAPTER 4

### RESULTS

#### 4.1 Geophysical Survey

##### 4.1.1 Bathymetry

In June and July of 2015, I conducted a multibeam echosounder survey (MBES), covering 14.1 km<sup>2</sup> of the Damariscotta River (Figure 4.1). Location maps (Figures 4.2 and 4.3) indicate the geographic location of figures and points, coves, bays and basins referenced. Pronounced depressions are present in Long Basin (between Fort Island Narrows and Wentworth Point, maximum depth 38.9 m), in Wadsworth Basin (between Wentworth Point and Merry Island Narrows, maximum depth ~28 m) and in Dodge Basin (from Glidden Ledge to Goose Ledge, maximum depth ~39 m). In the middle of the estuary, the area between Fort Island and Dodge Point, the basin and sill morphology dominates the system and the rough bathymetry suggests the sills are exposed or blanketed by sand and/or gravel deposits.

North of Dodge Point, the bedrock constrictions identified by Shipp (1989) do not appear as prominently (Figure 4.1). In this region the bathymetry is smooth with a pronounced scoured thalweg. In the upper estuary the role of bedrock in the system's morphology is reduced and limited to discrete outcrops along the edges of the channel (e.g. immediately north of Perkins Point and Goose Ledges, Figure 4.1). Scoured channels mark the thalweg of the river and are indicative of tidal ravinement in the estuary. Areas neighboring the channel and subtidal flats appear smooth and noticeably shallower than the thalweg.



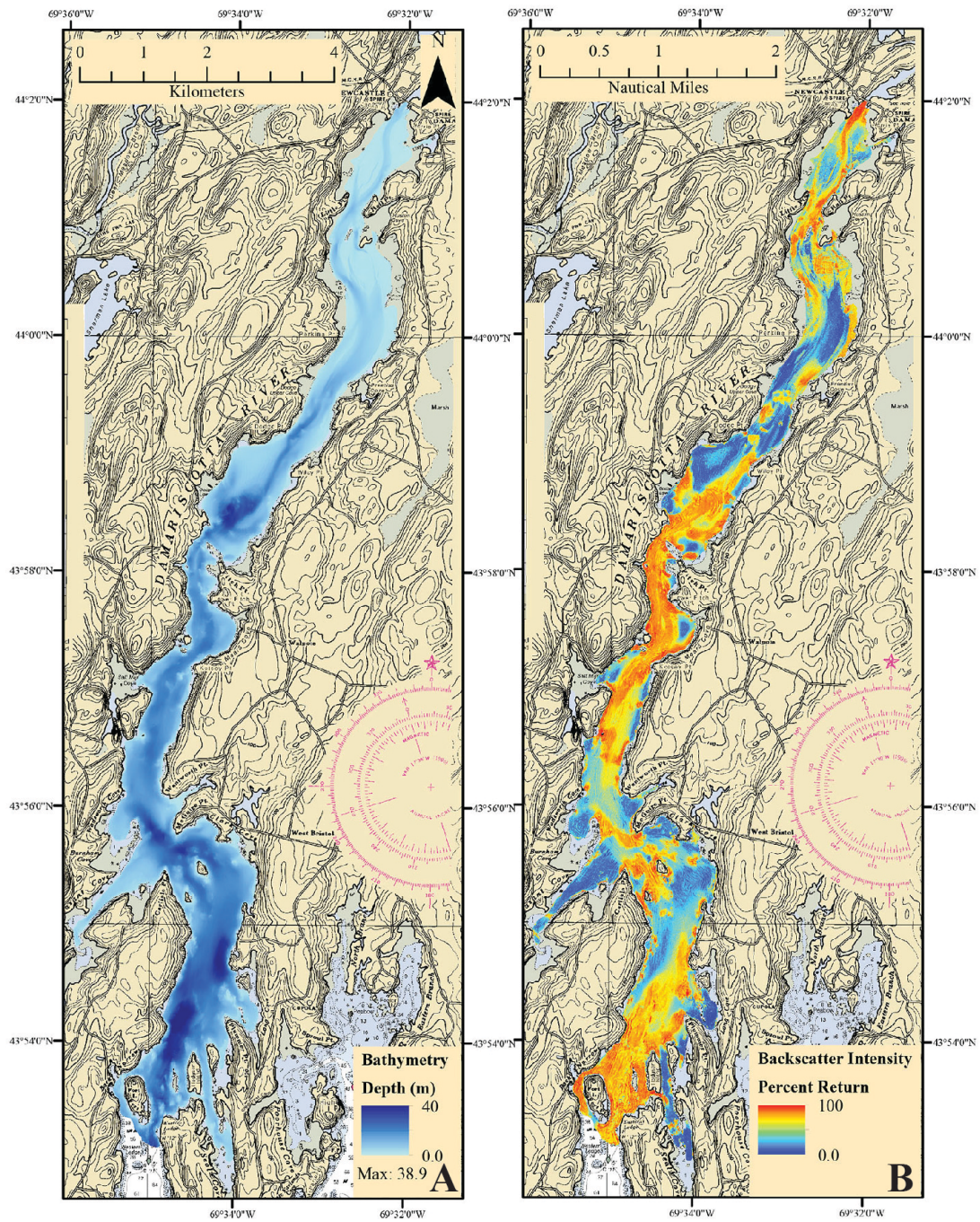


Figure 4.1: Maps generated with MBES. A) Bathymetry and B) backscatter intensity results for the Damariscotta River. Unmapped areas at the edges of the data are intertidal or shallow rocky areas.

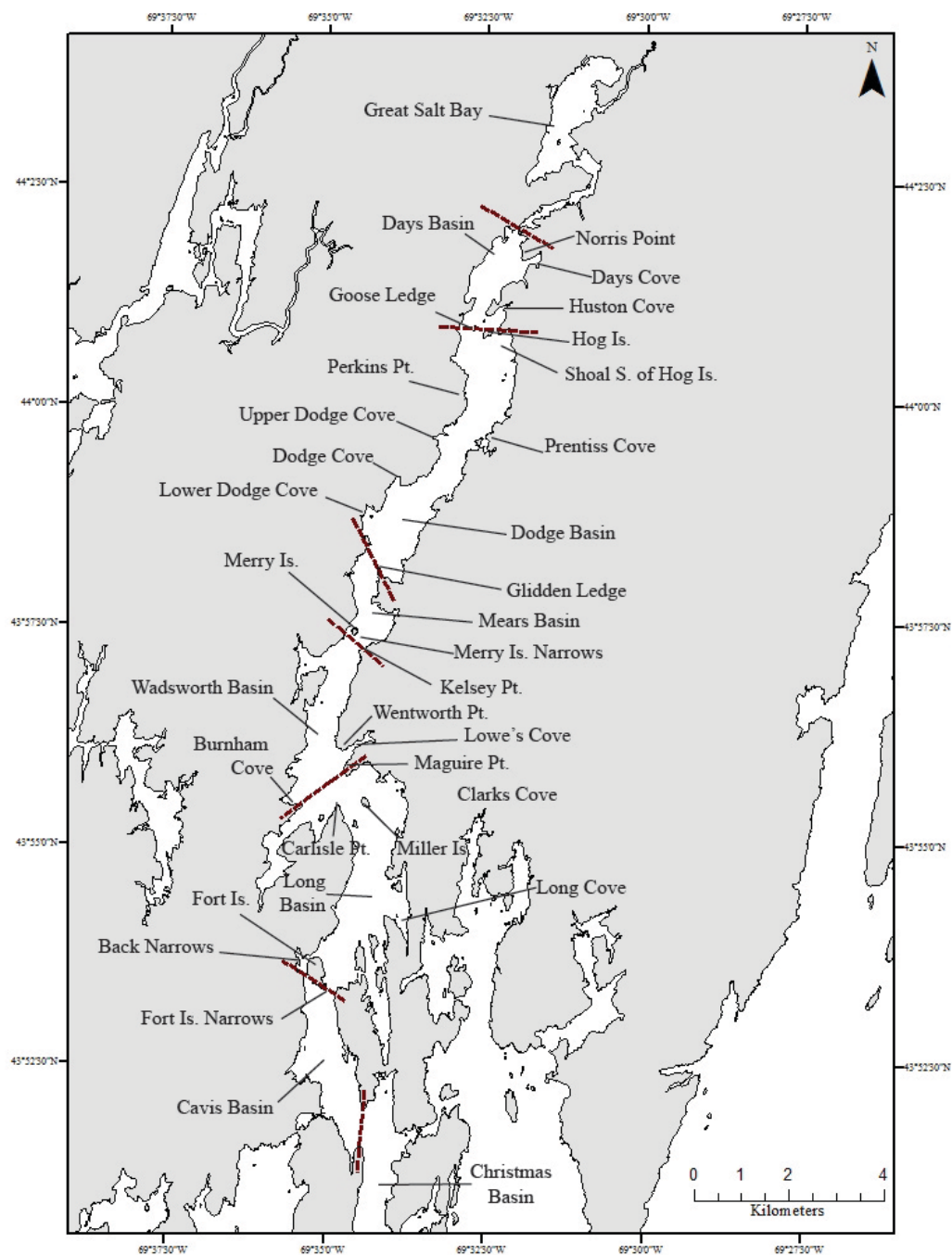


Figure 4.2: Location map indicating places referenced in text. Brown dashed lines indicate the location of bedrock constriction points from Shipp (1989).



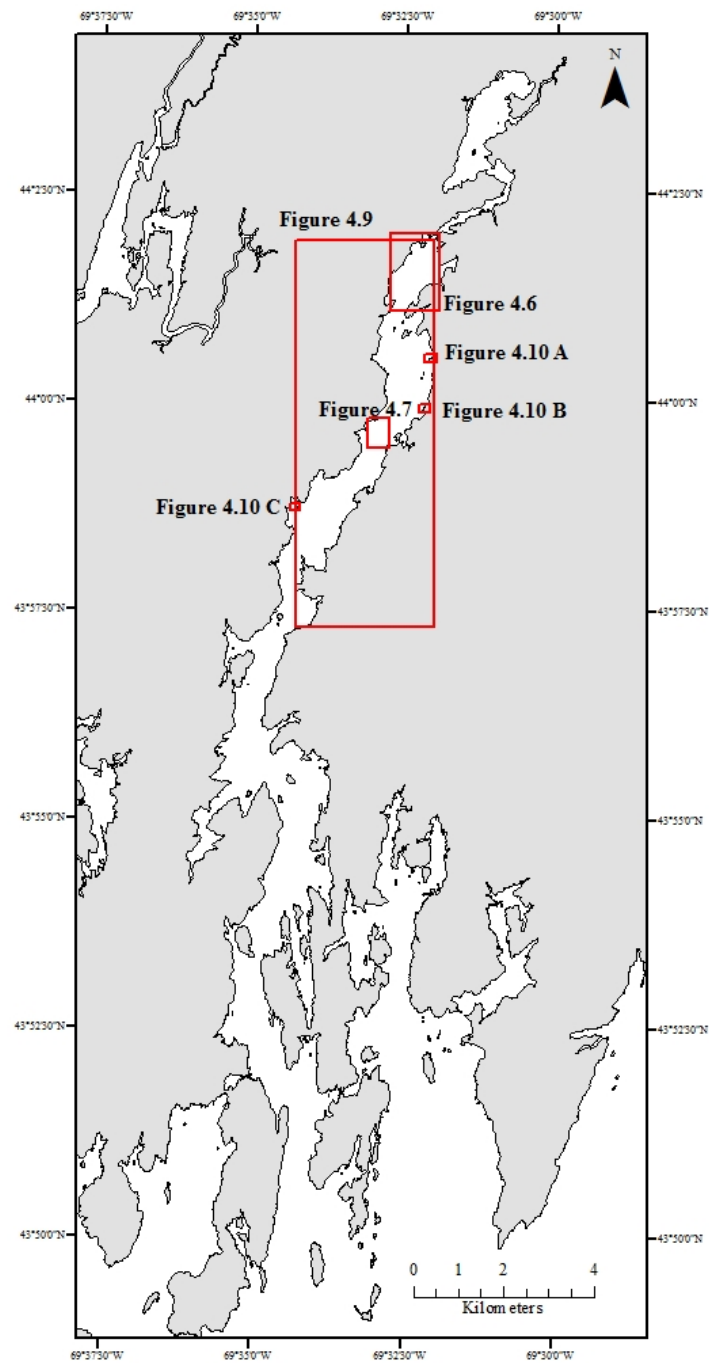


Figure 4.3: Location map indicating the location of figures included in this text.

#### 4.1.2 Estuarine Volume

Using the bathymetry, I calculated the distribution of subtidal water volume throughout the estuary by depth (Figure 4.4). The exponential decay trend in the volume distribution illustrates the extent of the surface waters, which are of particular significance for light-dependent biological processes within the estuary, as well as the temperature of the system. That less than five percent of the estuarine volume is restricted to the deepest 20 meters of the river reiterates the role of tidal currents in scouring the estuarine thalweg within the system.

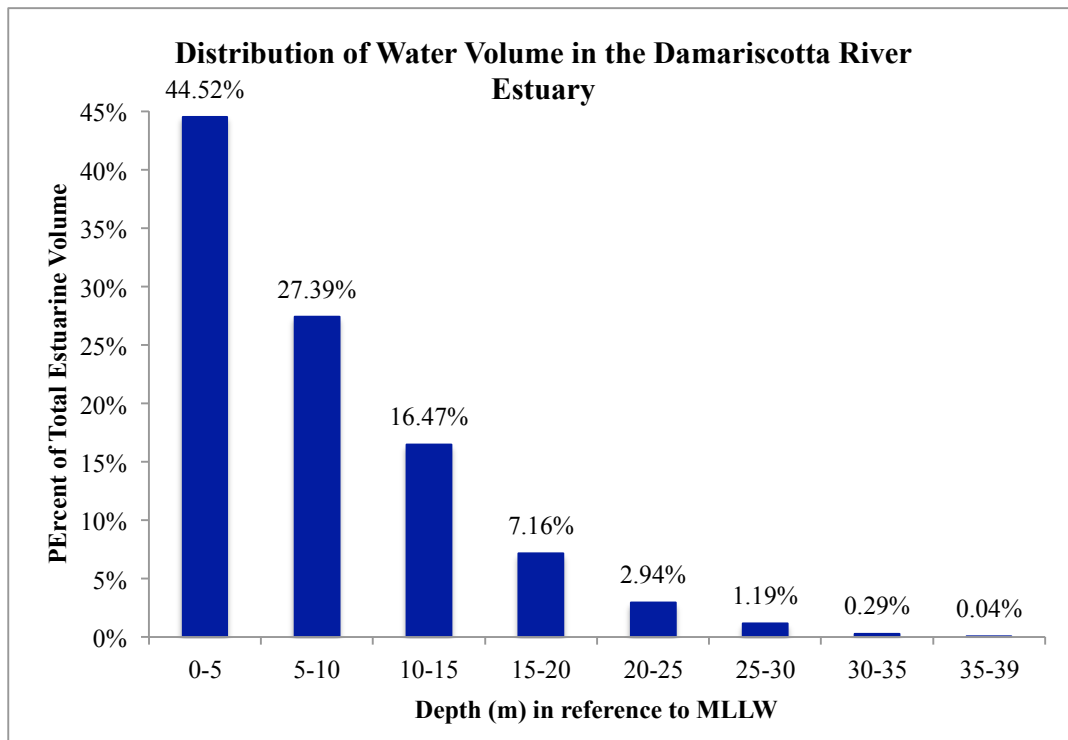


Figure 4.4: Hypsometry of the Damariscotta River estuary. The distribution of water volume is calculated from MBES bathymetry data. All depths are in reference to MLLW and water volumes represent subtidal volume.

## 4.2 Sediment Characterization

In addition to bathymetric data, backscatter intensity data, which result from the strength of the MBES return signal, yield additional insights into seafloor composition. In areas where a higher return signal is recorded, I infer a harder and/or rougher substrate; conversely in areas where a weaker backscatter intensity value is measured, the substrate is softer and/or smoother.

### 4.2.1. Grab Sample Analysis

Grain size analysis of sediment bottom grab samples confirms that MBES backscatter intensity data can be used as a proxy for sediment bottom type. Analysis of 22 bottom grab samples indicates a significant relationship exists between increasing backscatter intensity and increasing sand and gravel composition (expressed as a percent of total mass; Figure 4.5).

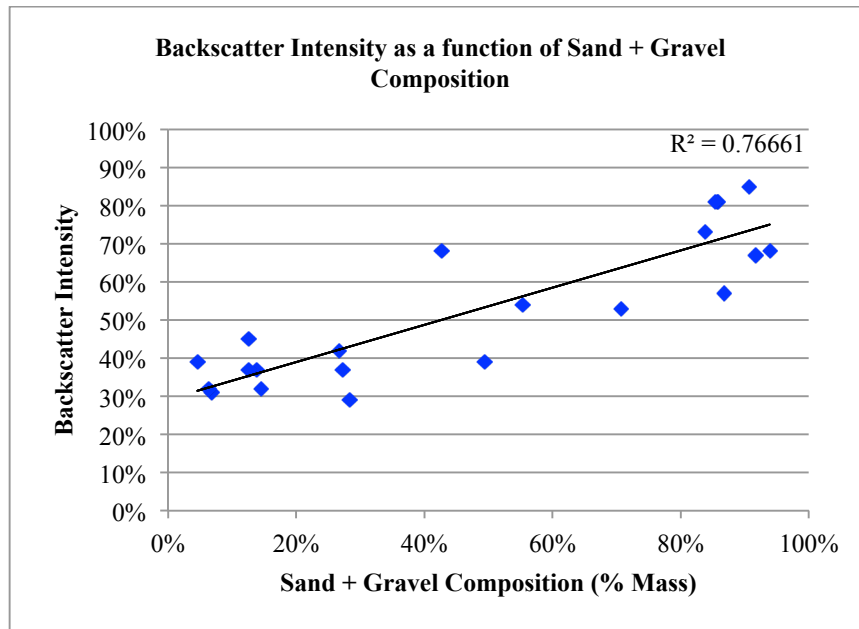


Figure 4.5: Backscatter intensity vs. sand and gravel content. Mass of the total sample.  $N = 22$ . The correlation coefficient is significant at the 0.05 level.

#### 4.2.2. Backscatter Intensity

Detailed backscatter intensity data were recorded throughout the survey area (Figure 4.1). Higher, more reflective returns were recorded in the Narrows by Fort Island, between Carlisle Point and Miller Island, from Maguire Point to Burnham Cove and between Dodge and Kelsey Points (Figure 4.4). These areas are constrictions that result from the bedrock geometry of the estuarine system. The backscatter values for these areas are greater than 50% and correspond with substrate comprised of generally more than 50% sand and gravel and/or exposed bedrock. The edges of the survey area, particularly in the middle and outer estuary, correspond to higher backscatter values (e.g. the shorelines between Carlisle Point and the Back Narrows) that are associated with the steep, cliffed shorelines that are characteristic this region of the river.

Areas with softer backscatter returns, associated with finer bottom sediment, are common in the many coves that border the river and adjacent to the thalweg. While the upper river (north of Glidden Ledge) exhibits a softer return than the lower river, it is harder than the coves and areas adjacent to the thalweg.

### 4.3 Submerged Landforms

#### 4.3.1 River Thalweg

Bedrock constriction points and deep basins, first identified by Shipp (1989), dominate large-scale morphology and control the thalweg of the river. North of Glidden Ledge, the thalweg is delineated by bathymetric depressions associated with tidal scouring and ravinement (Figure 4.1). Particularly in Days Basin, the thalweg is also associated with more reflective sediments (Figure 4.6). However the bathymetric

definition of the thalweg is reduced south of Perkins Point and all but eliminated south of Glidden Ledge. Near constriction points (e.g., between Glidden Ledge and Kelsey Point, and the Fort Island Narrows), more intense backscatter data indicates a harder, more reflective substrate. In other cases, such as near Maguire Point and Miller Island and east of Upper Dodge Point, more reflective backscatter data that stretch across the river appear to be more isolated constriction points.

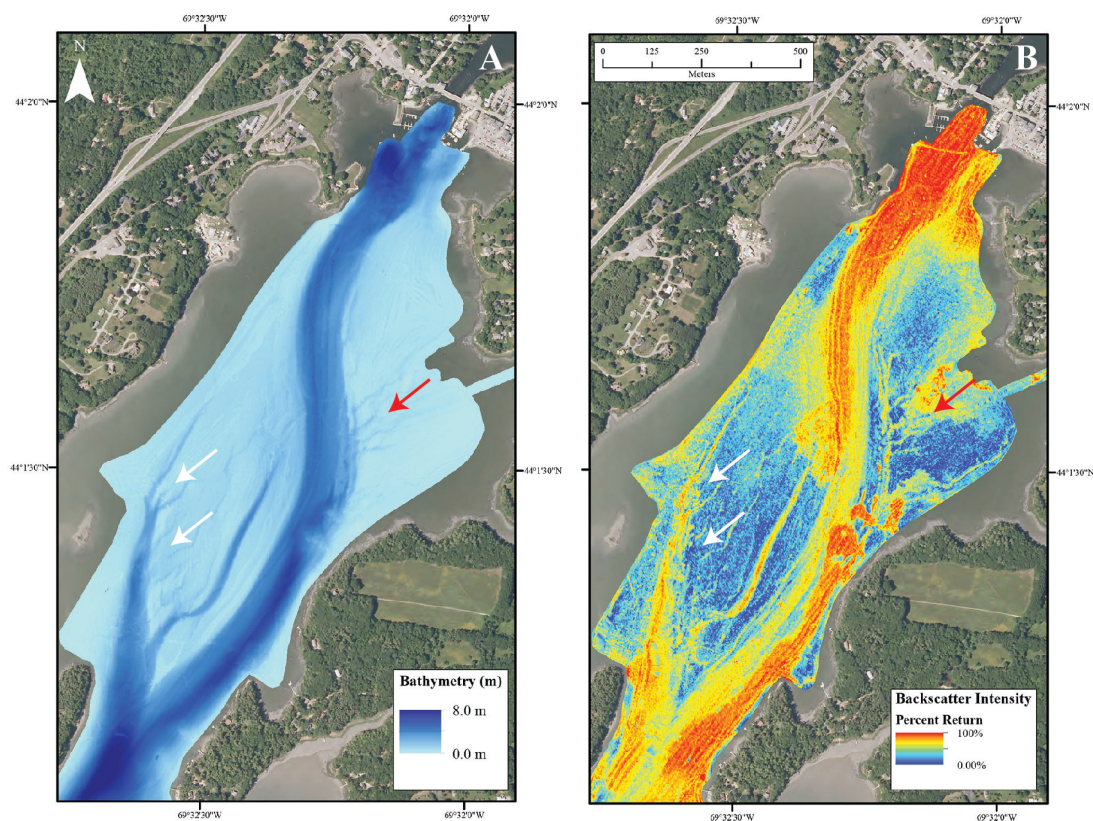


Figure 4.6: MBES data in Days Basin. A) bathymetry and B) backscatter, indicating primary and secondary channels as well as drainage networks associated with the intertidal and subtidal flats, shown by white and red arrows. Note that the unmapped areas on the margins of the MBES data are shallow intertidal regions (generally < 2 m deep at high tide).

#### 4.3.2 Subtidal Drainage Networks

While MBES data-collection in coves and shallow regions was limited by water depth and tidal state, we successfully mapped several networks of submarine drainage networks in Days Basin (Figure 4.6). Most prominently, just west of the primary river thalweg, a network of small channels (Figure 4.6, white arrows) drains into a larger channel that joins the thalweg just south of Little Point. The mapped channels, mostly submerged at low tide, may connect to intertidal channels, and serve as the drainage network for tidal flats. Much like the primary thalweg, the subtidal drainage channels also exhibit a more reflective backscatter return, associated with coarser sediment. On the east side of the river, just off Days Cove and Norris Point, a second, smaller network of channels is also evident (Figure 4.6, red arrows). These channels are evident both as bathymetric depressions and elevated backscatter intensity. They are also separated by a submerged field of large cobbles and small boulders, associated with the erosion of the Norris Point bluff.

#### 4.3.3 Current Lineations

The vicinity of Perkins Point marks a transition in the estuarine system. North of Perkins Point, a prominent thalweg is present in the bathymetry and backscatter intensity (approximately Km 23 – 34 in Figure 2.3). South of Perkins Point, however, bedrock constrictions dominate bathymetry and the backscatter data. Between Perkins Point and Upper Dodge Cove, current lineations, oriented parallel to river channel, are present on the western side of the estuary. Evident in both bathymetry and backscatter intensity data, the lineations form topographic ridges and troughs that are approximately 100 m in width and 700 m in length (Figure 4.7, Figure 4.8). These lineations are also visible in archived

side-scan sonar tracks for this area (Belknap, unpub. data). Perkins Point, to the north, is a rocky bluff. At its base, a shallow shoal ( $\sim 2.3$  m depth,  $\sim 750$  m in length) extends  $\sim 375$  m into the river and is marked by high backscatter intensity values. To the south, Upper Dodge Cove is also shallow (less than  $\sim 2$  m) and corresponds with softer backscatter intensity values.

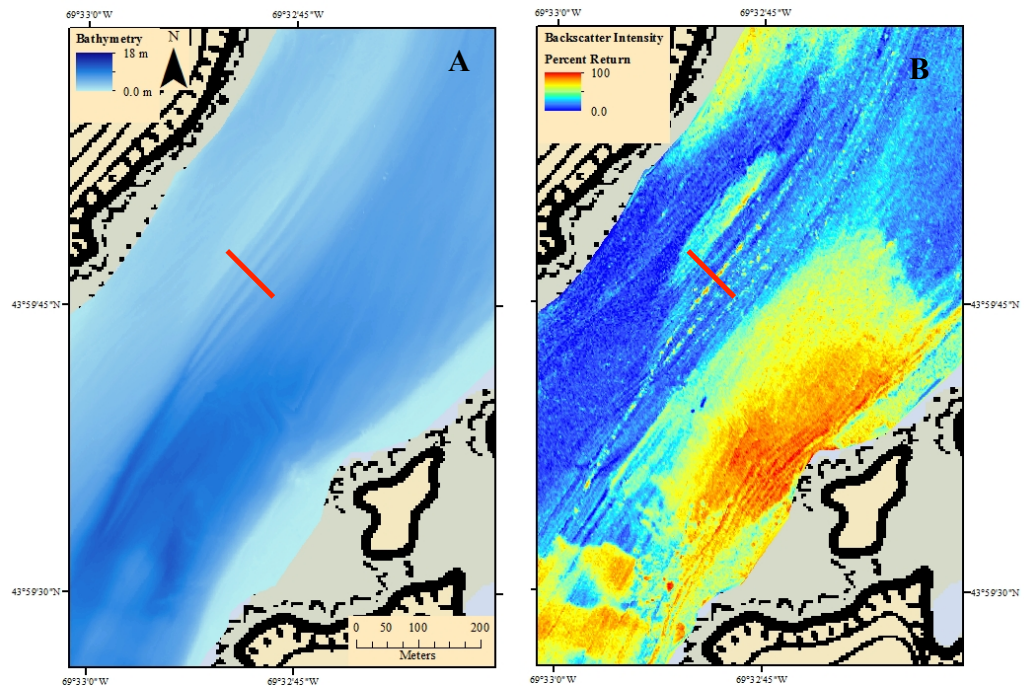


Figure 4.7. Current-oriented striations present on the seafloor. A) bathymetry and B) backscatter intensity, indicate current lineations located between Perkins Point and Upper Dodge Cove. The red line indicates the location of the profile shown in Figure 4.8.

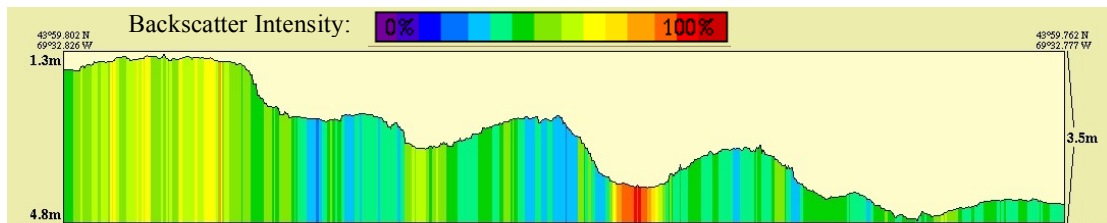


Figure 4.8: Vertical relief and backscatter intensity of current lineations. The location of the profile is indicated by red line in Figure 4.7.

#### 4.3.4 Relict and Modern Oyster Beds

Dodge Cove, a relatively shallow ( $< \sim 4$  m, MLLW) cove with quite soft backscatter intensity values, is known as the site of relict oyster beds (Figure 4.1; Shipp, 1989; Leach, 2007; Leach et al., 2007; Davies, 1992). The shoal, blanketed by soft sediments, extends beyond the concavity of the shoreline, west and south into the main channel of the river (Figure 4.9). While less pronounced than in the upper river, the thalweg borders the southeast edge of relict oyster beds in Dodge Cove, between Dodge Point and Glidden Ledge.

Immediately south of Hog Island is a prominent shoal that is characterized by depths less than  $\sim 1.5$  m (MLLW) and high backscatter intensity values (Figure 4.9). A number of oyster aquaculture leases are presently in use on and around this shoal, indicating that it is likely a modern oyster bed. While its bathymetry (shallow, with little topographic variation) is similar to the relict oyster beds in Dodge Cove, the backscatter intensity is distinctly opposite.



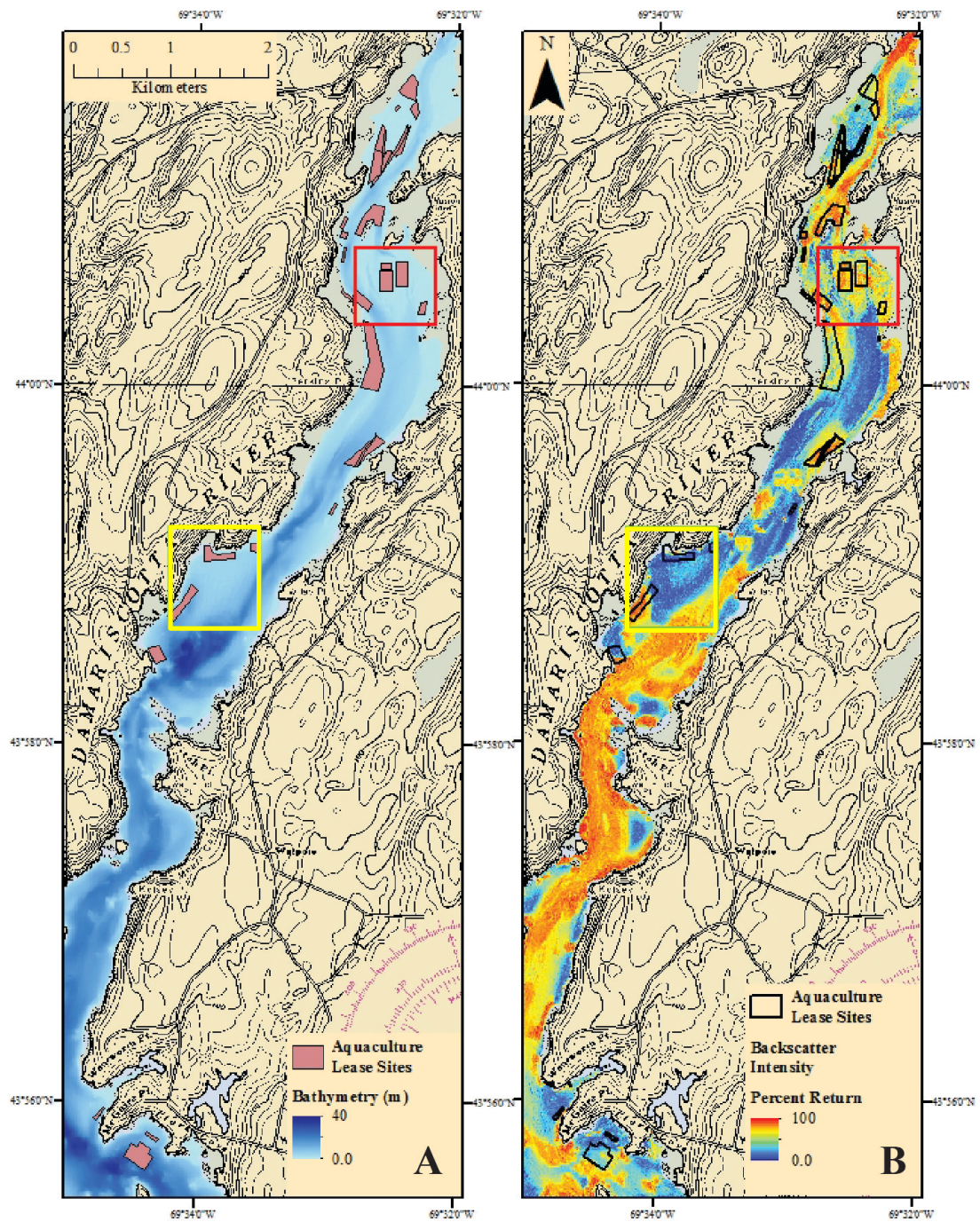


Figure 4.9: Dodge Cove relict and Hog Island modern oyster beds. A) Bathymetry, Maine DMR Aquaculture lease sites and location of relict (yellow) and modern (red) oyster beds. B) Backscatter intensity data are distinctly different for Dodge Cove and the shoal south of Hog Island.

#### 4.3.5 Recessional Moraines

The Damariscotta River is bordered by a series of marginal moraines associated with retreat of the Laurentide Ice Sheet (Figure 4.10). Oriented approximately east-west and perpendicular to the estuarine trend, several of the moraines exist as eroding bluffs along the Damariscotta River shoreline. Two moraines are located on the eastern shore, between Prentiss Cove and Huston Cove (Figure 4.10 A & B). Isolated and eroding moraines are also present in Lower and Upper Dodge Coves (Figure 4.10 C). In Upper Dodge Cove, at low tide, Presumpscot Formation glaciomarine clay can be seen draped over eroding till. Seaward of these moraines, large cobbles and boulder fields are present in intertidal and subtidal waters.

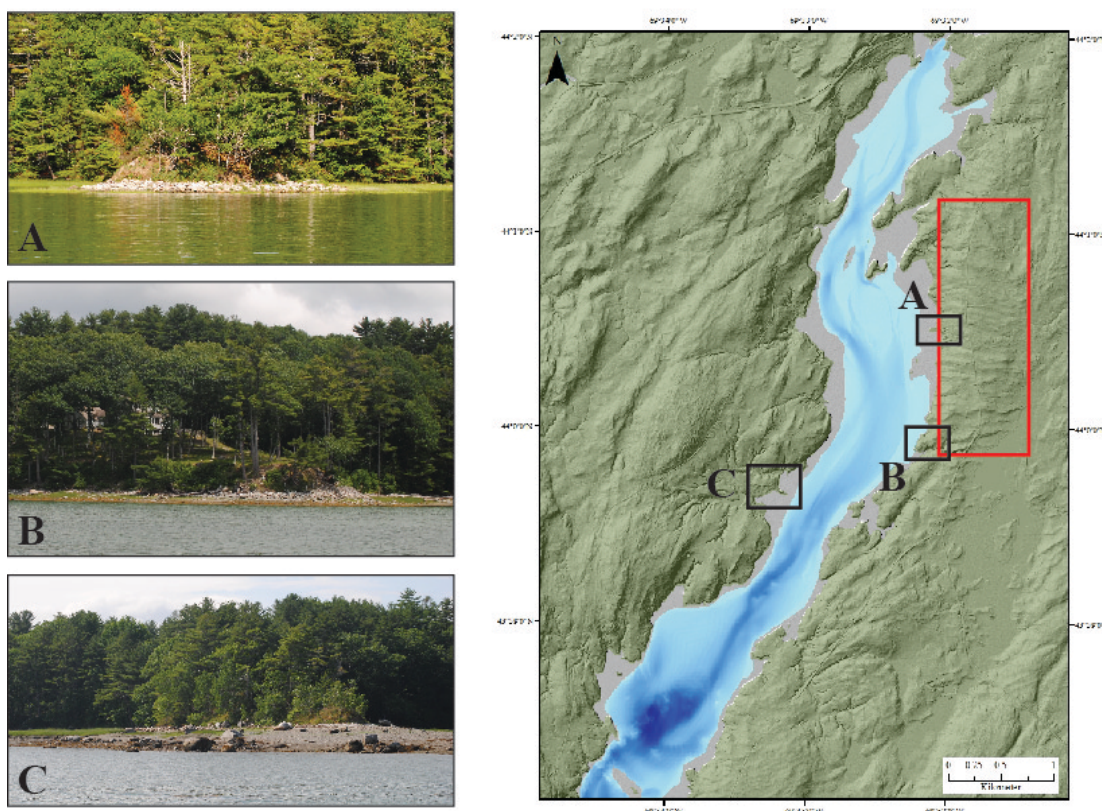


Figure 4.10: Recessional moraines in the Damariscotta River estuary. A, B and C indicate the location of moraines; the red box indicates a recessional moraines belt evident in the LiDAR Hillshade DEM (from Maine Office of GIS (<https://www1.maine.gov/megis/>)). Moraines A and B are found on the east shore, due east of Perkins Point. Moraine C is located in Upper Dodge Cove.

#### 4.4 Sediment Accumulation Patterns

##### 4.4.1 Sediment Cores

Four short piston cores were collected from coves throughout the estuary (Table 4.1; Figures 4.10 and 4.11; Appendix B). DR-PC-15-02, collected from Long Cove, consists primarily of uniform, fine-grained estuarine sediment. Layers of shell fragments are present at 4-6 cm, 10-13 cm, 20-22 cm and 55-59 cm. Small organic fragments, including wood and pine needles, are present occasionally throughout the core and are less common from 120-140 cm. The core catch, present from 155 – 170 cm, contains estuarine sediment.

DR-PC-15-04 (Figure 4.11), collected from Lowe's Cove, consists of uniform fine-grained estuarine sediment, with decreasing water content throughout the core. The top 12 cm of the core are quite high in water content and soupy, whereas the water content decreases from 12 – 30 cm and sediment is increasingly stiff. Sand content increases from 15 cm to 86 cm and fine mica fragments are present between 50 cm and 117 cm. A layer rich in wood and shell fragments is present at 66 – 68 cm. A sandy layer with shell fragments is present from 87 – 97 cm. The core catcher, from 104 – 117 cm, did not capture any sediment.

Table 4.1: Piston core sites, locations and core lengths.

| <b>Piston Core Identification</b> | <b>Core Site Name</b>     | <b>Core Site Location</b>       | <b>Core Length</b> |
|-----------------------------------|---------------------------|---------------------------------|--------------------|
| DR-PC-15-02                       | Long Cove                 | 43° 0.306' N<br>069° 33.836' W  | 1.71 m             |
| DR-PC-15-04                       | Lowe's Cove               | 43° 55.977' N<br>069° 34.723' W | 1.17 m             |
| DR-PC-15-07                       | Upper Dodge Cove          | 43° 59.602' N<br>069° 33.031' W | 1.04 m             |
| DR-PC-15-08                       | Shoal south of Hog Island | 44° 0.306' N<br>069° 32.368' W  | 1.40 m             |

Table 4.2: Piston core sediment samples utilized in radionuclide analysis.

| <b>Piston Core Identification</b> | <b>Core Site Name</b>     | <b>Core Utilized in Radionuclide Analysis</b> |
|-----------------------------------|---------------------------|---|
| DR-PC-15-02                       | Long Cove                 | 0 – 15 cm                                     |
| DR-PC-15-04                       | Lowe's Cove               | 0 – 17 cm                                     |
| DR-PC-15-07                       | Upper Dodge Cove          | 0 – 14 cm                                     |
| DR-PC-15-08                       | Shoal south of Hog Island | 0 – 21 cm                                     |



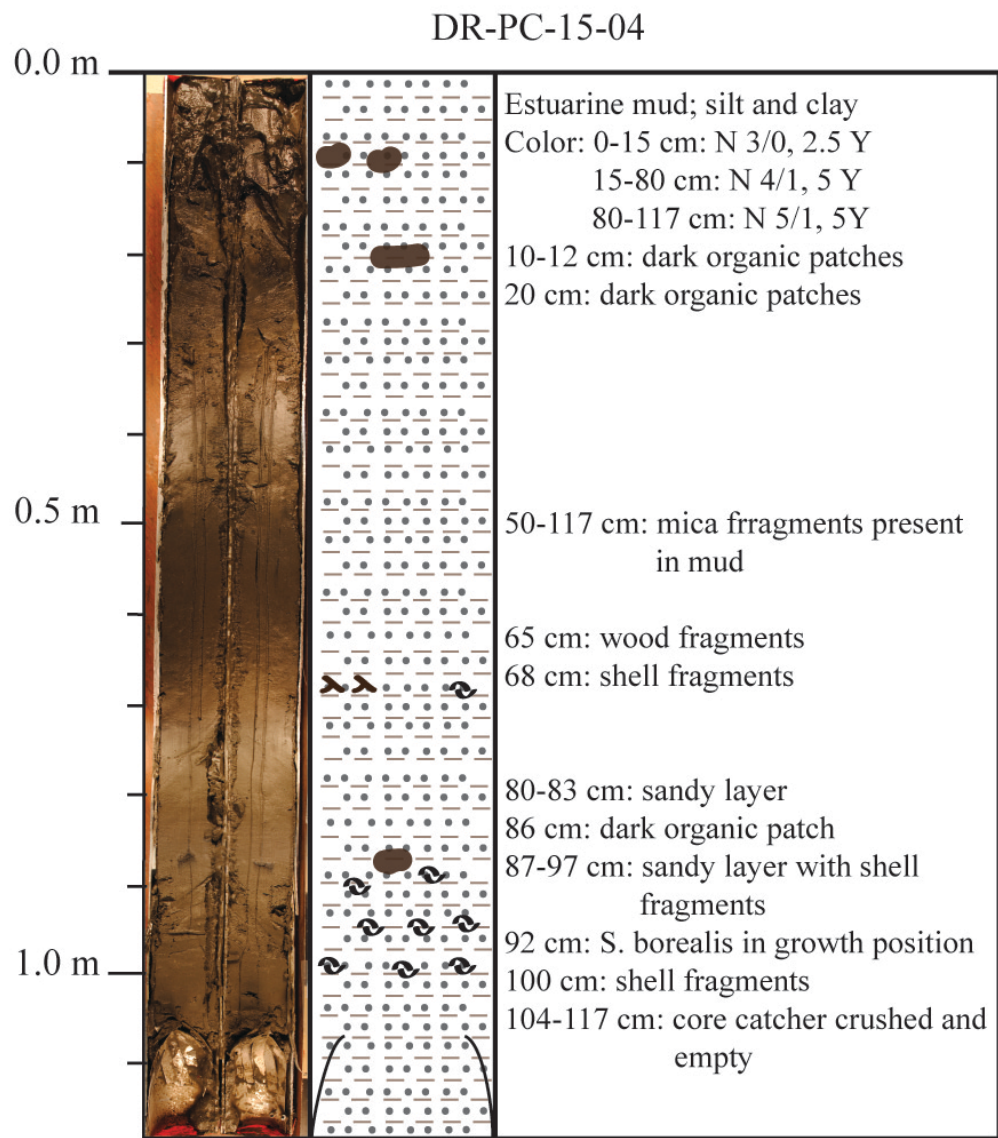


Figure 4.11: DR-PC-15-04 sediment core log from Lowe's Cove.

The core from Upper Dodge Cove, DR-PC-15-07, is the shortest of the cores. Composed of fine-grained estuarine sediment, the water content decreases from 0 to 25 cm. Several wood fragments were identified at 20, 59 and 97 cm depth and mussel shell fragment at 4 – 5 cm. A pebble (measuring approximately 5.5 x 2 x 3.5 cm) was found at 20 – 26 cm depth. Sediment remains roughly uniform in water content from 25 – 104 cm, though some shell fragments are present in the core catcher (93 – 104 cm) at 94 – 95 cm.

The core collected from the shoal south of Hog Island, DR-PC-15-08, is the longest of the cores at 1.71 m. The fine-grained estuarine sediment is high in water content at the top of the core and decreases gradually. The top 0 – 5 cm of the core is particularly soupy, with a slight increase in cohesion between 5 and 10 cm. Cohesion continues to increase from 10 to 30 cm and from 30 – 40 cm, sediment is pocked and crumbly in a several places. From 50 – 140 cm, the plasticity of the sediment is greater than in the upper core and a marbled appearance between 60 and 75 cm may be indicative of burrows. A razor clam (*Ensis directus*) shell was lodged in the sediment between 82 and 90 cm and a layer of shell fragments is present at 108 – 112 cm. Several isolated wood and shell fragments are present between 118 and 130 cm and the core catch occupies 125 – 140 cm of the core.

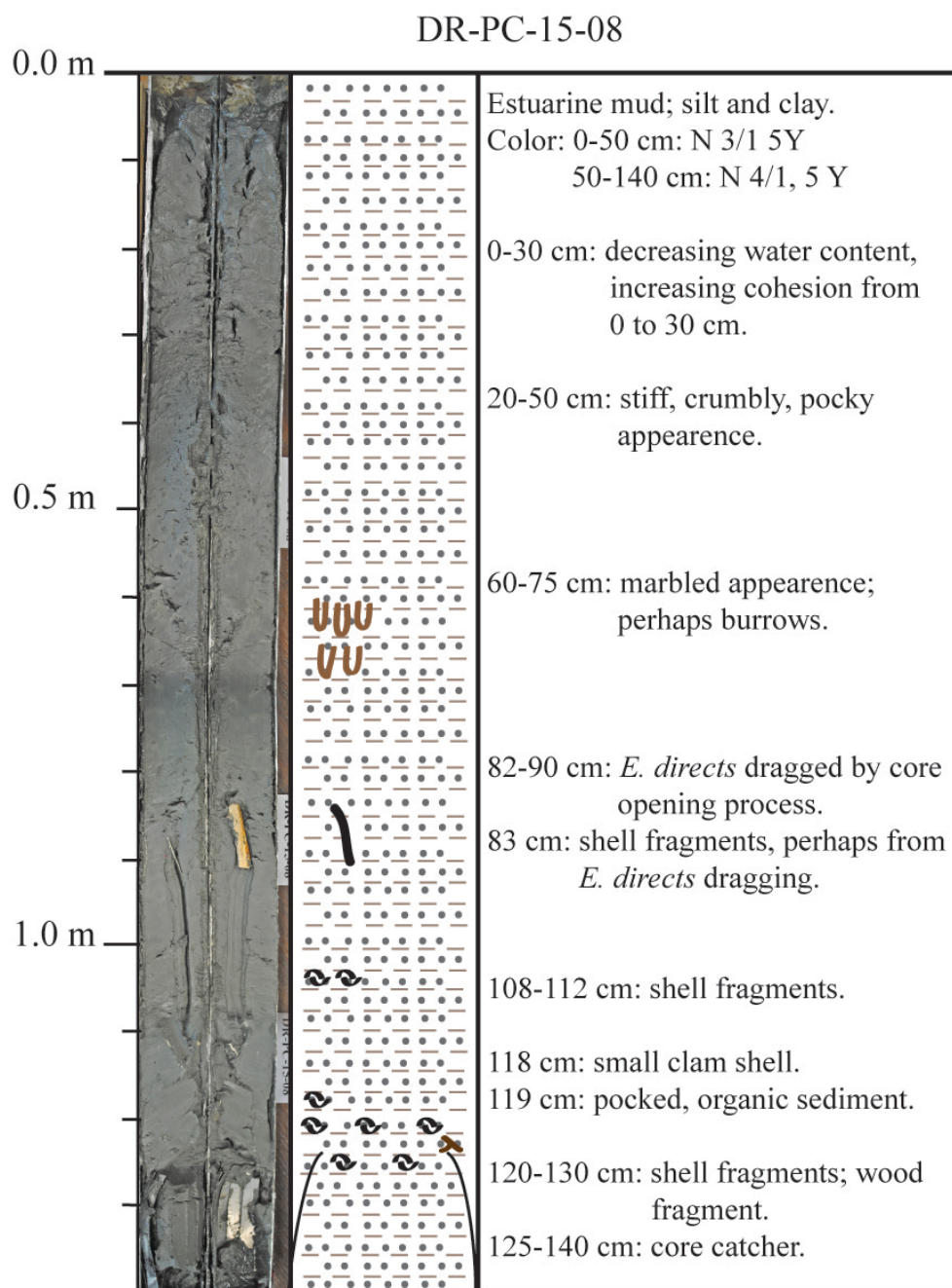


Figure 4.12: DR-PC-15-08 sediment core log from the shoal south of Hog Island.

#### 4.4.2 Radionuclide Analysis

Radionuclide analysis of four sediment cores yielded specific activity profiles for of  $^{210}\text{Pb}$  and  $^{137}\text{Cs}$  (Figures 4.11 – 4.14, Table 2, Appendix D). The specific activity of  $^{210}\text{Pb}$  decays rapidly to background, supported levels in the top 3 cm of DR-PC-15-02, whereas DR-PC-15-07 and DR-PC-15-08 decay over approximately 9 cm. The specific activity of  $^{210}\text{Pb}$  in DR-PC-15-04 is more variable, although a trend of decay is evident between approximately 6.5 and 13.5 cm. Background, supported activities are considered to be those where the specific activity of  $^{210}\text{Pb}$  ceases to vary significantly with depth.

$^{137}\text{Cs}$  specific activities are considerably lower than those of  $^{210}\text{Pb}$  (Figures 4.15 and 4.16).  $^{137}\text{Cs}$  specific activities in DR-PC-15-02 and DR-PC-15-07 are much lower than DR-PC-15-04 and DR-PC-15-08. The cores with higher specific activities also show substantially more variability, with values ranging from 0.0002 Bq/g to 0.021 Bq/g. The oscillating specific activities in DR-PC-15-04 and DR-PC-15-08 show multiple peaks of varying height whereas the quieter cores, DR-PC-15-02 and DR-PC-15-07, exhibit only minor peaks.



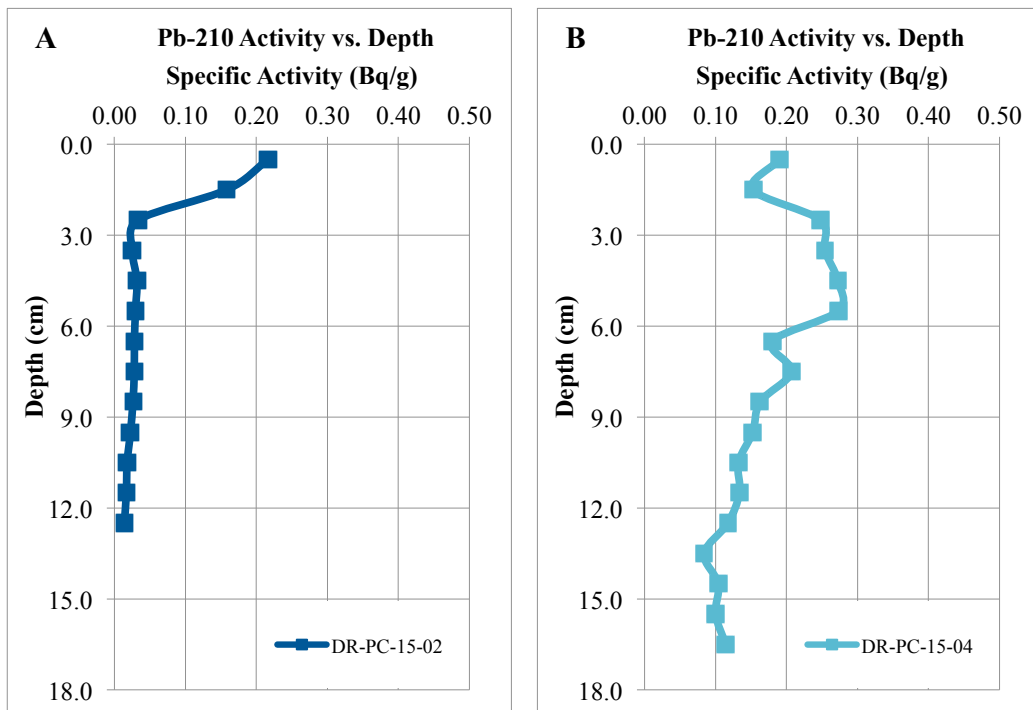


Figure 4.13: Specific activity of  $^{210}\text{Pb}$  in sediment cores from the southern estuary. A) Activities in DR-PC-15-02 and B) activities in DR-PC-15-04.

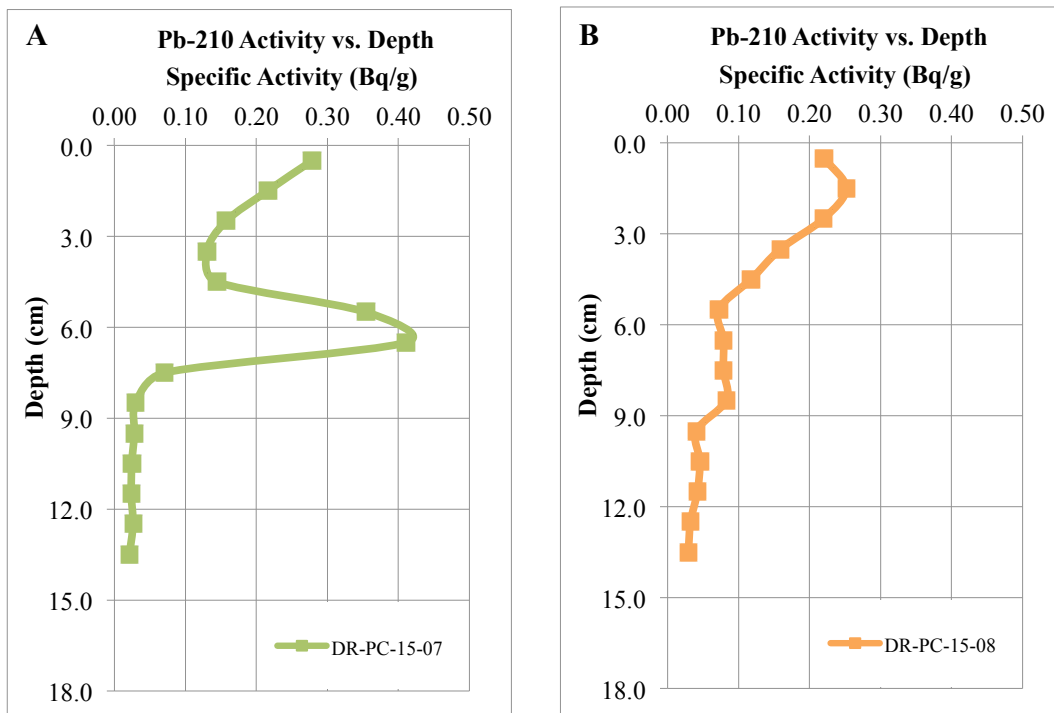


Figure 4.14: Specific activity of  $^{210}\text{Pb}$  in sediment cores from the northern estuary. A) Activities in DR-PC-15-07 and B) activities in DR-PC-15-08.

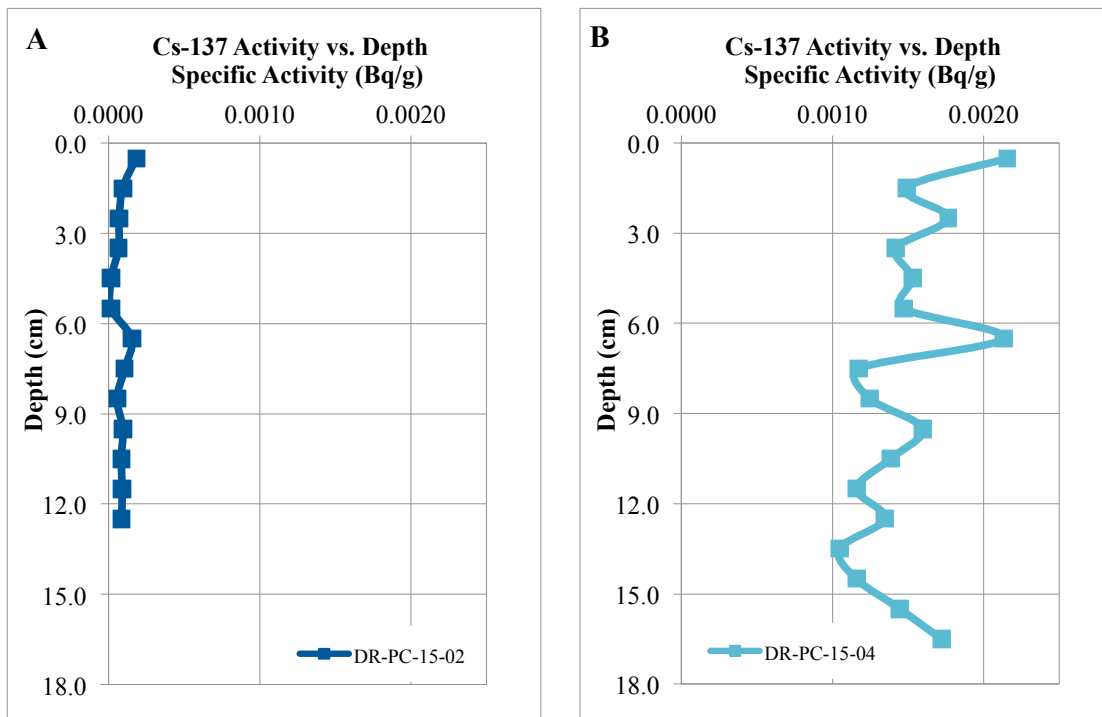


Figure 4.15: Specific activity of  $^{137}\text{Cs}$  in sediment cores from the southern estuary. A) Activities in DR-PC-15-02 and B) activities in DR-PC-15-04.

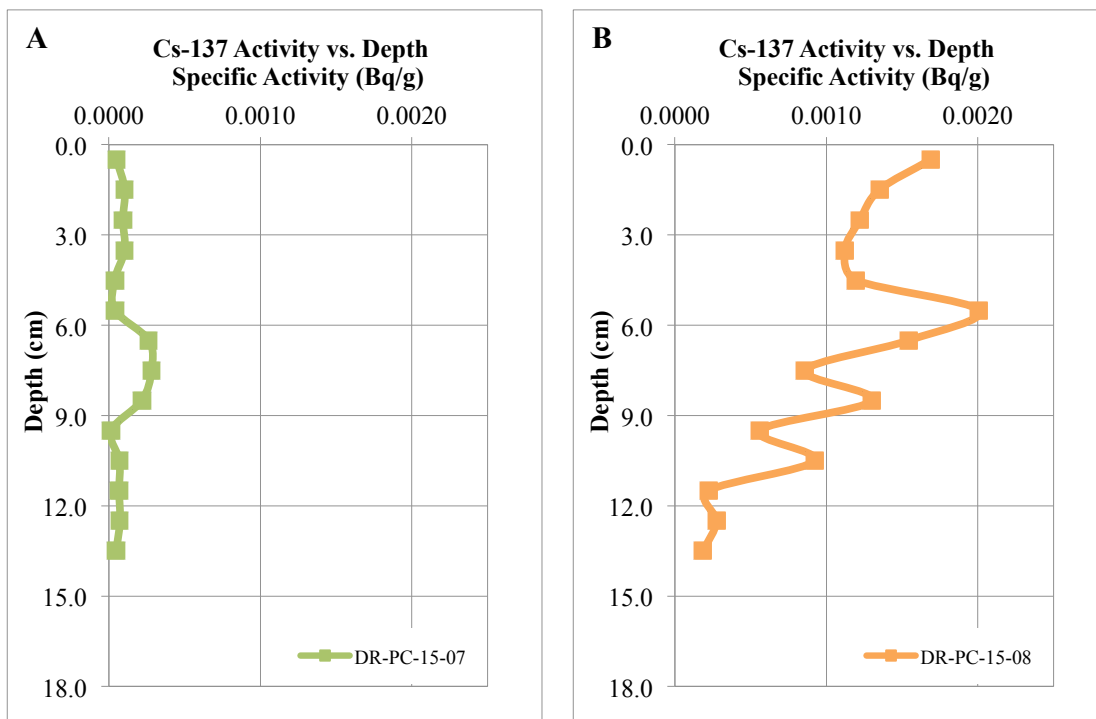


Figure 4.16: Specific activity of  $^{137}\text{Cs}$  in sediment cores from the northern estuary. A) Activities in DR-PC-15-07 and B) activities in DR-PC-15-08.

## CHAPTER 5

### DISCUSSION

#### 5.1 Sediment Accumulation Patterns

Radionuclide analysis of  $^{210}\text{Pb}$  and  $^{137}\text{Cs}$  activities in sediment cores is intended to provide insights into sediment accumulation patterns and rates at each core site. Such insights include the degree of sediment stability and/or reworking of sediment at core sites, as well as the sources of sediment to the estuary. Sediment sources could be predominantly reworked Pleistocene glaciomarine mud and Holocene estuarine sediments or the estuary may receive new, terrestrial input. Sediment accumulation patterns are considered in the context of backscatter intensity datasets and estuarine location (i.e., coves, channels and flats).

$^{210}\text{Pb}$  specific activities (Figures 4.13 and 4.14) measured for this study are consistent with previous studies utilizing the same method (Mayer, et al., unpub. data) and are generally quite low. Regional terrestrial  $^{210}\text{Pb}$  inventories (Landis et al., 2016) are generally an order of magnitude greater than those in this study. While there is considerable variability between  $^{137}\text{Cs}$  specific activities in sediment cores (i.e., Figures 15 A and 16 A vs. Figures 15 B and 16 B), the specific activities are also quite low, and 1-2 orders of magnitude less than regional terrestrial inventories (Landis et al., 2016). This is indicative of both the comparatively old age of sediments within the Damariscotta River system as well as the relatively limited input of newer sediment to the system.

The specific activities of  $^{210}\text{Pb}$  measured throughout each core vary substantially. It is not unusual for surface sediments to exhibit some degree of homogeneity due to physical processes and bioturbation mixing the sediment (Nitttrouer et al., 1984; Smith et

al., 1986; Sharma, et al., 1987; Bentley et al., 2014). However, the depth of mixed sediment, referred to as the mixed zone, varies among cores.  $^{210}\text{Pb}$  specific activities in DR-PC-15-02 and DR-PC-15-07 (Figures 13A and 14A) decline rapidly with depth, suggesting that no mixed interval is present in these cores. The rapid decline could be a result of erosional events and/or environments at these cores sites, or due to disturbance and/or loss during the coring process. In the case of DR-PC-15-02, in which  $^{210}\text{Pb}$  activities appear to reach background levels by 2.5 cm depth, this setting is likely erosive and an area of comparatively low deposition rate. Multiple shelly and sandy layers present in the core (Figure 4.12) are indicative of disturbance and/or episodic deposition at that site. Interpreting  $^{210}\text{Pb}$  results from DR-PC-15-07, collected at Upper Dodge Cove and immediately south of the current lineations (Figures 4.7 and 4.8, requires a better understanding of the historical hydrodynamics of this environment that could yield more insights into sediment dynamics at this site. It is noteworthy that DR-PC-15-07  $^{210}\text{Pb}$  activities do exhibit the expected exponential decay overall, however a significant disturbance is apparent at 5.5 – 6.5 cm depth within the core. A secondary analysis of samples from this section of the core was conducted and confirmed the disturbance was not a result of sampling or instrumental error (see Appendix A). The increase in  $^{210}\text{Pb}$  activity recorded at 5.5-6.5 cm in DR-PC-15-07 could be indicative of an influx of sediment new to the system or from an alternative source.

DR-PC-15-04 and DR-PC-15-08, collected from Lowe's Cove and the shoal south of Hog Island respectively, in contrast to DR-PC-15-02 and DR-PC-15-07, exhibit some degree of surface sediment mixing as seen in the  $^{210}\text{Pb}$  specific activities from the upper core. Specific activities of  $^{210}\text{Pb}$  in DR-PC-15-04 (Figure 13 B) oscillate between

the surface and 7.5 cm depth before declining steadily and reaching stable, background levels at 13.5 cm depth. The mixed interval evident in DR-PC-15-08 (Figure 14 B) is considerably smaller, from the surface to 2.5 cm depth, at which point  $^{210}\text{Pb}$  activities decline and reach background levels at 9.5 cm depth. While neither record illustrates a classic, exponential decay in  $^{210}\text{Pb}$  activities (such as Köster et al., 2007 from nearby Merrymeeting Bay), both provide an opportunity to utilize the radioactive decay of  $^{210}\text{Pb}$  to better understand sedimentation rates at these sites.

#### 5.1.1 Age Models and Sediment Accumulation Rates

Using a constant rate of supply (CRS) model and the specific activity of  $^{210}\text{Pb}$ , age models were developed for each core to determine sediment ages and accumulation rates (Table 5.1). Inherent in this approach is the assumption that sediment accumulation is constant; it does not account of disturbances such as reworking or mixing of sediment or for periods of non-deposition. Excluding the uppermost 1 cm (where sedimentation rates are substantially higher than elsewhere in each core), average sediment accumulation rates determined by the CRS age-depth model are similar in each core and generally  $< 0.2$  cm/yr (Table 5.1).

Sediment accumulation rates derived from  $^{210}\text{Pb}$  activities for DR-PC-15-04 and DR-PC-15-08 are reinforced by  $^{137}\text{Cs}$  activities in those cores.  $^{137}\text{Cs}$  was introduced into the marine environment in 1952 as a result of nuclear bomb tests and discharges from nuclear reactor facilities and reached peak fallout levels in 1963 (Sugai et al., 1994; Baskaran and Naidu, 1995).  $^{137}\text{Cs}$  activities in these cores do not exhibit the ideal singular, isolated peaks rather they are complicated. However, the activities are greatest

at core depths that coincide (within the margin of error) with 1963 (6.5 cm depth in DR-PC-15-04; 5.5 cm depth in DR-PC-15-08). Because boundary ages and sediment accumulation rates are based in the assumption that sediment accumulation is constant and not disturbed, and because the many mechanisms exist for the disturbance and reworking of sediment in this environment, ages and accumulation rates should be regarded with a degree of skepticism.

Table 5.1: Sedimentation rates and ages determined from CRS model.

| Depth (cm)         | Age (years) | Year +/- | Lower Boundary Age | Sediment Accumulation Rate (cm/yr) |
|--------------------|-------------|----------|--------------------|------------------------------------|
| <b>DR-PC-15-04</b> |             |          |                    |                                    |
| 0.5                | 0.00        | 0.00     | 2015               | 3.45                               |
| 1.5                | 2.58        | 1.67     | 2013               | 0.49                               |
| 2.5                | 4.10        | 4.13     | 2009               | 0.29                               |
| 3.5                | 9.46        | 6.28     | 2003               | 0.16                               |
| 4.5                | 16.23       | 8.22     | 1995               | 0.13                               |
| 5.5                | 25.42       | 10.29    | 1983               | 0.08                               |
| 6.5                | 41.34       | 13.12    | 1969               | 0.07                               |
| 7.5                | 52.42       | 14.78    | 1953               | 0.06                               |
| 8.5                | 74.24       | 17.58    | 1929               | 0.04                               |
| 9.5                | 99.88       | 28.65    | 1906               | 0.04                               |
| 10.5               | 120.22      | 38.15    | 1897               | 0.11                               |
| <b>DR-PC-15-08</b> |             |          |                    |                                    |
| 0.5                | 0.00        | 0.00     | 2013               | 0.47                               |
| 1.5                | 6.28        | 5.13     | 2005               | 0.12                               |
| 2.5                | 16.45       | 8.29     | 1994               | 0.09                               |
| 3.5                | 27.70       | 10.76    | 1983               | 0.09                               |
| 4.5                | 38.66       | 13.94    | 1972               | 0.09                               |
| 5.5                | 49.21       | 16.68    | 1964               | 0.12                               |
| 6.5                | 55.44       | 18.31    | 1956               | 0.13                               |
| 7.5                | 65.13       | 19.71    | 1942               | 0.07                               |
| 8.5                | 83.13       | 22.09    | 1910               | 0.03                               |
| 9.5                | 128.37      | 29.70    | 1881               | 0.03                               |

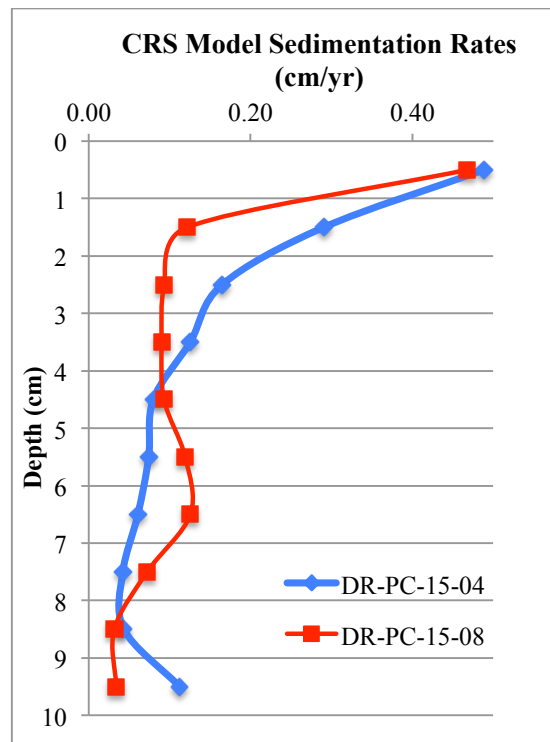


Figure 5.1: Sedimentation rates determined from CRS age-depth model. The blue line indicates results for DR-PC-15-04 (Lowe's Cove) and the red line indicates results for DR-PC-15-08 (shoal south of Hog Island). In both cases, the surface data point is excluded.

Mixing of sediment due to biological and physical processes, as well as low sediment accumulation rates ( $<0.1$  cm/yr), are important factors to consider when interpreting  $^{210}\text{Pb}$  activities and derived geochronologies. The significance of mixed surface sediments and their complicating role in the use of  $^{210}\text{Pb}$  to determine sediment accumulation rates is well studied (Bentley et al., 2014; Nittrouer et al., 1984; Sharma, et al., 1987; Smith et al., 1986). The issues associated with extensive surface sediment mixing are exacerbated in areas of low sedimentation, where the degree of mixing affects a greater period of time in the record. Each core shows evidence of sediment mixing at the surface, or a mixed layer associated with physical and biological processes, which calls into question the value of using a  $^{210}\text{Pb}$  geochronology to such data (Figures 4.11

and 4.12; Bentley et al., 2014; Nitttrouer et al., 1984; Sharma, et al., 1987; Smith et al., 1986).

Mechanisms for sediment disturbance in the Damariscotta River estuary, and at these core sites specifically, are abundant. Bioturbation and physical mixing cause sediments to be reworked and homogenized in the upper core. Furthermore, the process of collecting, transporting and processing sediment cores in the lab may also contribute to mixing of core sediments. Finally, anthropogenic activities that remobilize sediment, such as clamming in Lowe's Cove and trawling for oysters in bottom-seeded aquaculture sites, may also contribute to the reworking of surface sediments in the estuary. Considering the degree to which sediments can be reworked, the CRS age-depth model ages and sediment accumulation rates should be treated with great caution.



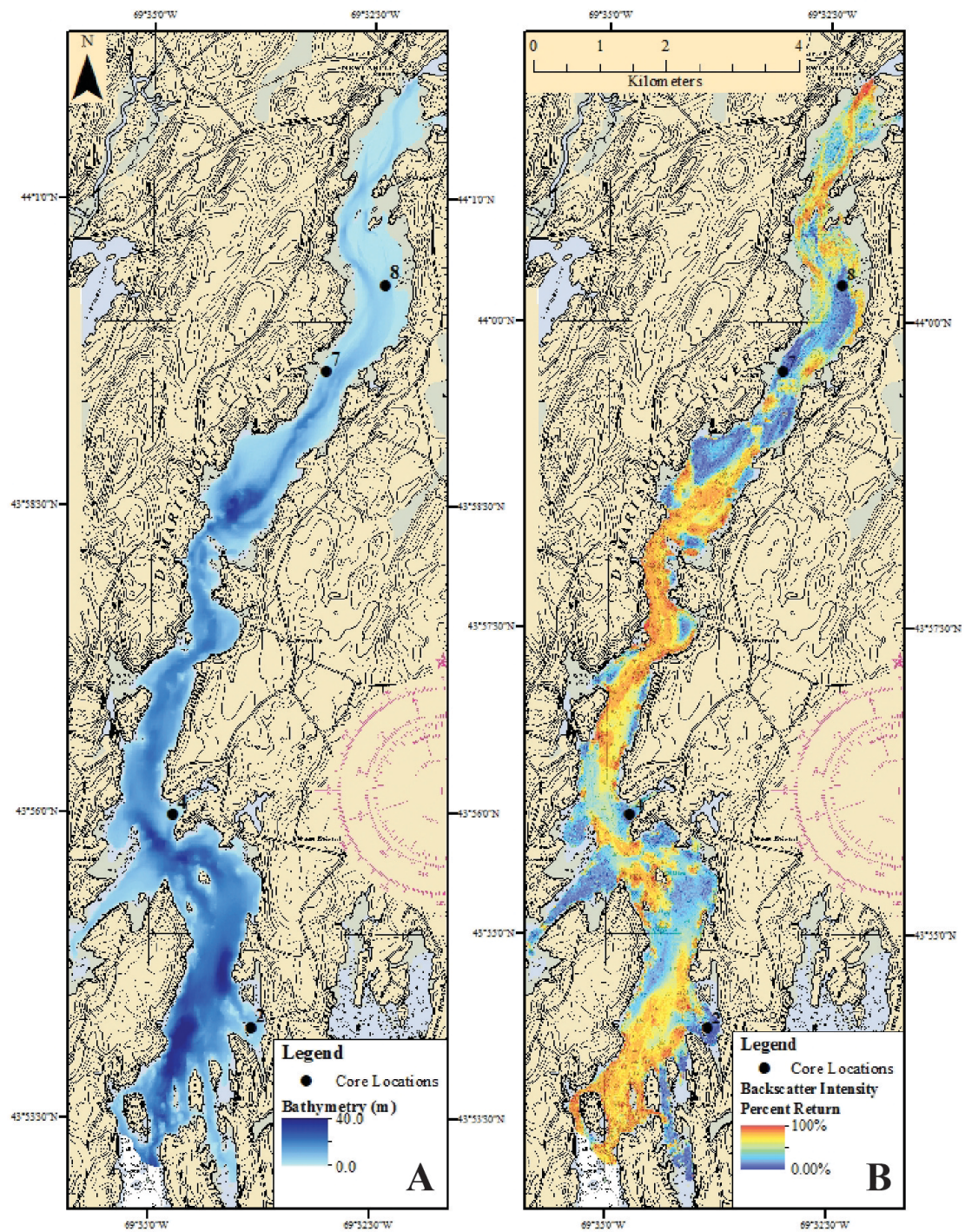


Figure 5.2: Core locations in the context of MBES data. A) Bathymetry and B) backscatter intensity, where core site numbers correspond to that last digit of core identification name (i.e., 2 is DR-PC-15-02).

### 5.1.2 Estimating Sediment Accumulation Rates

A second approach to interpreting  $^{210}\text{Pb}$  activities estimates upper bound of sediment accumulation rates while simultaneously taking into account the surface sediment mixed layer. By considering the specific activity of excess unsupported  $^{210}\text{Pb}$  integrated decay rate with core depth, it is possible to estimate an integrated sediment accumulation rate below the mixed layer depth and above background levels in the core (Figure 5.3; Table 5.2). Estimated sediment accumulation rates are determined using the  $^{210}\text{Pb}$  decay constant ( $0.03114 \text{ yr}^{-1}$ ) and the rate at which excess  $^{210}\text{Pb}$  activity decays with core depth.

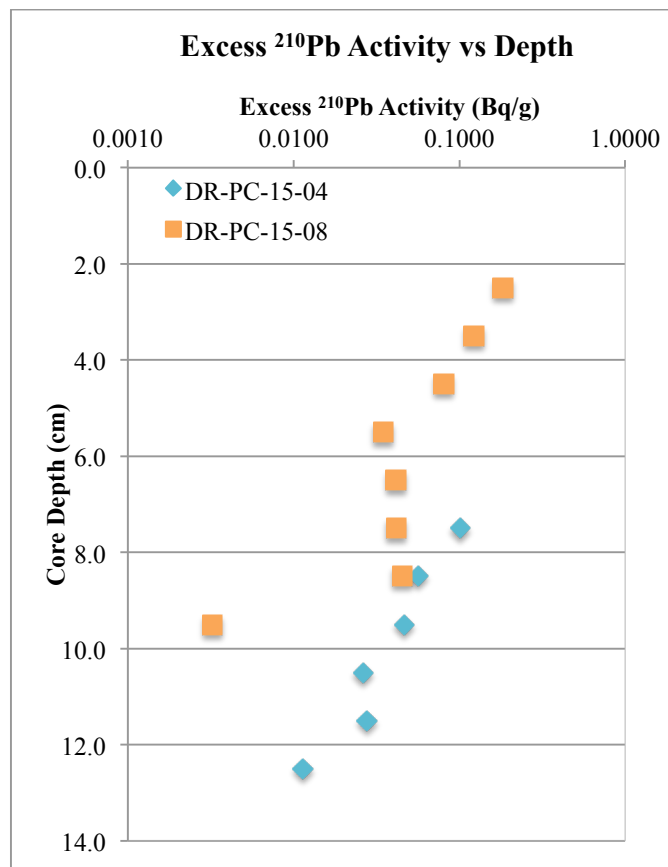


Figure 5.3: Excess  $^{210}\text{Pb}$  activities vs. core depth. The integrated rate of  $^{210}\text{Pb}$  decay with depth is used to estimate sediment accumulation rates at DR-PC-15-04 and DR-PC-15-08.

Table 5.2: Estimated sediment accumulation rates

| <b>Core</b> | <b>Mixed Sediment Layer Depth</b> | <b>Background Begins</b> | <b>Estimated Sediment Accumulation Rate</b> |
|-------------|-----------------------------------|--------------------------|---|
| DR-PC-15-04 | 7.5 cm                            | 13.5 cm                  | <0.075 cm/yr                                |
| DR-PC-15-08 | 2.5 cm                            | 9.5 cm                   | <0.053 cm/yr                                |

The discrepancy between sediment accumulation rates derived from the CRS age-depth model and estimated rates that account for mixed surface sediments reinforces the problematic nature of determining sediment accumulation rates for an estuarine system such as the Damariscotta River. Integrated sediment accumulation rates, which account of some degree of sediment mixing, suggest that accumulation in the Damariscotta estuary is low, generally less than ~0.075 cm/yr. Despite complicating factors associated with the use CRS age-depth model rates, model results reinforce low accumulation in this system. Both approaches demonstrate that quantifying sediment accumulation rates for an estuary such as the Damariscotta is difficult, particularly where the influx of freshwater and new sediment is very low compared to the magnitude of tidal mixing within the estuary.

Hydrodynamics associated with both core sites are complex, making it difficult to use accumulation rates to differentiate sediment accumulation trends within the estuary. The elongate estuarine geometry, coupled with low freshwater input, results in relatively little new, introduced sediment accumulating. Substantial tidal flushing (tidal prism:  $5.6 \times 10^6 \text{ m}^3$  with an estimated flushing time of 2-4 weeks, McAlice, 1977) likely reworks sediment extensively within the system. In addition to physical processes, surface sediment mixing, as well as burrows present in DR-PC-15-08 at 60-75 cm (Figure 4.12),

indicate the role that bioturbation plays in reworking sediment within the system (Bentley et al., 2014; Nittrouer et al., 1984; Sharma, et al., 1987; Smith et al., 1986).

A comparison of sediment accumulation rates across the North American Atlantic coast (Table 5.3) reveals that accumulation rates are an order of magnitude less than other estuaries in the region. This confirms that, in comparison to other estuaries in the region, Damariscotta River is a sediment-starved system, in which accumulation rates very quite low. The Damariscotta River has a small watershed area, in comparison to the other estuaries in the region (Table 5.3), which likely is an important factor in sedimentation trends.

Table 5.3: Regional comparison of sediment accumulation rates.

| Site                   | Rate (cm/yr) | Source                            |
|------------------------|--------------|-----------------------------------|
| Chesapeake Bay         | 0.3-0.8      | Goldberg et al., 1982; Brush 1984 |
| Hudson River, NY       | 0.1-0.4      | Slagle et al., 2006               |
| Great Bay Estuary, NH  | 30           | Bilgili et al., 2003              |
| Merrymeeting Bay, ME   | 0.243        | Köster et al., 2007               |
| Damariscotta River, ME | < ~0.075 cm  | This Study                        |

## 5.2 Estuarine Framework

Multibeam bathymetry data collected in this study add increased detail and precision to the existing bathymetry map (Shipp, 1989) and reinforce our understanding of the estuarine system as a series of basins punctuated by bedrock sills (Figure 4.1 A). The longitudinal geometry of the Damariscotta River is primarily a consequence of the bedrock framework, although sediment derived from eroding bluffs of glaciomarine mud and recessional moraines, and the hydrodynamics of the estuarine system are also important. Through the collection of extensive seismic reflection profiles, Shipp (1989, Figures 5.4 and 5.5) identified the basin and sill morphology of the system that serves as

the overarching geometric control on the Damariscotta River system. Shipp (1989) also described the distribution of sediment within it (Figure 5.6).

The degree of total (Holocene and Pleistocene) sediment stored in the Damariscotta River varies considerably from the inner to outer estuary. The thickest sediment deposits (in Long and Wadsworth Basins) are in the middle and outer estuary. While more sediment is stored in the upper estuary, deposits are not as thick as the isolated deep deposits in the middle and outer estuary. Accommodation space available in each basin, and likely the time at which each basin was reincorporated into the marine environment during the Holocene sea-level transgression, are critical factors governing sediment accumulation throughout the evolution of this system. Furthermore, the extent of erosion of sediment is critical in the preservation of the stratigraphic record and accumulation of sediment (Belknap et al., 1994). Erosion associated with the sea-level low-stand is evident basal unconformity seen in seismic reflection profiles, and the ravinement unconformity associated with the modern hydrodynamic regime,



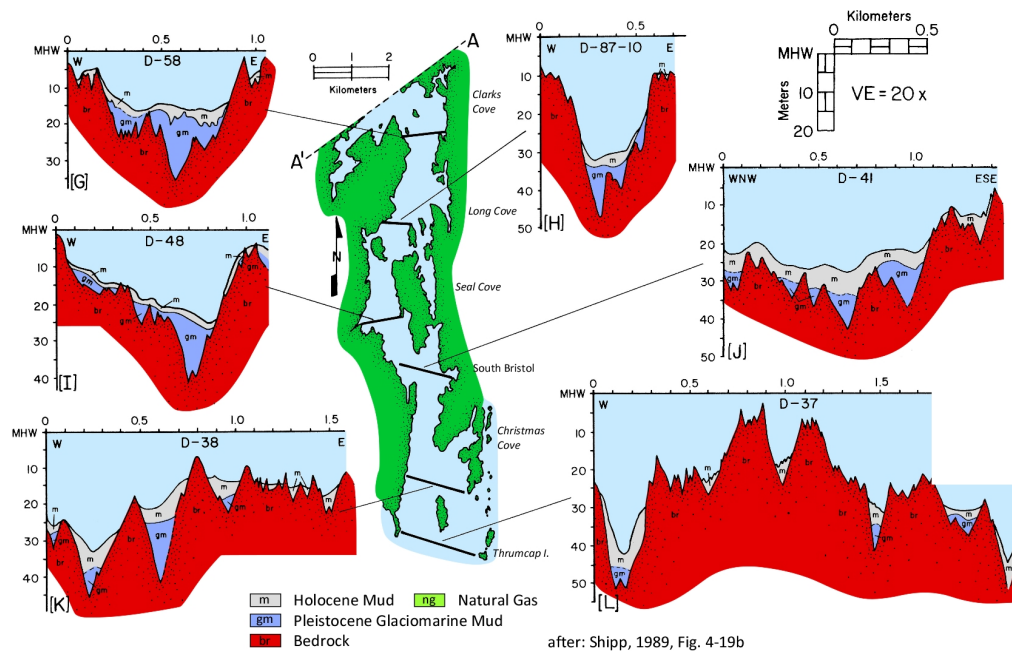


Figure 5.4: Selected seismic reflection profile cross-sections in the southern Damariscotta River. From Shipp (1989), modified by Belknap, D.F. Red represents bedrock, blue represents Pleistocene glaciomarine sediment, gray represents Holocene sediment and green represents natural gas.

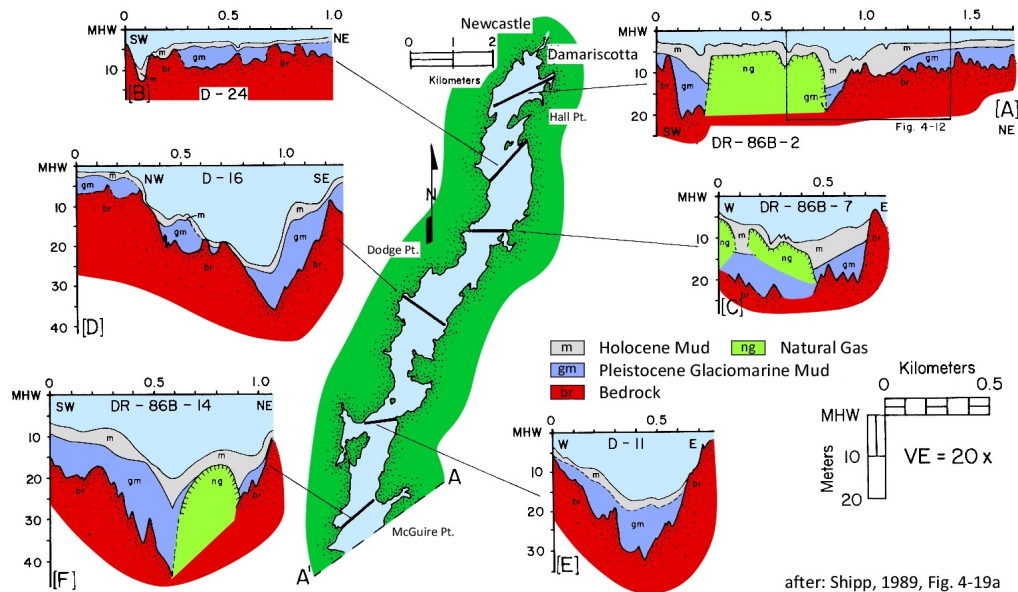


Figure 5.5: Selected seismic reflection profile cross-sections in the northern Damariscotta River. From Shipp (1989), modified by Belknap, D.F. Legend is described in Figure 5.4.

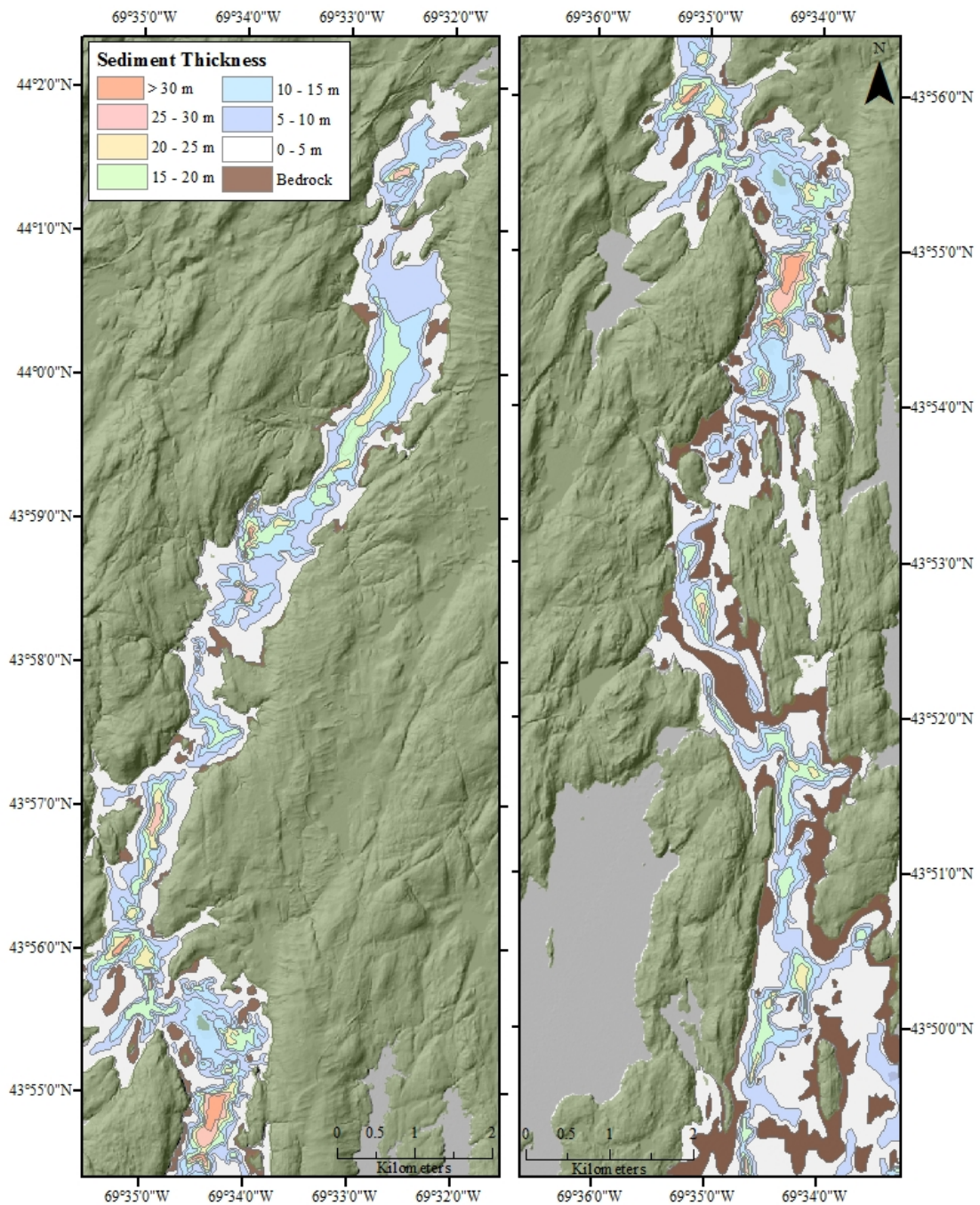


Figure 5.6: Total sediment thickness in the Damariscotta River estuary. Sediment thickness is determined from seismic reflection profiles. Digitized from Shipp, (1989, Figure 4-21). Areas shown as white are predominantly areas for which data does not exist. LiDAR Hillshade DEM is from the Maine Office of GIS (<https://www1.maine.gov/megis/>).

The bathymetry of the river system (Figure 4.1 A) illustrates the roles of bedrock and sediment distribution in estuarine hydrodynamics. Where the bathymetry of the southern Damariscotta River (south of Perkins Point) is controlled primarily by the basin and sill morphology and associated bedrock constriction points (described by Shipp, 1989), the bathymetry of the northern estuary is controlled more by the distribution of sediment and the estuarine thalweg. With little sediment preserved in the outer estuary (Shipp, 1989, Belknap et al., 1994; Figures 5.2, 5.4), any semblance of a thalweg has been largely removed with the erosion of sediment, leaving behind exposed bedrock sills and deep basins. Bedrock constriction points are stripped of sediment, but pockets of sediment are preserved in basins (Figure 5.5; Figure 4.1 B). It is noteworthy, however, that the deepest bathymetric points in the middle and outer basins (i.e., Long and Wadsworth Basins) are adjacent to bedrock constriction points (i.e., Fort Island Narrows and Wentworth Point sill) and are not areas with greatest sediment thickness. Thus, deep depressions result from hydrodynamic processes scouring and eroding sediments adjacent to constriction points, whereas the thickest sediment deposits are located elsewhere in the basin, where hydrodynamic processes have a lesser effect on sediment accumulation and preservation.

In the middle and outer estuary (south of Perkins' Point), where sediment appears generally coarser and harder (Figure 4.1 B), finer sediment is associated with coves (e.g., Dodge Cove, Pleasant Cove) and areas adjacent to coves, where the channel widens sufficiently (e.g., near Lowe's and Clark's Coves) to alter the hydrodynamics and allow for sediment to be preserved at depth. The accumulation of increasingly softer and finer sediment in coves adjacent to the middle and outer estuary reinforces Shipp's (1989)



observation that coves exhibit the same tripartite zonation as the estuarine system (Figure 2.5), but on a smaller scale.

While bedrock constriction points are present throughout the system (Figure 2.3, Figure 4.1), their role in the hydrodynamics of the estuary depends, in part, on the volume of sediment preserved throughout the system. For example, the Goose Ledge Sill, located at the southern end of Day's Basin, (Figure 2.3, Figure 4.1) has a lesser impact on the sediment distribution and volume preserved near Days and Dodge Basin than Glidden Ledge Narrows does on lower Dodge Basin and Wadsworth and Mears Basins (Figures 2.3 and 4.3). The greater volume of sediment stored near the head of the estuary (Figure 2.4) impacts the hydrodynamics of the estuarine system, resulting in a pronounced estuarine thalweg in sediment-choked Days and upper Dodge Basins. In the upper estuary, the volume of sediment appears to play a greater role in the hydrodynamics of the estuarine system than the bedrock framework.

Relict oyster reefs in Dodge Cove protrude into the channel. Erosion-resistant oyster bioherms in other Northeast estuaries play an important role in the hydrodynamics (Carbotte, et al., 2014). Furthermore, modern oyster bioherms may be present near the head of the estuary and could result from modern aquaculture (e.g., the shoal south of Hog Island). These bioherms, combined with the sediment choking, likely affect estuarine hydrodynamics in the upper estuary.

Surficial sediment preserved in the upper estuary is, in general, finer and/or softer than the sediment preserved in the outer estuary (Figure 4.1). Finer sediments in the upper estuary are generally restricted to areas adjacent to the estuarine tidal channel thalweg and in coves, as evidenced by the softer backscatter intensity returns, whereas

harder returns are associated with the thalweg and bedrock constriction points (Figure 4.1). On a smaller scale, this trend was also seen in Days and Lowe's Coves, where similar sub-tidal drainage networks were associated with harder sediments and neighboring flats were softer and muddier.

Current lineations, such as those identified between Perkins Point and Upper Dodge Cove (Figure 4.7), are longitudinal bedforms found in high current areas of estuaries, parallel to the predominant direction of flow (McKinney et al., 1974; Flood, 1983). In the Damariscotta River they appear to indicate a transition from the upper estuarine environment to the middle and outer estuary, in which the basin and sill morphology is the dominant control. North of this area, intertidal and shallow sub-tidal flats are ubiquitous features that border the river thalweg. As a result, the volume and distribution of sediment are critical components of the hydrodynamics in this region of the estuarine system. South of Perkins Point and the current lineations, where the basin and sill morphology is dominant, the bathymetry and surficial sediment are rougher, with only with shallow pockets of softer sediment restricted to coves and areas away from the primary channel of the river. Given their location within the system, the current lineations appear to be a consequence of the shift in factors controlling estuarine hydrodynamics. The breadth of the lineations widens from north to south, as the estuarine thalweg also widens and ultimately becomes defined by the constriction points in the middle and outer estuary.

### 5.3 Estuarine models

In the simplest sense, the Damariscotta River estuary conforms to previously described estuarine models (Pritchard, 1967; Belknap et al., 1986; Dalrymple et al., 1992). The farthest upstream extent of tidal processes and mixing of saline water is Great Salt Bay. Utilizing purely the chemical definition of an estuary (Pritchard, 1967), as the region in which the salinity changes from fresh water to marine, the Damariscotta River estuary stretches from Great Salt Bay to the Narrows at Fort Island, where the salinity transitions to fully marine (McAlice, 1974). The outer extent of the estuary is likely not stationary and may vary, to some degree, with seasons and precipitation events.

Because the freshwater input to the Damariscotta River estuary is low, the effect of fluvial processes in the river is minimal in comparison to marine processes. Tides dominate marine influence here because the elongate geometry restricts the impact of waves to the outer estuary. Unlike the standard conceptual stratigraphic model of a tidally dominated estuary (Dalrymple et al., 1992), in which a tide-dominated estuary is choked by marshes and tidal sand bars, the geometry of the Damariscotta River is ultimately a consequence of the bedrock framework (Shipp, 1989; Belknap et al., 1994). Marshes are scarce in the estuary and fringe features that border coves and the shoreline in the upper estuary. In the outer estuary, steep rocky shorelines and deep basins of the Damariscotta River valley prohibit the development of salt marsh systems. Tidal sand bars, described by Dalrymple et al., (1992) are not features found in the Damariscotta River because of the steep topography of the river valley, limited riverine input of sediment, and the generally fine, marine sediment in the system. Instead, however, tidal and subtidal flats are ubiquitous in the upper estuary north of Perkins Point, particularly in Days Basin and

Great Salt Bay. In contrast to the standard tide-dominated model of estuarine energetics, morphology and sediment facies (Dalrymple et al., 1992), the bedrock geometry is critical to development of the Damariscotta River system and necessary to understanding the hydrodynamics of this environment.

In addition to impacting the hydrodynamics of the estuary, the role of the bedrock geometry of the system is also critical for biological and chemical processes with the estuarine environment. Glidden Ledge, a substantial constriction point separating Dodge Basin from Mears Basin, effectively bisects the estuary into distinctly different environments, in which salinity and temperature vary considerably up- and downstream of this point (Coupland, 2016). In addition to affecting the transgressive development of the estuarine system in a valley incised into glaciomarine sediments and bedrock, the bedrock framework is critical to the establishment and maintenance of modern physical and biological processes acting the estuary.

While the role of bedrock in northeast estuaries was earlier acknowledged (Roman et al., 2000), it is not well documented nor understood. The tripartite zonation model of Maine estuaries (Figure 2.5; Belknap et al., 1986; Kelley, 1987) aptly describes the generalized distribution of sediment within the Damariscotta River yet fails to capture the role of bedrock geometry and constriction points. The rockbound coast of Maine and bathymetry of other estuaries in this region suggest that the role of bedrock in controlling estuarine hydrodynamics is not unique to the Damariscotta River estuary.

While the role of the bedrock framework in the evolution of the Damariscotta River is clear and well studied (Shipp, 1989 and Belknap et al., 1994), a generalized schematic rendering that results from this study incorporates the role of bedrock and

constriction points in the estuarine system (Figure 5.7). Similar to the tripartite zonation described by Belknap et al. (1986), Kelley (1987) and Shipp et al. (1987), I recognize three generalized zones within the Damariscotta River estuary. The upper estuary, from its head in Great Salt Bay to Perkins Point, is sediment choked with extensive intertidal and subtidal flats. A pronounced thalweg, as well as secondary channels cut into the flats and are well defined both by topographic relief and harder, coarser sediments in the channels. Similar channel networks are present in coves throughout the estuary (e.g., Lowe's and Day's Coves). Eroding bluffs, comprised moraines and glacial till deposits may contribute to the sediment supply in the upper estuary. Fringe salt marshes are also present along the shoreline.

The middle estuary is delineated at its innermost extent by the dispersion of the river thalweg and current lineations (e.g., immediately south of Perkins Point), whereas the outer extent is generalized and not well defined. Salt marshes are absent from the middle estuary, with the exception of adjacent coves, and the extent of intertidal and subtidal flats is significantly reduced. While the middle estuary is not sediment choked, erosion resistant relict oyster reefs do affect the hydrodynamics of the system even as the estuary widens. Surface sediment is harder and coarser in the middle of the channel than the inner estuary, yet extensive regions of soft and fine sediment appears well before reaching the coves.

Steep cliffs and rocky shorelines characterize the outer estuary, which is generally devoid of marshes and flats. The bedrock framework determines the breadth of the estuary and surface sediment is generally coarser than in the middle and inner estuary. Eroding bluffs are not present in the outer estuary and marshes or tidal flats are restricted

to coves. The seaward extent of the outer estuary is the Fort Island Narrows, where the salinity transitions to fully marine, though this boundary may vary seasonally and with storm events.

Throughout the estuary, narrow bedrock constriction points, comprised of islands and ledges, punctuate the estuarine system. In addition to creating the overall elongate geometry of the system, the bedrock framework impacts the distribution of sediment within the estuary. Because constriction points create areas of increased current velocities, they are marked by coarse, gravelly sediment and/or exposed bedrock. Thus, even in the upper estuary, marshes and tidal flats are not associated with constriction points. In addition to affecting the distribution of sediment in the estuary, constriction points such as Glidden Ledge, which nearly bisects the estuary, also impact physical, chemical and biological processes in the system.

Together the generalized description of sediment distribution in the Damariscotta River and the idealized models of Maine estuaries (Belknap et al., 1986; Kelley, 1987; Shipp et al., 1987) capture the tripartite zonation of estuaries on the Maine coast and recognize the role bedrock plays systems such as the Damariscotta River. Further analysis is required to determine how closely the generalized tripartite zonation described by Belknap et al. (1986), Kelley (1987) and Shipp et al. (1987) coincides with the estuarine zonation described here and evident in the Damariscotta, however there is some overlap in zone descriptions (i.e. the presence of marshes and tidal flats in the upper estuary). For example, a more detailed study using a combination of sediment cores and sediment traps, to measure net sediment accumulation and gross sedimentation

respectively, would help constrain how tripartite sedimentation zones correspond the estuarine zonation seen in the Damariscotta River.

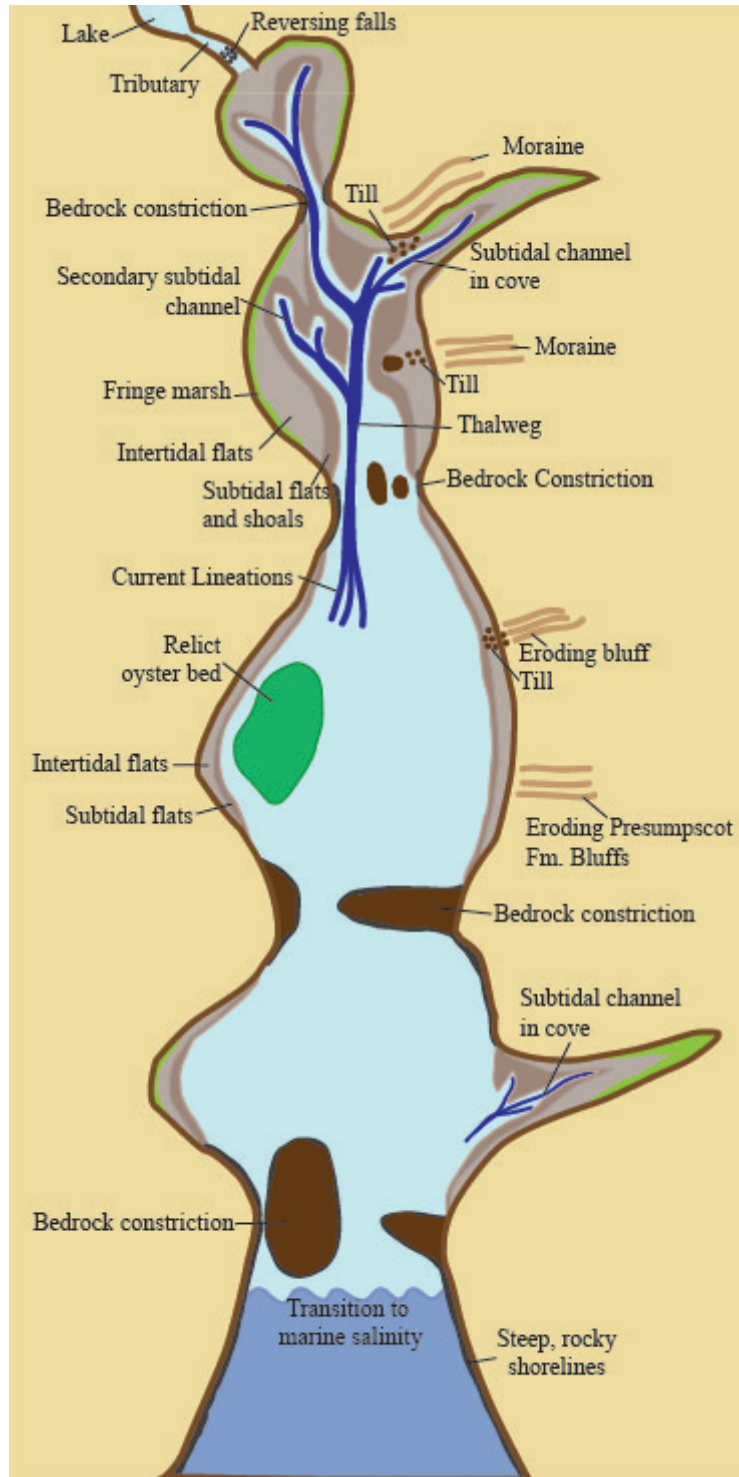


Figure 5.7: A schematic rendering of the Damariscotta River estuary.

The role of bedrock constriction points in the Damariscotta River likely applies to other estuaries in Maine and the northeastern United States and Canadian Maritimes that occupy drowned river valleys. The Saco River estuary, located in the southwestern arcuate embayment compartment of the coast (Figure 1.1; Kelley, 1987) is also punctuated by a series of bedrock constriction points. In contrast to the Damariscotta River and many estuaries in the region, it has considerable freshwater input that is a source of sediment to Saco Bay and neighboring beach systems (Manthorp, 1995; Brothers et al., 2009; Kelley and Brothers, 2008).

In contrast to bedrock constriction points in the Saco and Damariscotta Rivers, the bathymetry of the Sheepscot River that results from the bedrock framework of the estuary is deeper than that of neighboring Kennebec and Damariscotta Rivers. There are no major constriction points in the Sheepscot River until a reversing falls in the town of Sheepscot at the head of the estuary (Belknap et al., 1986). Because of its deep bathymetry, the Sheepscot River experiences significant intrusion of shelf water from the Gulf of Maine, making much of the lower estuary an extension of the ocean (Stickney, 1959). In contrast to the pronounced bedrock sills that prevent such intrusion in the Damariscotta estuary, the introduction of cool, low pH water from offshore into the Sheepscot estuary may make it particularly susceptible to effects of ocean acidification (Thornton and Mayer, 2015).

The role of bedrock constriction points in the Cobscook Bay estuary, an irregularly shaped estuary in the northeast, cliffed shoreline coastal compartment (Kelley, 1987), was recognized and described by Kelley and Kelley (2004). Much like the basin and sill morphology that persists in the Damariscotta River, weaker rock formations in



the Cobscook Bay region were eroded away by glacial and other weathering processes, leaving behind erosion-resistant formations that comprise peninsulas and outcrops within the estuary (Kelley and Kelley, 2004). Because of the complex role of bedrock in rocky and formerly glaciated estuaries such as Cobscook Bay and the Damariscotta River, existing conceptual estuarine models are of limited use in describing the spatial distribution of sediments (Kelley and Kelley, 2004).

While estuarine systems in Maine and the northeast vary considerably in many regards (i.e., volume of freshwater input, the degree of tidal dominance and the extent of bedrock influence), the bedrock framework is critical to distribution of sediment and hydrodynamics within these systems. The role of bedrock is also important in understanding the distribution and circulation contaminants and pollutants in these estuaries, particularly in the context of global climate change and as shoreline development and aquaculture expand along the coast of Maine in the 21<sup>st</sup> century.

## **CHAPTER 6**

### **CONCLUSION**

The bedrock framework of the Damariscotta River valley is critical to the evolution and development of the modern estuary. Multibeam sonar surveys, grab samples and radionuclide analysis of sediment cores reinforce the significance of the basin and sill morphology described by Shipp (1989) and Belknap et al. (1994) and describe the impact of bedrock constriction points on the distribution of sediment within the estuarine system. Furthermore, analyses reveal three estuarine zones similar to those described by Belknap et al. (1986), Kelley (1987) and Shipp et al., (1987). Throughout the system, narrow bedrock constriction points punctuate estuarine zonation and interrupt the distribution of sediment by creating areas of increased current velocities that greatly impact the distribution of sediment within the estuary.

The role of bedrock framework in modern estuarine hydrodynamics is not unique to the Damariscotta River and likely applies to many estuaries on the Maine coast and in the region, such as the Saco and Kennebec, Sheepscot Rivers, as well as Cobscook Bay and likely others. Not only does the bedrock framework have implications for sediment distribution, but also chemical and biological processes and the distribution of chemicals and pollutants within the estuary. In the context of global climate change, and with the continued shoreline development and expansion of aquaculture in the state of Maine, understanding the role that the bedrock framework of drowned river valleys impacts modern estuaries is critically important.

## REFERENCES CITED

Anderson, F.E., Black, L., Watling, L.E., Mook, W., and Mayer, L.M., 1981, A temporal and spatial study of mudflat erosion and deposition: *Journal of Sedimentary Petrology*, v. 51, p. 729-736.

Anderson, R.F., Schiff, S.L., and Hesslein, R.H., 1987, Determining sediment accumulation and mixing rates using  $^{210}\text{Pb}$ ,  $^{137}\text{Cs}$ , and other tracers: Problems due to postdepositional mobility or coring artifacts: *Canadian Journal of Fisheries and Aquatic Sciences*, v. 44, p. s231-s250.

Anderson, R.S., Miller, N.G., Davis, R.B., and Nelson, R.E., 1990, Terrestrial fossils in the marine Presumpscot Formation: implications for Late Wisconsinan paleoenvironments and isostatic rebound along the coast of Maine: *Canadian Journal of Earth Sciences*, v. 27, p. 1241-1246.

Appleby, P., and Oldfield, F., 1983, The assessment of  $^{210}\text{Pb}$  data from sites with varying sediment accumulation rates, *in* *Paleolimnology*: Springer, p. 29-35.

Barnhardt, W.A., Belknap, D.F., and Kelley, J.T., 1997, Stratigraphic evolution of the inner continental shelf in response to late Quaternary relative sea-level change, northwestern Gulf of Maine: *Geological Society of America Bulletin*, v. 109, p. 612-630.

Baskaran, M., and Naidu, A., 1995,  $^{210}\text{Pb}$ -derived chronology and the fluxes of  $^{210}\text{Pb}$  and  $^{137}\text{Cs}$  isotopes into continental shelf sediments, East Chukchi Sea, Alaskan Arctic: *Geochimica Et Cosmochimica Acta*, v. 59, p. 4435-4448.

Belknap, D.F., Andersen, B.G., Anderson, R.S., Anderson, W.A., Borns, H.W., Jr., Jacobson, G., Jr., Kelley, J.T., Shipp, R.C., Smith, D.C., Stuckenrath, R. Jr., Thompson, W.B., and Tyler, D.A., 1987, Late Quaternary sea-level changes in Maine: In: D. Nummedal, O.H. Pilkey, Jr. and J.D. Howard, eds., *Sea-Level Fluctuation and Coastal Evolution*, Society of Economic Paleontologists and Mineralogists Special Pub. 41, p. 71-85.

Belknap, D.F., Kelley, J.T. and Shipp, R.C., 1987, Quaternary stratigraphy of representative Maine estuaries: initial examination by high-resolution seismic reflection profiling: In: D.M. FitzGerald and P.S. Rosen, eds. *Glaciated Coasts*, Academic Press, San Diego p. 177-207.

Belknap, D.F., Kraft, J.C., and Dunn, R.K., 1994, Transgressive valley-fill lithosomes: Delaware and Maine: *Incised-Valley Systems: Origin and Sedimentary Sequences*, v. 1, p. 303.

Belknap, D.F. and Shipp, R.C., 1986, Quaternary geology of the Damariscotta estuary: In: D.W. Newberg, ed., Guidebook for Field Trips in Southwestern Maine; NEIGC 78<sup>th</sup> Ann Mtg., Bates College, Lewiston, ME. Trip B-9, p. 254-274.

Belknap, D.F. and Shipp, R.C., 1991, Seismic stratigraphy of glacial-marine units, Maine inner shelf: In: J.B. Anderson and G.M. Ashley, eds., Glacial-Marine Sedimentation; Paleoclimatic significance, Geological Society of America Special Paper 261, p. 137-157.

Belknap, D.F., Shipp, R.C., and Kelley, J.T., 1986, Depositional setting and Quaternary stratigraphy of the Sheepscot Estuary, Maine: a preliminary report: *Géographie Physique et Quaternaire*, v. 40, p. 55-69.

Bentley, S.J., Swales, A., Pyenson, B., and Dawe, J., 2014, Sedimentation, bioturbation, and sedimentary fabric evolution on a modern mesotidal mudflat: A multi-tracer study of processes, rates, and scales: *Estuarine, Coastal and Shelf Science*, v. 141, p. 58-68.

Bilgili, A., Swift, M., Lynch, D., and Ip, J., 2003, Modeling bed-load transport of coarse sediments in the Great Bay Estuary, New Hampshire: *Estuarine, Coastal and Shelf Science*, v. 58, p. 937-950.

Bloom, A.L., 1963, Late-Pleistocene fluctuations of sea level and postglacial & crustal rebound in coastal Maine: *American Journal of Science*, v. 261, pp. 862-879.

Borns, H.W., Jr., Doner, L.A., Dorion, C.C., Jacobson, G.L., Jr., Kaplan, M.R., Kreutz, K.J., Lowell, T.V., Thompson, W.B. and Weddle, T.K., 2004, The deglaciation of Maine, U.S.A., in: J. Ehlers and P.L. Gibbard, eds., Quaternary Glaciations - Extent and Chronology, Part II, Elsevier B.V., p. 89-109.

Bratton, J.F., Colman, S.M., Thieler, E.R., and Seal, R.R., 2002, Birth of the modern Chesapeake Bay estuary between 7.4 and 8.2 ka and implications for global sea-level rise: *Geo-Marine Letters*, v. 22, p. 188-197.

Brothers, L., Belknap, D., Kelley, J., and Janzen, C., 2008, Sediment transport and dispersion in a cool-temperate estuary and embayment, Saco River estuary, Maine, USA: *Marine Geology*, v. 251, p. 183-194.

Brush, G.S., 1984, Patterns of recent sediment accumulation in Chesapeake Bay (Virginia—Maryland, USA) tributaries: *Chemical Geology*, v. 44, p. 227-242.

Brush, G.S., 1989, Rates and patterns of estuarine sediment accumulation. *Limnology and Oceanography*, v. 34, p. 1235-1246.

Brush, G.S., Martin, E.A., DeFries, R.S., and Rice, C.A., 1982, Comparisons of <sup>210</sup>Pb and pollen methods for determining rates of estuarine sediment accumulation: *Quaternary Research*, v. 18, p. 196-217.

Cahl, D.L., 2012, Diffusion coefficients calculated using  $^{137}\text{Cs}$  profiles applied to  $^{210}\text{Pb}$  dating in lake core sediments: M.S. Thesis, Physics, University of Maine, Orono, 108 pp.

Carbotte, S., Bell, R., Ryan, W., McHugh, C., Slagle, A., Nitsche, F., and Rubenstone, J., 2004, Environmental change and oyster colonization within the Hudson River estuary linked to Holocene climate: *Geo-Marine Letters*, v. 24, p. 212-224.

Colman, S.M., and Bratton, J.F., 2003, Anthropogenically induced changes in sediment and biogenic silica fluxes in Chesapeake Bay: *Geology*, v. 31, p. 71-74.

Cooper, S.R., and Brush, G.S., 1991, Long-term history of Chesapeake Bay anoxia. *Science*(Washington), v. 254, p. 992-996.

Coupland, C.M., 2016, Understanding shellfish growth in the Damariscotta River Estuary using a coupled modeling approach: *Estuarine and Coastal Modeling Conference*, 14<sup>th</sup>, Kingston, RI., Abstracts, v. 1., p. 4.

Cronin, T., Willard, D., Karlsen, A., Ishman, S., Verardo, S., McGeehin, J., Kerhin, R., Holmes, C., Colman, S., and Zimmerman, A., 2000, Climatic variability in the eastern United States over the past millennium from Chesapeake Bay sediments: *Geology*, v. 28, p. 3-6.

Cronon, W., 1983, *Changes in the Land: Indians, Colonists, and the Ecology of New England* (New York: Hill and Wang, 1983).

Dalrymple, R.W., Zaitlin, B.A., and Boyd, R., 1992, Estuarine facies models: conceptual basis and stratigraphic implications: perspective: *Journal of Sedimentary Research*, v. 62, no. 6., p.1130-1146.

Davies, C.P., 1992, Estuarine preservation potential model for archaeological sites in coastal Maine: M.S. Thesis, Inst. Quaternary Studies, University of Maine, Orono, 195 pp.

Dorion, C.C., Balco, G.A., Kaplan, M.R., Kruetz, K., Wright, J.D., and Borns, H.W., 2001, Stratigraphy, paleoceanography, chronology, and environment during deglaciation of eastern Maine: *Special Papers-Geological Society of America*, p. 215-242.

Flood, R.D., 1983, Classification of sedimentary furrows and a model for furrow initiation and evolution: *Geological Society of America Bulletin*, v. 94, p. 630-639.

Folk, R.L., 1957, *Petrology of sedimentary rocks*: Hemphill Publishing Company. 190 p.

Goldberg, E.D., Hodge, V., Koide, M., Griffin, J., Gamble, E., Bricker, O.P., Matisoff, G., Holdren, G.R., and Braun, R., 1978, A pollution history of Chesapeake Bay: *Geochimica Et Cosmochimica Acta*, v. 42, p.1413-1425.

- Grizzle, R.E., Brodeur, M.A., Abeels, H.A., and Greene, J.K., 2008, Bottom habitat mapping using towed underwater videography: subtidal oyster reefs as an example application: *Journal of Coastal Research*, p. 103-109.
- Hannum, M.B., 1997, Late Quaternary Evolution of the Kennebec and Damariscotta River Estuaries, Maine. M.S. Thesis, Dept. Geological Sciences, Univ. Maine, Orono, 98 pp.
- Kelley, J.T., 1987, Inventory of Coastal Environments and Classification of Maine's Glaciated Shoreline: *Glaciated Coasts*. Academic Press, Inc. New York, p 151-176.
- Kelley, J.T., Belknap, D.F., and Claesson, S., 2010, Drowned coastal deposits with associated archaeological remains from a sea-level "slowstand": Northwestern Gulf of Maine, USA: *Geology*, v. 38, p. 695-698.
- Kelley, J.T., Belknap, D.F., Kelley, A.R., and Claesson, S.H., 2013, A model for drowned terrestrial habitats with associated archeological remains in the northwestern Gulf of Maine, USA: *Marine Geology*, v. 338, p. 1-16.
- Kelley, J.T., and Brothers, L.L., 2009, Camp Ellis, Maine: A small beach community with a big problem... its jetty: *Geological Society of America Special Papers*, v. 460, p. 1-20.
- Kelley, J.T., and Kelley, A.R., 2004, Controls on surficial materials distribution in a rock-framed, glaciated, tidally dominated estuary: Cobscook Bay, Maine: *Northeastern Naturalist*, v. 11, p. 51-74.
- Köster, D., Lichter, J., Lea, P.D., and Nurse, A., 2007, Historical eutrophication in a river-estuary complex in mid-coast Maine: *Ecological Applications*, v. 17, p. 765-778.
- Landis, J.D., Renshaw, C.E., and Kaste, J.M., 2016, Beryllium-7 and lead-210 chronometry of modern soil processes: The Linked Radionuclide accumulation model, *LRC: Geochimica et Cosmochimica Acta*, v. 180, p. 109-125.
- Leach, P.A., 2007, Marine geoarchaeological investigation of Damariscotta River, Maine, USA: Unpublished M.S. Thesis, Climate Change Institute, University of Maine, Orono, 164 pp.
- Leach, P.A. and Belknap, D.F., 2007, Marine geophysics and vibracoring applied to the search for submerged prehistory in Damariscotta River, Maine, USA. In: L. Wilson, P. Dickinson and J. Jeandron, eds., *Reconstructing Human-Landscape Interactions*, Cambridge Scholars Publishing, Newcastle, UK, Chapter 8, p. 141-158.
- Lu, X., and Matsumoto, E., 2005, Recent sedimentation rates derived from <sup>210</sup>Pb and <sup>137</sup>Cs methods in Ise Bay, Japan: *Estuarine, Coastal and Shelf Science*, v. 65, p. 83-93.

- Manthorp, P.A., 1995, Estuarine circulation and sediment transport in the Saco River estuary, Maine: M.S. Thesis, Boston University, Boston, MA, 230 pp.
- McAlice, B.J., 1977, A preliminary oceanographic survey of the Damariscotta River estuary, Lincoln County, Maine: Maine Sea Grant Technical Report.
- McKinney, T.F., Stubblefield, W.L., and Swift, D.J., 1974, Large-scale current lineations on the central New Jersey shelf: investigations by side-scan sonar: *Marine Geology*, v. 17, p. 79-102.
- Meade, R.H., 1982, Sources, sinks, and storage of river sediment in the Atlantic drainage of the United States: *The Journal of Geology*, p. 235-252.
- Molnia, B.F., 1974, A rapid and accurate method for the analysis of calcium carbonate in small samples: *Journal of Sedimentary Research*, v. 44.
- Nichols, F.H., Cloern, J.E., Luoma, S.N., and Peterson, D.H., 1986, The modification of an estuary. *Science*(Washington), v. 231, p. 567-573.
- Nittrouer, C., DeMaster, D., Mckee, B.A., Cutshall, N., and Larsen, I., 1984, The effect of sediment mixing on Pb-210 accumulation rates for the Washington continental shelf: *Marine Geology*, v. 54, p. 201-221.
- Nittrouer, C., Sternberg, R., Carpenter, R., and Bennett, J., 1979, The use of Pb-210 geochronology as a sedimentological tool: application to the Washington continental shelf: *Marine Geology*, v. 31, p. 297-316.
- Osberg, P.H., Hussey, A.M., Tucker, R.D., Boone, G.M., Loiselle, M.C., and Trefethen, J.M., 1985, Bedrock geologic map of Maine: Maine Geological Survey, Augusta, ME, 1:500,000.
- Pritchard, D.W., 1967, What is an estuary? Physical viewpoint, *in*, Lauff, G.H., ed., *Estuaries: American Association for the Advancement of Science, Publication 83*, p. 3-5.
- Roman, C.T., Jaworski, N., Short, F.T., Findlay, S., and Warren, R.S., 2000, Estuaries of the northeastern United States: habitat and land use signatures: *Estuaries*, v. 23, p. 743-764.
- Ryan, J.J., and Goodell, H., 1972, Marine geology and estuarine history of Mobile Bay, Alabama part 1. Contemporary sediments: *Geological Society of America Memoirs*, v. 133, p. 517-554.
- Sanger, D., and Belknap, D., 1987, Human responses to changing marine environments in the Gulf of Maine, *in* *Man and the Mid-Holocene Climatic Optimum: Proceedings of the 17'th Annual Chacmool Conference*, Dept. Archaeology, Univ. Calgary, p. 245-261.

Schnitker, D., Belknap, D.F., Bacchus, T.S., Friez, J.K., Lusardi, B.A. and Popek, D.M., 2001, Deglaciation of the Gulf of Maine, In: Weddle, T.K. and Retelle, M.J., eds., Deglacial History and Relative Sea-Level Changes, Northern New England and Adjacent Canada, Boulder Colorado, Geological Society of America Paper 351, p. 9-34.

Sharma, P., Gardner, L., Moore, W., and Bollinger, A., 1987, Sedimentation and bioturbation in a salt marsh as revealed by  $^{210}\text{Pb}$ ,  $^{137}\text{Cs}$ , and  $^7\text{Be}$  studies. *Limnology and Oceanography*, v. 32, p. 313-326.

Shipp, R.C., 1989, Late Quaternary sea-level fluctuations and geologic evolution of four embayments and adjacent inner shelf along the northwestern Gulf of Maine. Ph.D. Dissertation, Oceanography Program, Univ. of Maine, 832 pp.

Slagle, A., Ryan, W., Carbotte, S., Bell, R., Nitsche, F., and Kenna, T., 2006, Late-stage estuary infilling controlled by limited accommodation space in the Hudson River: *Marine Geology*, v. 232, p. 181-202.

Smith, J.N., Boudreau, B.P., and Noshkin, V., 1986, Plutonium and  $^{210}\text{Pb}$  distributions in northeast Atlantic sediments: subsurface anomalies caused by non-local mixing: *Earth and Planetary Science Letters*, v. 81, p. 15-28.

Stickney, A.P., 1959, Ecology of the Sheepscot River estuary: US Department of Interior, US Fish and Wildlife Service Special Scientific Report-Fisheries, 309, 21 p.

Stuiver, M. and H.W. Borns, Jr., 1975, Late Quaternary marine invasion in Maine: Its chronology and associated crustal movement: *Geological Society of America Bulletin*, v. 86, p. 99-104.

Sugai, S.F., Alperin, M.J., and Reeburgh, W.S., 1994, Episodic deposition and  $^{137}\text{Cs}$  immobility in Skan Bay sediments: a ten-year  $^{210}\text{Pb}$  and  $^{137}\text{Cs}$  time series: *Marine Geology*, v. 116, p. 351-372.

Thompson, W.B., Crossen, K., Borns Jr, H., and Andersen, B., 1989, Glaciomarine deltas of Maine and their relation to late Pleistocene–Holocene crustal movements, *in* *Neotectonics of Maine*: Maine Geological Survey Augusta, p. 43-67.

Thompson, W.B., Griggs, C.B., Miller, N.G., Nelson, R.E., Weddle, T.K., and Kilian, T.M., 2011, Associated terrestrial and marine fossils in the late-glacial Presumpscot Formation, southern Maine, USA, and the marine reservoir effect on radiocarbon ages: *Quaternary Research*, v. 75, p. 552-565.

Thompson, W.B. and Borns, H.W., Jr., 1985, Surficial Geologic Map of Maine, Maine Geological Survey, Augusta, Maine 1:500,000.

Thornton, K., and Mayer, L.M., 2015, Estuarine Monitoring Program Summary Report 2014: Maine Coastal Observing Alliance (MCOA).



Wilson, K.R., Kelley, J.T., Tanner, B.R., and Belknap, D.F., 2010, Probing the origins and stratigraphic signature of salt pools from north-temperate marshes in Maine, USA: *Journal of Coastal Research*, v. 26, p. 1007-1026.

Wolman, M.G., 1967, A cycle of sedimentation and erosion in urban river channels: *Geografiska Annaler, Series A, Physical Geography*, p. 385-395.

## APPENDIX A: SECONDARY ANALYSIS OF CORE DR-PC-15-07

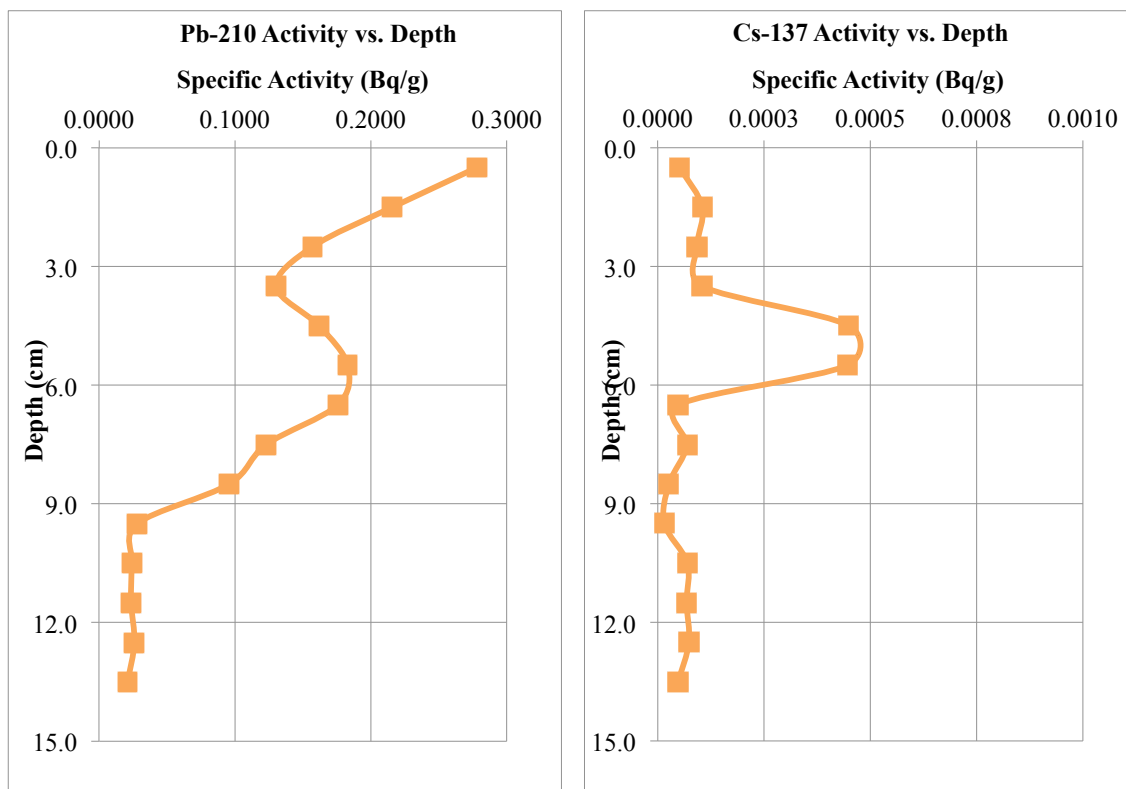


Figure A.1. Secondary analysis of DR-PC-15-07. A secondary analysis of radionuclides  $^{210}\text{Pb}$  and  $^{137}\text{Cs}$  activities included only samples at 4.5, 5.5, 6.5 and 7.5 cm depth in the core. Other data are from the initial analysis of Dr-PC-15-07.

## APPENDIX B: SEDIMENT CORE PHOTOS AND LOGS

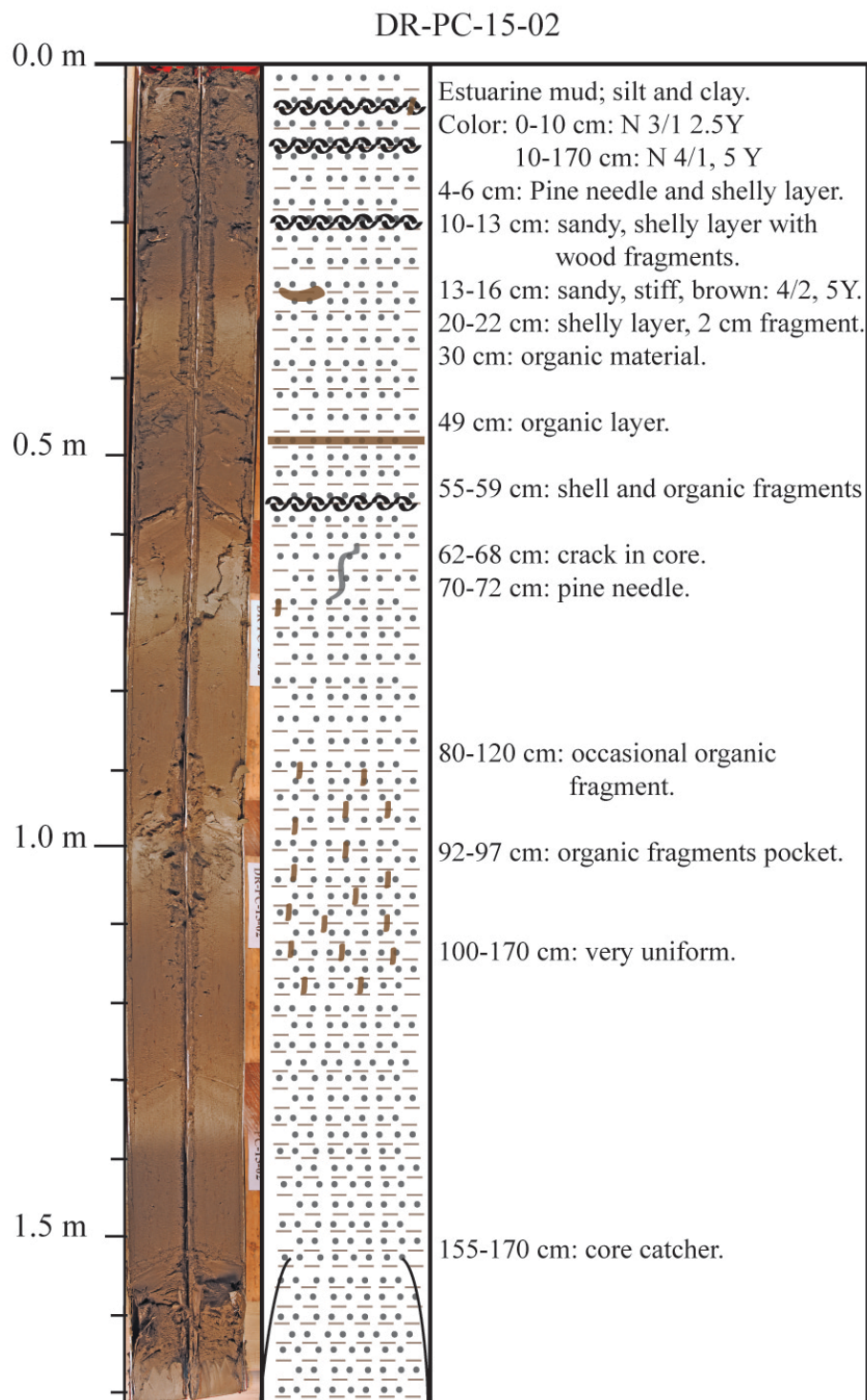


Figure B.1. DR-PC-15-02 sediment core log from Long Cove.

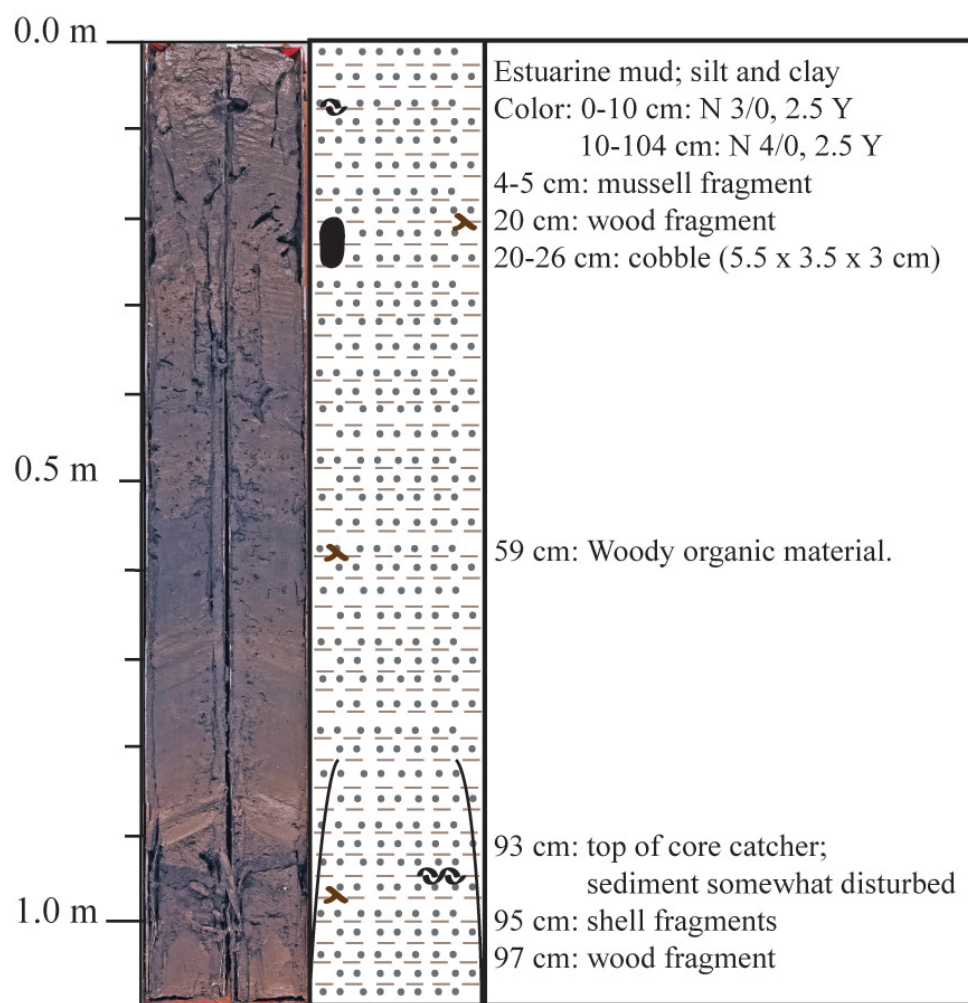


Figure B.2: DR-PC-15-07 sediment core log from Upper Dodge Cove.

## APPENDIX C: SEDIMENT GRAB SAMPLE SITES AND ANALYSIS

Table C.1: Sediment grab sample sites.

| <b>SAMPLE ID</b> | <b>NORTH<br/>LATITUDE</b> | <b>WEST<br/>LONGITUDE</b> | <b>LOCATION DESCRIPTION</b>                  |
|------------------|---------------------------|---------------------------|--|
| DR-BS-15-01      | 43 54.231                 | 69 33.998                 | Mouth of Long Cove                           |
| DR-BS-15-02      | 43 54.095                 | 69 34.223                 | Outer Mouth of Farmer's Cove                 |
| DR-BS-15-03      | 43 54.054                 | 69 34.169                 | Inner Mouth of Farmer's Cove                 |
| DR-BS-15-04      | 43 54.017                 | 69 34.143                 | Outer Farmer's Cove                          |
| DR-BS-15-05      | 43 53.804                 | 69 34.337                 | Outer Seal Cove                              |
| DR-BS-15-06      | 43 54.145                 | 69 34.427                 | Middle of River; NW of Seal Cove             |
| DR-BS-15-07      | 43 54.42                  | 69 34.478                 | Middle of River; W of Long Cove shoal        |
| DR-BS-15-08      | 43 54.68                  | 69 34.43                  | Middle of River, N of GB 8                   |
| DR-BS-15-09      | 43 55.609                 | 69 34.087                 | Outer Clark's Cove                           |
| DR-BS-15-10      | 43 55.725                 | 69 34.676                 | Immediately S of Maguire Point               |
| DR-BS-15-11      | 43 56.245                 | 69 35.043                 | Immediately S of Lowe's Cove, E shore        |
| DR-BS-15-12      | 43 56.112                 | 69 35.175                 | Due W of DMC Dock                            |
| DR-BS-15-13      | 43 55.935                 | 69 34.83                  | Mouth of Lowe's Cove                         |
| DR-BS-15-14      | 43 58.831                 | 69 33.838                 | Dodge Cove                                   |
| DR-BS-15-15      | 43 59.119                 | 69 33.336                 | SE of Dodge Point                            |
| DR-BS-15-16      | 43 59.734                 | 69 32.852                 | Current Lineations, Upper Dodge Cove         |
| DR-BS-15-17      | 43 59.742                 | 69 32.793                 | Current Lineations, Upper Dodge Cove         |
| DR-BS-15-18      | 43 59.742                 | 69 32.82                  | Current Lineations, Upper Dodge Cove         |
| DR-BS-15-19      | 43 59.74                  | 69 32.719                 | E of Current Lineations                      |
| DR-BS-15-20      | 43 59.665                 | 69 32.659                 | N of Prentiss Island                         |
| DR-BS-15-21      | 43 59.973                 | 69 32.493                 | Middle of River, S of "15", Mook Aquaculture |
| DR-BS-15-22      | 43 54.689                 | 69 34.247                 | Due E of GB9, NW of Peters Is.               |

Table C.2: Grain Size Analysis Results. Backscatter intensity values are taken from MBES dataset. All other values were determined through grain size analysis in the laboratory.

| Sample ID   | Backscatter Intensity (%) | Moisture Content % Water | Dry Sediment Composition |          |         |        |        |
|-------------|---------------------------|--------------------------|--------------------------|----------|---------|--------|--------|
|             |                           |                          | Gravel (g)               | Sand (g) | Mud (g) | % Silt | % Clay |
| DR-BS-15-01 | 29                        | 59.81%                   | 0.03                     | 15.70    | 39.75   | 36.62% | 35.04% |
| DR-BS-15-02 | 81                        | 26.76%                   | 20.77                    | 20.15    | 6.84    | 2.10%  | 12.23% |
| DR-BS-15-03 | 54                        | 55.05%                   | 0.30                     | 19.11    | 15.64   | 17.36% | 27.25% |
| DR-BS-15-04 | 37                        | 69.99%                   | 0.02                     | 3.10     | 19.39   | 22.18% | 63.98% |
| DR-BS-15-05 | 37                        | 67.94%                   | 0.07                     | 2.66     | 18.87   | 25.84% | 61.52% |
| DR-BS-15-06 | 57                        | 27.10%                   | 1.39                     | 66.23    | 10.22   | 1.32%  | 11.81% |
| DR-BS-15-07 | 81                        | 33.68%                   | 26.91                    | 16.21    | 7.08    | 1.80%  | 12.30% |
| DR-BS-15-08 | 42                        | 64.05%                   | 0.26                     | 7.05     | 20.06   | 8.68%  | 64.61% |
| DR-BS-15-09 | 39                        | 53.36%                   | 0.08                     | 18.17    | 18.67   | 17.40% | 33.18% |
| DR-BS-15-10 | 85                        | 14.04%                   | 60.90                    | 18.90    | 8.25    | 1.93%  | 7.44%  |
| DR-BS-15-11 | 68                        | 29.80%                   | 0.63                     | 46.09    | 3.05    | 1.40%  | 4.72%  |
| DR-BS-15-12 | 53                        | 41.01%                   | 0.51                     | 36.26    | 15.22   | 8.82%  | 20.45% |
| DR-BS-15-13 | 45                        | 61.32%                   | 0.00                     | 2.86     | 19.92   | 30.13% | 57.29% |
| DR-BS-15-14 | 31                        | 64.96%                   | 0.00                     | 1.88     | 25.73   | 48.22% | 44.96% |
| DR-BS-15-15 | 73                        | 35.05%                   | 22.88                    | 28.69    | 9.90    | 4.61%  | 11.50% |
| DR-BS-15-16 | 39                        | 60.69%                   | 0.00                     | 1.32     | 27.50   | 55.65% | 39.76% |
| DR-BS-15-17 | 37                        | 44.93%                   | 0.22                     | 13.45    | 36.49   | 32.72% | 40.04% |
| DR-BS-15-18 | 32                        | 59.24%                   | 0.01                     | 2.54     | 37.63   | 47.41% | 46.24% |
| DR-BS-15-19 | 68                        | 39.51%                   | 3.73                     | 22.88    | 35.76   | 23.56% | 33.78% |
| DR-BS-15-20 | 81                        | 38.26%                   | 19.51                    | 32.75    | 8.96    | 5.82%  | 8.81%  |
| DR-BS-15-21 | 32                        | 61.56%                   | 0.02                     | 5.67     | 33.64   | 40.19% | 45.33% |
| DR-BS-15-22 | 67                        | 31.91%                   | 1.06                     | 62.33    | 5.70    | 0.83%  | 7.42%  |

## APPENDIX D: SEDIMENT CORE ANALYSIS

Table D.1: Summary of sediment core and radionuclide analysis.

| DR-PC-15-02: Long Cove   |                |                 |                 |  |  |  |
|--------------------------|----------------|-----------------|-----------------|--|--|--|
| Depth (cm)               | Wet Sample (g) | % Water by Mass | % LOI (organic) | <sup>210</sup> Pb Specific Activity (Bq/g) | <sup>210</sup> Pb Specific Activity +/- (Bq/g) | <sup>137</sup> Cs Specific Activity (Bq/g) |
| 0.0-1.0                  | 4.5427         | 58.31%          | 10.88%          | 21.651%                                    | 0.037%   | 0.018%                                     |
| 1.0-2.0                  | 3.3589         | 44.03%          | 6.60%           | 15.852%                                    | 0.033%   | 0.009%                                     |
| 2.0-3.0                  | 4.3491         | 40.41%          | 5.05%           | 3.312%                                     | 0.015%   | 0.007%                                     |
| 3.0-4.0                  | 4.5974         | 30.76%          | 3.26%           | 2.513%                                     | 0.012%   | 0.007%                                     |
| 4.0-5.0                  | 4.1471         | 18.58%          | 1.89%           | 3.161%                                     | 0.012%   | 0.002%                                     |
| 5.0-6.0                  | 4.4754         | 24.04%          | 2.88%           | 2.962%                                     | 0.011%   | 0.002%                                     |
| 6.0-7.0                  | 2.9276         | 24.85%          | 4.72%           | 2.815%                                     | 0.016%   | 0.015%                                     |
| 7.0-8.0                  | 3.0355         | 22.24%          | 2.37%           | 2.795%                                     | 0.015%   | 0.011%                                     |
| 8.0-9.0                  | 3.3544         | 20.86%          | 1.73%           | 2.610%                                     | 0.012%   | 0.006%                                     |
| 9.0-1.0                  | 3.2817         | 16.65%          | 1.83%           | 2.261%                                     | 0.012%   | 0.009%                                     |
| 10.0-11.0                | 3.5902         | 21.59%          | 2.23%           | 1.790%                                     | 0.011%   | 0.008%                                     |
| 11.0-12.0                | 3.4404         | 12.99%          | 1.12%           | 1.679%                                     | 0.010%   | 0.009%                                     |
| 12.0-13.0                | 3.7537         | 19.47%          | 2.05%           | 1.398%                                     | 0.010%   | 0.009%                                     |
| DR-PC-15-04: Lowe's Cove |                |                 |                 |  |  |  |
| Depth (cm)               | Wet Sample (g) | % Water by Mass | % LOI (organic) | <sup>210</sup> Pb Specific Activity (Bq/g) | <sup>210</sup> Pb Specific Activity +/- (Bq/g) | <sup>137</sup> Cs Specific Activity (Bq/g) |
| 0.0-1.0                  | 2.1864         | 62.16%          | 9.31%           | 1.900E-01                                  | 5.824E-04                                      | 2.154E-03                                  |
| 1.0-2.0                  | 2.6746         | 62.95%          | 9.85%           | 1.527E-01                                  | 4.583E-04                                      | 1.488E-03                                  |
| 2.0-3.0                  | 3.8925         | 60.67%          | 9.19%           | 2.475E-01                                  | 4.671E-04                                      | 1.766E-03                                  |
| 3.0-4.0                  | 3.6523         | 60.66%          | 8.63%           | 2.539E-01                                  | 4.965E-04                                      | 1.420E-03                                  |
| 4.0-5.0                  | 3.1853         | 62.33%          | 9.06%           | 2.722E-01                                  | 5.447E-04                                      | 1.529E-03                                  |
| 5.0-6.0                  | 2.8788         | 57.36%          | 9.19%           | 2.730E-01                                  | 5.443E-04                                      | 1.469E-03                                  |
| 6.0-7.0                  | 4.3448         | 57.00%          | 8.86%           | 1.799E-01                                  | 3.894E-04                                      | 2.131E-03                                  |
| 7.0-8.0                  | 3.4509         | 60.93%          | 8.36%           | 2.072E-01                                  | 4.501E-04                                      | 1.177E-03                                  |
| 8.0-9.0                  | 3.2172         | 61.14%          | 8.17%           | 1.628E-01                                  | 4.408E-04                                      | 1.244E-03                                  |

| Depth (cm) | Wet Sample (g) | % Water by Mass | % LOI (organic) | <sup>210</sup> Pb Specific Activity (Bq/g) | <sup>210</sup> Pb Specific Activity +/- (Bq/g) | <sup>137</sup> Cs Specific Activity (Bq/g) | <sup>137</sup> Cs Specific Activity +/- (Bq/g) |
|------------|----------------|-----------------|-----------------|--|--|--|--|
| 9.0-1.0    | 3.0772         | 61.24%          | 9.24%           | 1.524E-01                                  | 4.412E-04                                      | 1.597E-03                                  | 2.232E-04                                      |
| 10.0-11.0  | 3.6512         | 64.05%          | 9.83%           | 1.323E-01                                  | 3.989E-04                                      | 1.386E-03                                  | 2.064E-04                                      |
| 11.0-12.0  | 3.4816         | 63.16%          | 9.22%           | 1.337E-01                                  | 4.036E-04                                      | 1.159E-03                                  | 2.067E-04                                      |
| 12.0-13.0  | 3.1017         | 63.23%          | 9.56%           | 1.174E-01                                  | 3.987E-04                                      | 1.348E-03                                  | 2.220E-04                                      |
| 13.0-14.0  | 4.1591         | 62.31%          | 9.06%           | 8.385E-02                                  | 2.878E-04                                      | 1.046E-03                                  | 1.664E-04                                      |
| 14.0-15.0  | 3.4828         | 62.31%          | 9.02%           | 1.038E-01                                  | 3.413E-04                                      | 1.158E-03                                  | 1.935E-04                                      |
| 15.0-16.0  | 3.5252         | 62.37%          | 9.97%           | 1.001E-01                                  | 3.379E-04                                      | 1.446E-03                                  | 2.055E-04                                      |
| 16.0-17.0  | 3.0160         | 62.70%          | 9.99%           | 1.141E-01                                  | 3.886E-04                                      | 1.719E-03                                  | 2.350E-04                                      |

**DR-PC-15-07: Upper Dodge Cove**

| Depth (cm) | Wet Sample (g) | % Water by Mass | % LOI (organic) | <sup>210</sup> Pb Specific Activity (Bq/g) | <sup>210</sup> Pb Specific Activity +/- (Bq/g) | <sup>137</sup> Cs Specific Activity (Bq/g) | <sup>137</sup> Cs Specific Activity +/- (Bq/g) |
|------------|----------------|-----------------|-----------------|--|--|--|--|
| 0.0-1.0    | 2.3509         | 49.30%          | 9.69%           | 2.785E-01                                  | 5.614E-04                                      | 5.232E-05                                  | 1.331E-04                                      |
| 1.0-2.0    | 2.7594         | 43.68%          | 7.13%           | 2.158E-01                                  | 4.457E-04                                      | 1.047E-04                                  | 1.075E-04                                      |
| 2.0-3.0    | 3.6888         | 48.69%          | 6.99%           | 1.571E-01                                  | 3.201E-04                                      | 9.241E-05                                  | 7.634E-05                                      |
| 3.0-4.0    | 3.8346         | 47.62%          | 6.39%           | 1.304E-01                                  | 2.831E-04                                      | 1.040E-04                                  | 7.714E-05                                      |
| 4.0-5.0    | 3.0389         | 46.00%          | 6.53%           | 1.439E-01                                  | 3.325E-04                                      | 3.721E-05                                  | 9.619E-05                                      |
| 5.0-6.0    | 3.0420         | 50.68%          | 6.69%           | 3.544E-01                                  | 6.107E-04                                      | 3.957E-05                                  | 8.656E-05                                      |
| 6.0-7.0    | 2.9359         | 51.55%          | 7.91%           | 4.109E-01                                  | 6.500E-04                                      | 2.637E-04                                  | 1.023E-04                                      |
| 7.0-8.0    | 3.2914         | 51.60%          | 8.50%           | 7.053E-02                                  | 2.415E-04                                      | 2.813E-04                                  | 9.717E-05                                      |
| 8.0-9.0    | 3.2819         | 49.33%          | 7.87%           | 3.009E-02                                  | 1.580E-04                                      | 2.178E-04                                  | 9.019E-05                                      |
| 9.0-1.0    | 3.7871         | 48.70%          | 7.17%           | 2.818E-02                                  | 1.407E-04                                      | 1.542E-05                                  | 6.309E-05                                      |
| 10.0-11.0  | 3.2810         | 48.82%          | 6.49%           | 2.444E-02                                  | 1.418E-04                                      | 6.969E-05                                  | 7.051E-05                                      |
| 11.0-12.0  | 3.2706         | 46.91%          | 7.09%           | 2.369E-02                                  | 1.366E-04                                      | 6.757E-05                                  | 7.345E-05                                      |
| 12.0-13.0  | 3.0454         | 47.66%          | 6.05%           | 2.609E-02                                  | 1.500E-04                                      | 7.331E-05                                  | 8.316E-05                                      |
| 13.0-14.0  | 3.4421         | 47.96%          | 6.97%           | 2.109E-02                                  | 1.257E-04                                      | 4.803E-05                                  | 8.128E-05                                      |

**DR-PC-15-08: Shoal south of Hog Island**

| Depth (cm) | Wet Sample (g) | % Water by Mass | % LOI (organic) | <sup>210</sup> Pb Specific Activity (Bq/g) | <sup>210</sup> Pb Specific Activity +/- (Bq/g) | <sup>137</sup> Cs Specific Activity (Bq/g) | <sup>137</sup> Cs Specific Activity +/- (Bq/g) |
|------------|----------------|-----------------|-----------------|--|--|--|--|
| 0.0-1.0    | 3.6441         | 58.55%          | 8.06%           | 2.204E-01                                  | 4.663E-04                                      | 1.688E-03                                  | 1.993E-04                                      |
| 1.0-2.0    | 3.2514         | 56.20%          | 7.84%           | 2.514E-01                                  | 4.744E-04                                      | 1.349E-03                                  | 1.825E-04                                      |
| 2.0-3.0    | 3.2784         | 58.55%          | 8.19%           | 2.199E-01                                  | 4.779E-04                                      | 1.221E-03                                  | 1.825E-04                                      |
| 3.0-4.0    | 3.3041         | 57.75%          | 7.50%           | 1.591E-01                                  | 4.158E-04                                      | 1.122E-03                                  | 1.767E-04                                      |



| Depth (cm) | Wet Sample (g) | % Water by Mass | % LOI (organic) | <sup>210</sup> Pb Specific Activity (Bq/g) | <sup>210</sup> Pb Specific Activity +/- (Bq/g) | <sup>137</sup> Cs Specific Activity (Bq/g) | <sup>137</sup> Cs Specific Activity +/- (Bq/g) |
|------------|----------------|-----------------|-----------------|--|--|--|--|
| 4.0-5.0    | 3.3725         | 56.69%          | 7.28%           | 1.176E-01                                  | 3.654E-04                                      | 1.197E-03                                  | 1.805E-04                                      |
| 5.0-6.0    | 4.7824         | 56.49%          | 7.12%           | 7.200E-02                                  | 2.463E-04                                      | 2.007E-03                                  | 1.637E-04                                      |
| 6.0-7.0    | 4.2240         | 55.37%          | 7.23%           | 7.854E-02                                  | 2.719E-04                                      | 1.546E-03                                  | 1.660E-04                                      |
| 7.0-8.0    | 4.0579         | 48.67%          | 7.39%           | 7.871E-02                                  | 2.824E-04                                      | 8.599E-04                                  | 1.363E-04                                      |
| 8.0-9.0    | 3.3018         | 51.42%          | 7.52%           | 8.265E-02                                  | 3.030E-04                                      | 1.303E-03                                  | 1.664E-04                                      |
| 9.0-1.0    | 5.7996         | 54.83%          | 7.21%           | 4.047E-02                                  | 1.670E-04                                      | 5.581E-04                                  | 8.449E-05                                      |
| 10.0-11.0  | 4.3989         | 53.36%          | 7.07%           | 4.533E-02                                  | 2.021E-04                                      | 9.222E-04                                  | 1.119E-04                                      |
| 11.0-12.0  | 4.4423         | 48.62%          | 7.11%           | 4.207E-02                                  | 2.050E-04                                      | 2.200E-04                                  | 7.357E-05                                      |
| 12.0-13.0  | 5.1081         | 53.26%          | 6.73%           | 3.229E-02                                  | 1.655E-04                                      | 2.752E-04                                  | 6.923E-05                                      |
| 13.0-14.0  | 5.6849         | 51.87%          | 6.70%           | 2.917E-02                                  | 1.461E-04                                      | 1.872E-04                                  | 5.602E-05                                      |

## **BIOGRAPHY OF AUTHOR**

Emily Archer Chandler in Portland, Maine and was raised in North Yarmouth and Phippsburg, Maine. She attended Tabor Academy, in Marion, Massachusetts and graduated with Naval Honors in 2005. In May 2009, Emily graduated from Bates College with a Bachelor of Arts degree in Geology and German. Her undergraduate honors Geology thesis focused on the modern and historical development of Seawall Beach, a barrier beach system in Phippsburg, Maine while her German thesis studied Austrian identity in the twentieth century.

After completing her under-graduate degree, Emily taught marine science aboard the schooner *SSV Tabor Boy*, while sailing in coastal Maine and Massachusetts. Emily joined the faculty of Tabor Academy in 2011, where she taught Chemistry and Coral Reef Ecology, coached the girls' rowing and cross-country teams and served as a houseparent until 2014.

Emily returned to Maine in 2014 to begin her graduate studies at the University of Maine. She is a candidate for the Master of Science degree in Earth and Climate Sciences from the University of Maine in August 2016.